ICASE

GEOMETRIC METHODS IN COMPUTATIONAL FLUID DYNAMICS

Peter R. Eiseman

Report No. 80-11

April 18, 1980

INSTITUTE FOR COMPUTER APPLICATIONS IN SCIENCE AND ENGINEERING
NASA Langley Research Center, Hampton, Virginia

Operated by the

UNIVERSITIES SPACE USRA RESEARCH ASSOCIATION

182

TABLE OF CONTENTS

INTRODUCTION

When the flow of a fluid is numerically simulated in a region with a complicated geometry, the theoretical basis for the simulation is a combination of numerical, fluid dynamic, and geometric analyses. In turbomachinery problems, the level of geometric complexity is usually considerable. With increasing amounts of available computational power, with computational fluid dynamic methods reaching a certain level of maturity, and with geometric methods in a fairly primitive state, there is a need to develop geometric analyses in order to consider applications to problems with practical geometries. As a consequence, the emphasis here shall be on geometric methods in computational fluid dynamics. Throughout the development, a general viewpoint shall be adopted so that geometric computational fluid dynamic algorithms can be formulated in a manner which is applicable to broad classes of problems. The geometric description of the flow regions will be given by coordinate generation techniques. To express the equations of motion and the boundary conditions relative to a coordinate system, the methods of tensor analysis must be considered. After a sufficient amount of tensor analysis is presented, general forms for the equations of motion and the boundary conditions are developed. Moreover, with the consequent increase in the possible number of terms in the equations to be solved, numerical methods are considered in a manner for which large numbers of terms can be handled in a systematic manner without the need to explicitly write or code each term on a term by term basis.

GEOMETRIC METHODS IN COMPUTATIONAL FLUID DYNAMICS

Peter R. Eiseman

Institute for Computer Applications in Science and Engineering

and

Universities Space Research Association

ABSTRACT

General methods are presented for the construction of geometric computational fluid dynamic algorithms that can be applied to simulate a wide variety of flow fields in various nontrivial regions. Particular emphasis is given to the highly constrained geometric regions which readily occur in turbomachinery applications. The analysis includes basic developments with tensors, various forms for the equations of motion, generalized numerical methods and boundary conditions, and various methods for coordinate generation to meet the strong geometric constraints of turbomachines. Coordinate generation is considered in enough generality to yield mesh descriptions from one or more transformations that are smoothly joined together to form a composite mesh.

This paper was prepared for the short course on "Shock-Boundary Layer Interaction in Turbomachines" at the von Karman Institute for Fluid Dynamics in June 1980 and in compliance with AGARD Contract No. AGARD/OTAN/DPP/80/11007. This paper pertains to the part of the course entitled "Theoretical Solutions to the Navier-Stokes Equations for Transonic Flow." Partial support was supplied under NASA Contracts No. NAS3-22117 and No. NAS1-15810.

BASIS TENSOR ANALYSIS

The geometric complexity of the various regions within a typical turbomachine is a major factor in the fluid dynamic analysis of any particular region. Although the various regions are parts of Euclidian space, the complexity is caused by region boundaries. To mathematically describe and anlyze flows through such regions, the application of coordinate transformations is a very effective method. Since the physical laws governing fluid flow are independent of any particular coordinate transformation, the mathematical description must also be coordinate invariant. Tensor analysis, however, is a study of the pertinent coordinate invariant quantities. As a result, the mathematical description will be expressed in a tensor form. Since parts of Euclidian space are bounded in some complicated fashion, tensor analysis for our purpose shall be resticted to Euclidian space.

Preliminaries

To start our examination of tensor analysis, let R^n denote an n-dimension Euclidian space, let $\hat{u}_1, \hat{u}_2 \ldots, \hat{u}_n$ denote unit vectors along the axes of a fixed Cartesian coordinate system on R^n, and let $\vec{x}$ be a position vector in R^n. Since R^n is a vector space, the position vector can be expressed by the linear combination

$$\vec{x} = x^i \hat{u}_i \tag{1}$$

where the Einstein summation convention has been employed. In particular, when an index appears as both a subscript and a superscript it is assumed to be summed from 1 to n. This convention shall also be assumed without any more mention in the subsequent discussion. In Eq. 1, the

coefficients x^i are the Cartesian coordinates of the point $\vec{x}$ which is commonly denoted by $(x^1,x^2,\ldots,x^n)$. A two-dimensional illustration of Eq. 1 is given in Figure 1 where the geometric relationship is clearly displayed. Relative to the fixed Cartesian coordinates, let $y^1,y^2,\ldots y^n$ be a system of curvilinear coordinates. The relationship with the fixed Cartesian coordinates is then given in the form

$$\vec{x} = x^i(y^1,\ldots y^n)\hat{u}_i \tag{2}$$

by definition of the functions on the right hand side. When all except one of the curvilinear coordinates are fixed, Eq. 2 defines a coordinate curve with the non-fixed curvilinear coordinate as a parameterization.

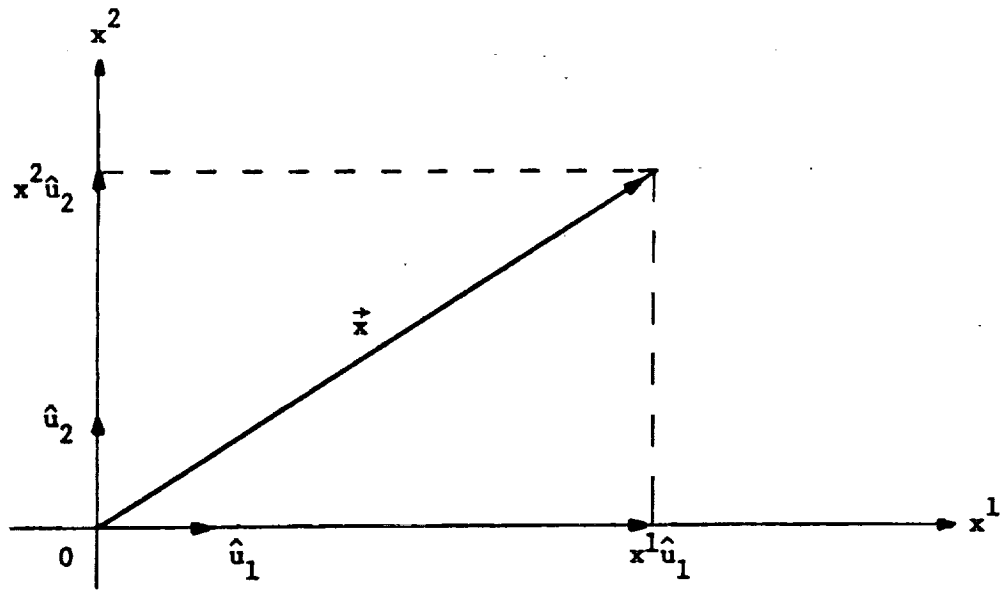

Figure 1. The Cartesian Decomposition of the Position Vector in Two-Dimensions

Upon differentiation with respect to the non-fixed coordinate, a natural tangent vector to the coordinate curve is obtained. Since partial derivatives are taken by holding fixed all except the variable to be differentiated, the natural tangent vectors to coordinate curves are just partial derivatives of the position vector given in Eq. 2. In symbols, the natural tangent vector $\vec{e}_j$ to coordinate curves in the curvilinear variable y^j is given by

$$\vec{e}_j = \frac{\partial \vec{x}}{\partial y^j} \quad . \tag{3}$$

Since the natural tangent vector of Eq. 3 is defined at every point in the domain of the coordinate transformation, it is a vector field as opposed to a single vector. In parallel with Figure 1, a two-dimensional illustration of the natural tangent vectors at a point $\vec{x}$ is depicted in Figure 2.

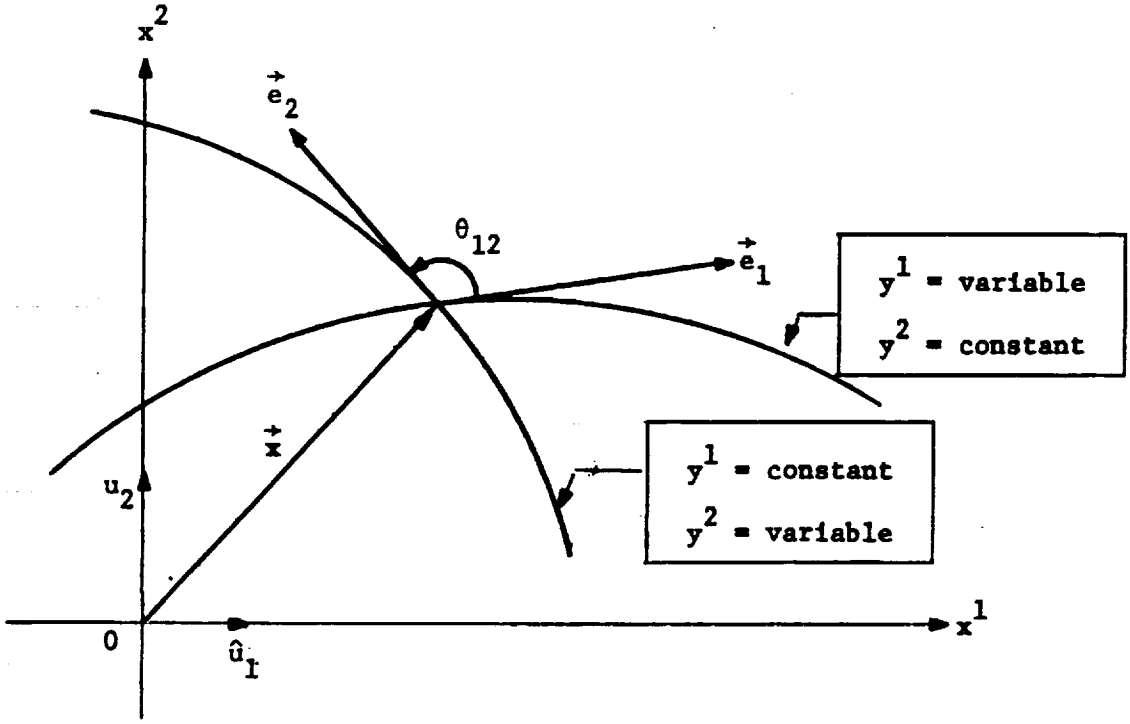

Figure 2. The Natural Tangent Vectors at a Point in Two-Dimensions.

When the transformation of Eq. 2 is inserted into expression for the natural tangent vector field of Eq. 3, we obtain

$$\vec{e}_j = \frac{\partial}{\partial y^j}(x^i \hat{u}_i) = \frac{\partial x^i}{\partial y^j}\hat{u}_i \quad , \tag{4}$$

where the last equality is valid because derivatives of the constant vectors $\hat{u}_i$ vanish. Alternatively, the constancy of each $\hat{u}_i$ implies from Eq. 1 that $\hat{u}_i = \partial\vec{x}/\partial x^i$ which, in turn, leads to Eq. 4 when it is inserted into a chain rule expansion of Eq. 3. To interpret Eq. 4, a Cartesian basis of the vector space R^n is transformed into the set of natural tangent vectors by a Jacobian transformation. If the transformation is nonsingular, then the natural tangent vectors are also a basis of R^n. In particular, the Jacobian

$$J = \det\left(\frac{\partial x^i}{\partial y^j}\right) \quad , \tag{5}$$

must then be non-zero. In the two-dimensional illustration of Figure 2, the Jacobian is non-zero at the point $\vec{x}$ because the natural tangent vectors displayed there are clearly a basis of R^2. Had $\vec{e}_1$ and $\vec{e}_2$ been pointing in the same direction or had either one of them vanished, then the transformation (Eq. 4) would have been singular and Jacobian would have vanished. As a consequence, the pointwise coordinate transformation of Eq. 2 would have mapped a one or two dimensional object into one of lesser dimension. A common example is given by the polar singularity where the one-dimensional segment corresponding zero radius is mapped onto the origin which is zero-dimensional. In general, a singularity is associated with a degeneracy in dimensionality of the pointwise transformation of Eq. 2. When the transformation is nonsingular, there is no loss

in dimensionality and the inverse transformation

$$\vec{y} = \vec{y}(x^1,\ldots,x^n) \tag{6}$$

is valid in a neighborhood of the nonsingular points by virtue of the inverse function theorem.

The Metric

Angles between coordinate curves and rates of change along coordinate curves can be measured with dot products of the natural tangent vector fields of Eq. 4. For notational convenience, let the dot products be represented by

$$g_{ij} \equiv \vec{e}_i \cdot \vec{e}_j \tag{7}$$

which is symmetric in the indices i and j each of which vary from 1 to n. The similar set of dot products of unit Cartesian vectors $\hat{u}_i$ is, however, of a special form: it is given by $\hat{u}_k \cdot \hat{u}_\ell = \delta_{k\ell}$ where $\delta_{k\ell}$ is the Kronecker delta symbol which is unity if the indices are equal and vanishes otherwise. When Eq. 4 is inserted into Eq. 7 and when the special form of the Cartesian dot products is applied, the dot products of the natural tangent vectors are given by

$$\begin{aligned} g_{ij} &= \left(\frac{\partial x^k}{\partial y^i}\,\hat{u}_k\right) \cdot \left(\frac{\partial x^\ell}{\partial y^j}\,\hat{u}_\ell\right) \\ &= \frac{\partial x^k}{\partial y^i}\,\frac{\partial x^\ell}{\partial y^j}\,\hat{u}_k \cdot \hat{u}_\ell \\ &= \frac{\partial x^k}{\partial y^i}\,\frac{\partial x^\ell}{\partial y^j}\,\delta_{k\ell} \\ &= \frac{\partial x^k}{\partial y^i}\,\frac{\partial x^k}{\partial y^j} \end{aligned} \tag{8}$$

where the sum over k after the last equality is a slight abuse of the summation convention since two superscripts are summed rather than a subscript-superscript pair. From Eq. 8 with $i = j$, the magnitude of the natural tangent vector field to coordinate curves in the y^j variable (Eq. 4) becomes

$$\sqrt{g_{jj}} = \left[\left(\frac{\partial x^1}{\partial y^j}\right)^2 + \left(\frac{\partial x^2}{\partial y^j}\right)^2 + \ldots + \left(\frac{\partial x^n}{\partial y^j}\right)^2\right]^{\frac{1}{2}} , \tag{9}$$

which can also be recognized as the derivative of coordinate curve arc length with respect to the curve parameterization y^j. Since the index j appears on both sides of the equation, note that its repetition which is not summed does not conflict with a summation convention. With the magnitudes (Eq. 9) established for the natural tangent vector fields (Eq. 4), unit tangent vector fields can be defined along the coordinate curves provided that the magnitudes do not vanish and can consequently be used for the respective normalizations. When dot products of the unit vector fields obtained by the normalizations are computed, angles between coordinate curves can be determined. For the coordinate curves in the y^i and y^j variables, respectively, the dot product which determines the angle θ_{ij} between them is given by

$$\cos\theta_{ij} = \left(\frac{\vec{e}_i}{\sqrt{g_{ii}}}\right) \cdot \left(\frac{\vec{e}_j}{\sqrt{g_{jj}}}\right) = \frac{g_{ij}}{\sqrt{g_{ii}g_{jj}}} . \tag{10}$$

A two-dimensional illustration of the angle θ_{12} is displayed in Figure 2. Unlike the higher dimensional cases, $\theta_{12} = \theta_{21}$ is the only angle that needs to be determined there. In the illustration, the magnitudes $\sqrt{g_{11}}$, $\sqrt{g_{22}}$ and the angle θ_{12} are enough to determine the area of the

parallelogram defined by $\vec{e}_1$, $\vec{e}_2$ and appropriate parallel translates. The area, $\sqrt{g_{11}}[\sqrt{g_{22}}|\sin\theta_{12}|]$, upon substitution from Eq. 10, reduces to $\sqrt{g}$ where g is the determinant of the matrix (g_{ij}). Intuitively, the area should be equal to the Jacobian (Eq. 5), and consequently, the relationship $g = J^2$ should be valid. From Eq. 8, the validity can, in fact, be established not only for two-dimensions but more generally for any number of dimensions. Specificially, if A denotes the matrix from the Jacobian transformation of Eq. 4 and if A^t is the transpose of A, then the determinant of Eq. 8 becomes

$$g = \det(A^t A) = (\det A^t)(\det A) = (\det A)^2 = J^2 , \qquad (11)$$

from the determinant product rule and invariance with respect to transpose. The singularity or nonsingularity of a coordinate transformation can then clearly be considered from the matrix of dot products or from the Jacobian transformation.

With the determination of coordinate curve arc length from the dot products given in Eq. 9, a reasonable expectation is to determine the arc length of an arbitrary curve from the full set of dot products given in Eq. 8. Between two values $t = a$ and $t = b$ of a parameterization t for an arbitrary curve $\vec{x} = \vec{x}(\vec{y}(t))$, the curve arc length can be approximated by the linear distance between corresponding points on the curve. When a given level of accuracy is specified, it can be obtained for choices of a and b that are sufficiently close together. Moreover, in the limit towards differential sizes the appoximation converges to an exact equality, assuming that the curve is sufficiently smooth. The differential element of arc length ds is then given by

$$(ds)^2 = d\vec{x} \cdot d\vec{x} \quad . \tag{13}$$

From a chain rule expansion, the differential of the Cartesian vector field $\vec{x}$ of Eq. 2 becomes

$$d\vec{x} = \frac{\partial \vec{x}}{\partial y^i} dy^i = \vec{e}_i dy^i \quad , \tag{14}$$

where the natural tangent vector fields (Eq. 3) were inserted for the last equality. Upon substitution, the quadradic expression for the arc length differential becomes

$$(ds)^2 = (\vec{e}_i dy^i) \cdot (\vec{e}_j dy^j) = (\vec{e}_i \cdot \vec{e}_j) dy^i dy^j = g_{ij} dy^i dy^j \quad , \tag{15}$$

where the second equality results from dot product linearity; the third, from Eq. 7. Consequently, the rule for distance measurements with respect to curvilinear variables is given entirely by the set of all dot products between the natural tangent vector fields to coordinate curves (Eq. 7). The rule is referred to as a metric and the dot products g_{ij} are then called metric coefficients [1]. When the rule is applied to the earlier case of arc length along a coordinate curve in the y^j variable, the result corresponds to the earlier statement following Eq. 9. To obtain a specific coordinate curve in y^j, the remaining variables y^k for $k \neq j$ must be constants which, in turn, leads to the vanishing differentials: $dy^k = 0$ for $k \neq j$. Upon substitution, Eq. 15 reduces to the unsummed expression $(ds)^2 = g_{jj}(dy^j)^2$, establishing the expected correspondence. In Figure 3, an application of the metric is given for an arbitrary curve in two-dimensions where a differential element of arc length

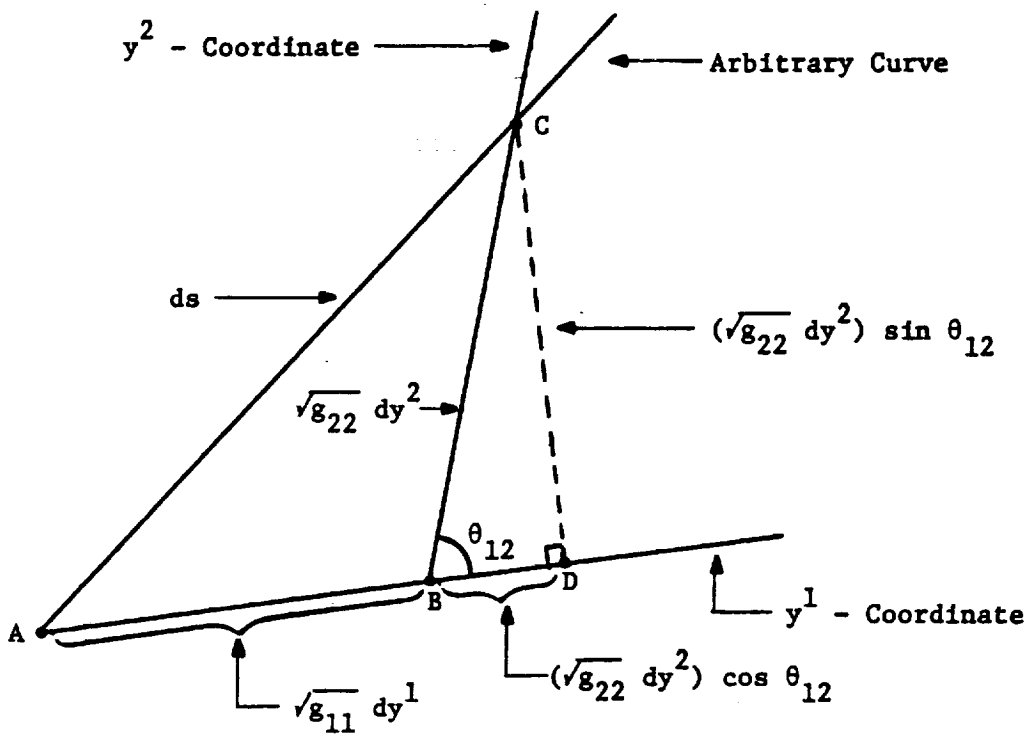

Figure 3. Differential Element of Arc Length for an Arbitrary Curve in Two-Dimensions.

is to be computed between A and C along the arbitrary curve. On a differential level, all curves can be represented by the straight line segments, as illustrated. The distances along the coordinate curves in y^1 and y^2 variables are given by $\sqrt{g_{11}}\ dy^1$ and $\sqrt{g_{22}}\ dy^2$ respectively along line segments AB and BC. From the angle θ_{12}, distances on the legs of the right triangle ADC can be obtained. By the Pythagorean theorem, the arc length expression is then

$$
\begin{aligned}
(ds)^2 &= \left[\sqrt{g_{11}}\, dy^1 + (\sqrt{g_{22}}\, dy^2)\cos\theta_{12}\right]^2 + \left[(\sqrt{g_{22}}\, dy^2)\sin\theta_{12}\right]^2 \\
&= g_{11}(dy^1)^2 + 2\sqrt{g_{11}g_{22}}\ (\cos\theta_{12})dy^1dy^2 + g_{22}(dy^2)^2 \\
&= g_{11}(dy^1)^2 + 2\, g_{12}dy^1dy^2 + g_{22}(dy^2)^2 \\
&= g_{ij}dy^i dy^j \quad ,
\end{aligned}
\tag{16}
$$

which as expected matches with the general form. The third equality in Eq. 16 was the result of a direct substitution from Eq. 10; the last, symmetry in the indices of the metric coefficients.

When the transformation of coordinates (Eq. 2) is nonsingular at a point, the natural tangent vectors (Eq. 3) form a basis of the vector space R^n. A new basis $\vec{e}^1, \vec{e}^2, \ldots, \vec{e}^n$ can be then be obtained by enforcement of the orthogonality relationship

$$
\vec{e}^i \cdot \vec{e}_j = \delta^i_j \tag{17}
$$

for $1 \leq i, j \leq n$. The symbol δ^i_j is a Kronecker delta which is equal to the earlier Kronecker delta δ_{ij}: it is unity when $i = j$ and vanishes otherwise. A two-dimensional illustration of the new (dual) basis is given in Figure 4. The orthogonality properties are geometrically viewed as the construction of vector fields which are perpendicular to coordinate curves. In the example, $\vec{e}^1$ is perpendicular to every y^2- coordinate curve at every point along each one. Similarly $\vec{e}^2$ is perpendicular to the y^1 - coordinate curve, as illustrated. Moreoever, in n-dimensions $\vec{e}^1$ is perpendicular to all coordinate surfaces corresponding to constant

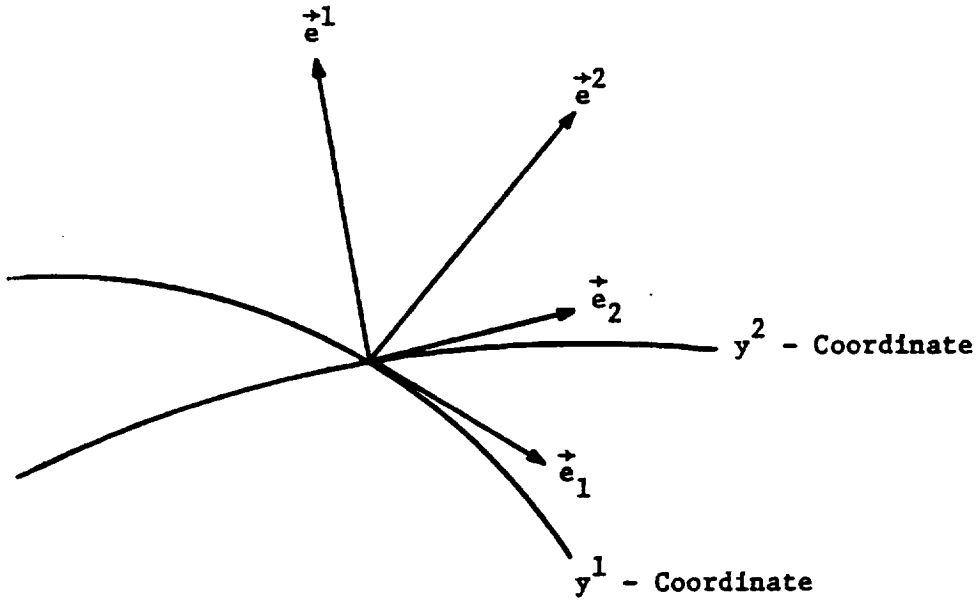

Figure 4. Dual Basis to the Natural Tangent Vectors in Two Dimensions

values of y^i at all points along those surfaces. Since $\vec{e}^i$ belongs to R^n, it can be expressed as a linear combination of the natural tangent vectors in the form $\vec{e}^i = a^{ik}\vec{e}_k$ for some coefficients a^{ik}. When the linear combination is inserted into Eq. 17 and subsequently when Eq. 7 is applied, we obtain $a^{ik}g_{kj} = \delta^i_j$ which indicates that the matrix (a^{ik}) is just the inverse of the matrix of metrics (g_{ij}) which exists since $g = J^2$ by Eq. 11 and J is nonvanishing by the nonsingularity of the transformation. For uniformity in the notation for metrics, the elements a^{ik} of the inverse matrix shall be denoted by g^{ik}. With the uniform metric notation, the transformation into the superscript basis is given by

$$\vec{e}^i = g^{ij}\vec{e}_j \,, \tag{18a}$$

for $i = 1,2,\ldots,n$. By matrix multiplication $g_{ki}\vec{e}^{i} = g_{ki}g^{ij}\vec{e}_j = \delta_k^j\vec{e}_j = \vec{e}_k$ which is

$$\vec{e}_k = g_{ki}\vec{e}^{i} \quad . \tag{18b}$$

In summary, transformations between subscripted and superscripted bases of R^n are obtained by using the form of the metric that is compatible with the Einstein summation convention of summing subscript-superscript pairs of indices. Since both subscripted and superscripted vectors are bases of R^n, any vector $\vec{v}$ can be expressed as

$$\vec{v} = v^k\vec{e}_k = v_i\vec{e}^{i} \quad , \tag{19}$$

where the coefficients are designated with superscripts and subscripts in correspondence with the summation convention. Upon a direct substitution from Eq. 18 and an application of linear independence, the coefficients of Eq. 19 are related by

$$v_i = g_{ik}v^k \quad , \tag{20a}$$

and

$$v^k = g^{ki}v_i \quad . \tag{20b}$$

Consequently, the metric can be used to raise and lower the indices of either the vector bases or their coefficients by adhering to the summation convention. As a matter of termonology, subscripted quantities, have been called covariant quantities: superscripted ones, contravariant [2].

When the dot products of the superscripted vectors are considered, a result similar to the metric expression in Eq. 7 could be anticipated. To form a superscripted version, the dot product of $\vec{e}^{k}$ with both sides of Eq. 18a is taken. The right hand side is given by $g^{ij}\vec{e}^{k} \cdot \vec{e}_j = g^{ij}\delta^k_j = g^{ik}$ where the definition of Eq. 17 has been applied. Thus, in parallel with the dot product representation of g_{ij}, the inverse to the matrix of metrics has elements given in the dot product form

$$g^{ik} = \vec{e}^{i} \cdot \vec{e}^{k} , \tag{21}$$

for $i,j = 1,2,\ldots,n$. Moreover, if A denotes the Jacobian transformation of Eq. 4 with transpose A^t and inverse A^{-1}, then for nonsingular A, the inverse metrics are given by

$$(g^{ij}) = (g_{km})^{-1} = (A^tA)^{-1} = A^{-1}(A^t)^{-1} = A^{-1}(A^{-1})^t . \tag{22}$$

When this matrix equation is converted into components, the inverse metric assumes the form

$$g^{ij} = \frac{\partial y^i}{\partial x^m}\,\frac{\partial y^j}{\partial x^m} , \tag{23}$$

which appears like an expanded form of Eq. 21. Upon substitution of both Eq. 23 and Eq. 4 into Eq. 18a, we obtain

$$\vec{e}^{i} = \frac{\partial y^i}{\partial x^m}\,\hat{u}_m , \tag{24}$$

after some simplifications. The result is a Cartesian expansion of $\vec{e}^{\,i}$ which is a parallel to the expansion of $\vec{e}_j$ in Eq. 4 and which establishes the connection between Eqs. 21 and 23.

Tensor Products

With the basis of natural tangents $\vec{e}_1, \vec{e}_2, \ldots \vec{e}_n$ and its dual $\vec{e}^{\,1}, \vec{e}^{\,2}, \ldots, \vec{e}^{\,n}$ with respect to dot products (Eq. 17), higher order bases of higher order spaces can be obtained from tensor products of the given bases. The formation of a higher order space from m existing spaces $W_1, W_2, \ldots, W_m$ is usually taken to be a Cartesian product $W_1 \times W_2 \times ,,, \times W_m$ where points are given by ordered m-tuples of the form $(w_1, w_2, \ldots w_m)$ for w_k in W_k and $k = 1,2,\ldots,m$. The Cartesian product is satisfactory when no algebraic properties are needed such as when the spaces W_i are just sets of points. However, when each W_i is a vector space, a product which is also a vector space is usually needed. The tensor product fulfills this need. It is defined by the enforcement of linearity in each position of the Cartesian m-tuples so that the new vectors (i.e., tensors) can be added, substracted, and scaled in the same manner as the original vectors in each W_i. To distinguish the tensor product from the Cartesian product, the Cartesian $\times$ shall be replaced by $\otimes$. The tensor product of the spaces W_i is then denoted by $W_1 \otimes W_2 \otimes \ldots \otimes W_m$ with elements $\vec{w}_1 \otimes \vec{w}_2 \otimes \ldots \otimes \vec{w}_m$ which for uniformity of notation also have the symbol $\otimes$. For $\vec{v}_k$ in W_k and a scalar a_k, the relationship that defines the tensor product is given by

$$\vec{w}_1 \otimes \ldots \otimes \vec{w}_{k-1} \otimes (a_k \vec{w}_k + \vec{v}_k) \otimes \vec{w}_{k+1} \otimes \ldots \otimes \vec{w}_m \qquad (25)$$

$$= a_k \left[\vec{w}_1 \otimes \ldots \otimes \vec{w}_m\right] + \left[\vec{w}_1 \otimes \ldots \otimes \vec{w}_{k-1} \otimes \vec{v}_k \otimes \vec{w}_{k+1} \otimes \ldots \otimes \vec{w}_m\right].$$

When the W_i are taken to be spaces of vector fields rather than vector spaces, the only difference is that the scalars a_k of Eq. 25 are functions rather than real numbers since vector fields are just an assignment of vectors at all points in the space over which they are defined. The functions a_k are given over the space of vector field definition which if collapsed to a point would be a real number and similarly the vector fields would reduce to vectors. Now let each W_i be the space of natural tangent vector fields for $i = 1,2,\ldots,p$ and let each W_j^* be the dual space for $j = 1,2,\ldots,q$. Then elements α of the tensor product space $W_1 \otimes \ldots \otimes W_p \otimes W_1^* \otimes \ldots \otimes W_q^*$ can be expressed in the form

$$\alpha = \alpha^{i_1 \ldots i_p}_{\quad j_1 \ldots j_q} \vec{e}_{i_1} \otimes \ldots \otimes \vec{e}_{i_p} \otimes \vec{e}^{\,j_1} \otimes \ldots \otimes \vec{e}^{\,j_q}, \qquad (26)$$

which is an expansion in the tensor product basis $\vec{e}_{i_1} \otimes \ldots \otimes \vec{e}^{\,j_q}$ with coefficients $\alpha^{i_1 \ldots i_p}_{\quad j_1 \ldots j_q}$. The Einstein summation convention for Eq. 26 is used here in the form where all indices can be raised and lowered by use of the metric (Eq. 20). In particular, blank spaces must exist below the indices i_k for $k = 1,2,\ldots,p$ and above the indices j_ℓ for $\ell = 1,2,\ldots,q$. As a matter of terminology, the tensor expression of Eq. 26 is referred to as a tensor of type (p,q) and rank $p+q$ to indicate the numbers of covariant and contravariant basis factors and the total number of basis factors respectively.

Differentiation of Tensors

To consider the differentiation of tensors, the first step is to consider the differentiation of each factor in the tensor product. Then the

differentiation process can be extended to expansions of the type given in Eq. 26 by the enforcement of a Leibnitz rule. The first factor is the scalar coefficient $\alpha^{i_1 \cdots i_p}_{j_1 \cdots i_q}$ where the derivative is already well defined by partial differentiation. In anticipation of the extension to general tensors, the derivative in the y^i - coordinate direction shall be denoted by the symbol D_i which reduces to the parital derivative $\partial/\partial y^i$ on application to functions. When D_i is applied to a natural tangent vector field $\vec{e}_j$ as representative element from the next group of factors, the result must be another vector field. To preserve the basis of natural tangents, the derivative can be expressed in the form

$$D_i \vec{e}_j = \Gamma^k_{ij} \vec{e}_k \quad , \tag{27}$$

where the coefficients Γ^k_{ij} in the linear combination are called Christoffel symbols of the second kind. Alternatively, the derivative can also be expressed in terms of the Cartesian basis $\hat{u}_1, \hat{u}_2, \ldots, \hat{u}_n$ which is constant for all values of $y^1, y^2, \ldots, y^n$ in correspondence with the domain of vector field definition. When D_i is directly applied to the Cartesian expansion for $\vec{e}_j$ in Eq. 4, only the nonconstant coefficients have non-trivial derivatives and the result is given by

$$D_i \vec{e}_j = \frac{\partial^2 x^k}{\partial y^j \partial y^i} \hat{u}_k \quad . \tag{28}$$

Since the order of partial differentiation is interchangeable, $D_i \vec{e}_j = D_j \vec{e}_i$ for vector fields on Cartesian spaces. Upon substitution from Eq. 27 and an application of linear independence, the symmetry property

$$\Gamma_{ij}^{k} = \Gamma_{ji}^{k} \quad , \tag{29}$$

of the Christoffel symbols is valid for all i,j,k. This property can be extended to non-Euclidian spaces by the definition of a Torsion tensor, the vanishing of which yields a slightly more complex statment than Eq. 29. For Euclidian space, vanishing torsion is given precisely by Eq. 29. Consequently, the symmetric lower indices for the Christoffel symbols which define the derivative of Eq. 27 yields a derivative which is called torsionless.

With the torsionless derivative for Euclidian space, the Christoffel symbols can be obtained from Eq. 28 when $\hat{u}_k$ is expanded in the basis of natural tangents. The expansion is obtained from

$$\hat{u}_k = \delta_k^i \hat{u}_i = \frac{\partial y^m}{\partial x^k} \frac{\partial x^i}{\partial y^m} \hat{u}_i = \frac{\partial y^m}{\partial x^k} \vec{e}_m \quad , \tag{30}$$

where the second equality follows from the inverse relationship for Jacobian transformations; the last, from Eq. 4. The substitution into Eq. 28 then yields

$$D_i \vec{e}_j = \frac{\partial y^m}{\partial x^k} \frac{\partial^2 x^k}{\partial y^j \partial y^i} \vec{e}_m = \frac{\partial y^k}{\partial x^m} \frac{\partial^2 x^m}{\partial y^j \partial y^i} \vec{e}_k \quad . \tag{31}$$

From Eq. 27 and the linear independence of the natural tangents, the Christoffel symbols are represented by

$$\Gamma_{ij}^{k} = \frac{\partial y^k}{\partial x^m} \frac{\partial^2 x^m}{\partial y^j \partial y^i} \quad , \tag{32}$$

which is a representation in terms of both the Cartesian and curvilinear coordinates. An alternate and more intrinsic representation would be an expression in terms of the metric as a function of the curvilinear coordinates. Representations which depend upon some fixed embedding, such as the Cartesian coordinate frame of reference, could not be considered to be intrinsic to the space under study. To obtain an intrinsic representation, the derivative D_i given in Eq. 27 will be applied to the metric expression (Eq. 7) given by the dot product of natural tangents. On application, we obtain

$$\begin{aligned}\frac{\partial g_{mj}}{\partial y^i} &= D_i(\vec{e}_m \cdot \vec{e}_j) \\ &= (D_i\vec{e}_m) \cdot \vec{e}_j + \vec{e}_m \cdot (D_i\vec{e}_j) \\ &= (\Gamma^r_{im}\vec{e}_r) \cdot \vec{e}_j + \vec{e}_m \cdot (\Gamma^r_{ij}\vec{e}_r) \\ &= g_{rj}\Gamma^r_{im} + g_{mr}\Gamma^r_{ij} \quad ,\end{aligned} \tag{33}$$

where the second equality is a Leibnitz rule; the third, a substitution from Eq. 27; and the fourth, a substitution from Eq. 7. When i and j are interchanged and when m and i are interchanged, Eq. 33 respectively is given by

$$\frac{\partial g_{mi}}{\partial y^j} = g_{ri}\Gamma^r_{jm} + g_{mr}\Gamma^r_{ji} \quad , \tag{34}$$

and

$$\frac{\partial g_{ij}}{\partial y^m} = g_{rj}\Gamma^r_{mi} + g_{ir}\Gamma^r_{mj} \quad . \tag{35}$$

On examination of the right hand sides of Eqs. 33-35, the Christoffel symbols are observed to appear in pairs: each symbol in the pair belongs to a different equation and each symbol differs from the other only in the ordering of its subscripts. When the torsionless condition (Eq. 29) which is valid for the derivative in Euclidian spaces is applied, the paired symbols become identical. Consequently, the subtraction of the metric derivative of Eq. 35 from the sum of the metric derivatives in Eqs. 33 and 34 collapses by cross cancellation into an expression with just one Christoffel symbol summation. Interchanging the sides of the expression, the result is given by

$$2\, g_{mr}\Gamma^{r}_{ij} = \frac{\partial g_{mj}}{\partial y^{i}} + \frac{\partial g_{mi}}{\partial y^{j}} - \frac{\partial g_{ij}}{\partial y^{m}} \quad . \tag{36}$$

Since $g^{km}g_{mr}\Gamma^{r}_{ij} = \delta^{k}_{r}\Gamma^{r}_{ij} = \Gamma^{k}_{ij}$, the metric formulation for the Christoffel symbols becomes

$$\Gamma^{k}_{ij} = \frac{g^{km}}{2}\left\{\frac{\partial g_{mj}}{\partial y^{i}} + \frac{\partial g_{mi}}{\partial y^{j}} - \frac{\partial g_{ij}}{\partial y^{m}}\right\} \quad . \tag{37}$$

With the assumption of a Cartesian frame, the metric formulation collapses into the earlier Cartesian representation (Eq. 32) by substitutions from the metric in Eq. 8 and its inverse in Eq. 23. However, the derivative in Eq. 27 with coefficients from Eq. 37 is not restricted to Euclidian spaces.

In continuation, the extension of the derivative to the next group of factors in Eq. 26 which are the dual vector fields $\vec{e}^{\,i}$ to the natural tangents are obtained by an application of the Leibnitz rule to the duality relationship of Eq. 17. Since the Kronecker symbol is a constant for any particular pair of indices, its derivative vanishes and the differentiated

duality relationship becomes

$$
\begin{aligned}
0 &= D_i(\vec{e}^k \cdot \vec{e}_j) \\
&= (D_i\vec{e}^k) \cdot \vec{e}_j + \vec{e}^k \cdot (D_i\vec{e}_j) \\
&= (D_i\vec{e}^k) \cdot \vec{e}_j + \vec{e}^k \cdot (\Gamma^r_{ij}\vec{e}_r) \\
&= (D_i\vec{e}^k) \cdot \vec{e}_j + \Gamma^k_{ij} \quad .
\end{aligned}
\tag{38}
$$

where the third equality comes from Eq. 27; the fourth, from duality. When the derivative of the dual vector field is written in terms of the dual basis, there are functions Λ^k_{ij} such that $D_i\vec{e}^k = \Lambda^k_{im}\vec{e}^m$. On substitution, Eq. 38 then becomes $-\Gamma^k_{ij} = (D_i\vec{e}^k) \cdot \vec{e}_j = (\Lambda^k_{im}\vec{e}^m) \cdot \vec{e}_j = \Lambda^k_{im}\delta^m_j = \Lambda^k_{ij}$ which determines the derivative coefficients. Consequently, the derivative of the dual vector field $\vec{e}^k$ in the $\vec{e}_i$-direction which preserves the dual basis is given by

$$
D_i\vec{e}^k = -\Gamma^k_{ij}\vec{e}^j \quad . \tag{39}
$$

With the derivative defined on both covariant (Eq. 27) and contravariant (Eq. 39) basis vector fields, the extension to a general tensor field (Eq. 26) is obtained directly from a Leibnitz rule. The general tensor field of Eq. 26 can be rewritten in the form

$$
\alpha = \alpha^{i_1\cdots i_p}_{\quad j_1\cdots j_q}\, e_{i_1\cdots i_p} \otimes e^{j_1\cdots j_q} \quad , \tag{40a}
$$

where

$$e_{i_1 \cdots i_p} = \vec{e}_{i_1} \otimes \cdots \otimes \vec{e}_{i_p} \quad , \tag{40b}$$

and

$$e^{j_1 \cdots j_q} = \vec{e}^{\,j_1} \otimes \cdots \otimes \vec{e}^{\,j_q} \quad , \tag{40c}$$

are respectively the groups of covariant and contravariant basis factors. When D_k is applied to the tensor α, the Leibnitz rule is used to obtain

$$\begin{aligned} D_k \alpha = & \left(\frac{\partial}{\partial y^k} \alpha^{i_1 \cdots i_p}{}_{j_1 \cdots j_q} \right) e_{i_1 \cdots i_p} \otimes e^{j_1 \cdots j_q} \\ & + \alpha^{i_1 \cdots i_p}{}_{j_1 \cdots j_q} (D_k e_{i_1 \cdots i_p}) \otimes e^{j_1 \cdots j_q} \\ & + \alpha^{i_1 \cdots i_p}{}_{j_1 \cdots j_q} e_{i_1 \cdots i_p} \otimes (D_k e^{j_1 \cdots j_q}) \quad . \end{aligned} \tag{41}$$

To evaluate the second term in Eq. 41, the Leibnitz rule is applied again to yield the factor

$$\begin{aligned} D_k e_{i_1 \cdots i_p} &= \sum_{m=1}^{p} \vec{e}_{i_1} \otimes \cdots \otimes (D_k \vec{e}_{i_m}) \otimes \cdots \otimes \vec{e}_{i_p} \\ &= \sum_{m=1}^{p} \Gamma^{r_m}_{k i_m} \vec{e}_{i_1} \otimes \cdots \otimes \vec{e}_{r_m} \otimes \cdots \otimes \vec{e}_{i_p} \quad . \end{aligned} \tag{42}$$

A similar application leads to

$$D_k e^{j_1 \cdots j_q} = -\sum_{m=1}^{q} \Gamma^{j_m}_{k r_m} \vec{e}^{\,j_1} \otimes \cdots \otimes \vec{e}^{\,r_m} \otimes \cdots \otimes \vec{e}^{\,j_q} \quad , \tag{43}$$

which appears in the third term. When Eqs. 42 and 43 are inserted into Eq. 41 and subsequently when r_m is interchanged (as a dummy index of summation) with the respective indices i_m and j_m, the derivative assumes the form

$$D_k\alpha = (D_k\alpha)^{i_1\cdots i_p}{}_{j_1\cdots j_q}\, e_{i_1\cdots i_p} \otimes e^{j_1\cdots j_q} , \tag{44a}$$

in the original basis with coefficients given by

$$\begin{aligned}(D_k\alpha)^{i_1\cdots i_p}{}_{j_1\cdots j_q} = {} & \frac{\partial}{\partial y^k}\, \alpha^{i_1\cdots i_p}{}_{j_1\cdots j_q} \\ & + \sum_{m=1}^{p} \Gamma^{i_m}_{kr_m}\, \alpha^{i_1\cdots r_m\cdots i_p}{}_{j_1\cdots j_q} \\ & - \sum_{m=1}^{q} \Gamma^{r_m}_{kj_m}\, \alpha^{i_1\cdots i_p}{}_{j_1\cdots r_m\cdots j_q} .\end{aligned} \tag{44b}$$

As a matter of terminology, the derivative is called the covariant derivative of the tensor field α in the direction $\vec{e}_k$.

The Gradient of a Tensor

In Cartesian coordinates, the gradient of a function f is given by the expression

$$\nabla f = \frac{\partial f}{\partial x^m}\, \hat{u}_m , \tag{45}$$

and moreover, is a vector field which is normal to the surfaces defined by constant values of f. To verify the latter statement, consider the

differential tangent vector $d\vec{x} = \hat{u}_i dx^i$ which at a point $\vec{x}(\vec{Q})$ on a constant f surface can be viewed as a limit of directed secants $\vec{x}(\vec{P}) - \vec{x}(\vec{Q})$ to the surface as $\vec{P}$ approaches $\vec{Q}$. By direct evaluation the dot product $(\nabla f) \cdot d\vec{x}$ is just df which vanishes when f is a constant and which in turn verifies the statement on the normality of the gradient. In curvilinear coordinates the gradient (Eq. 45) becomes

$$\nabla f = \frac{\partial f}{\partial y^i} \frac{\partial y^i}{\partial x^m} \hat{u}_m = \vec{e}^i \frac{\partial}{\partial y^i} (f) \quad , \tag{46}$$

where the first equality comes from the chain rule; the second, from Eq. 24. As an operator, the gradient can be removed from its application to functions in Eq. 46 and be given the obvious generalization to tensors which is

$$\nabla = \vec{e}^k \otimes D_k \quad . \tag{47}$$

In the generalization, the scalar product became a tensor product and partial derivatives became covariant derivatives (Eq. 44), each being the extension of the former.

To illustrate the general computation of gradients with Eq. 47, several useful examples will be considered. The simplest and most common example is that of a vector field $\vec{\alpha} = \alpha^i \vec{e}_i$. From the covariant derivative in Eq. 44, the gradient becomes

$$\begin{aligned} \nabla\vec{\alpha} &= \left(\frac{\partial \alpha^i}{\partial y^k} + \alpha^m \Gamma^i_{km}\right) \vec{e}^k \otimes \vec{e}_i \\ &= g^{kr} \left(\frac{\partial \alpha^i}{\partial y^k} + \alpha^m \Gamma^i_{km}\right) \vec{e}_r \otimes \vec{e}_i \end{aligned} \tag{48}$$

where the last equality follows by using the metric to lower an index (Eq. 18a). In fluid mechanics, the next most common tensor is the stress tensor which is a second rank tensor. Second rank tensors are often called dyadics. As the final example, the gradient of a dyadic $\alpha = \alpha^{ij}\vec{e}_i \otimes \vec{e}_j$ is then given by

$$\nabla\alpha = \left(\frac{\partial\alpha^{ij}}{\partial y^k} + \alpha^{rj}\,\Gamma^i_{kr} + \alpha^{ir}\,\Gamma^j_{kr}\right)\vec{e}^k \otimes \vec{e}_i \otimes \vec{e}_j \quad , \tag{49}$$

from a direct application of Eq. 44, as before.

The Divergence of a Tensor

The divergence operator is a modification of the gradient operator (Eq. 47) obtained when the tensor product is replaced by a dot product. In symbols, the divergence $\nabla\cdot$ is given by

$$\nabla\cdot = \vec{e}^k \cdot D_k \quad . \tag{50}$$

Upon application to a Cartesian coordinate expression of a vector field $\vec{\alpha} = \alpha^i \hat{e}_i$, the easily recognized form

$$\nabla\cdot\vec{\alpha} = \frac{\partial\alpha^i}{\partial x^i} \quad , \tag{51}$$

is obtained from Eq. 48 where $y^i = x^i$, Christoffel symbols vanish, and the dot product replacement becomes a Kronecker delta.

To obtain the divergence of a vector field in curvilinear coordinates, the general expression of Eq. 50 shall be applied to a vector field in the covariant basis $\vec{e}_i$ of natural tangents. The simplest case occurs when the

vector field is a particular natural tangent. For each fixed subscript i, the divergence is given by

$$\nabla \cdot \vec{e}_i = \vec{e}^k \cdot D_k \vec{e}_i = \vec{e}^k \cdot (\Gamma^j_{ki} \vec{e}_j) = \Gamma^j_{ki} \delta^k_j = \Gamma^j_{ij} \quad . \tag{52}$$

From Eq. 37, the sum of Christoffel symbols becomes

$$\Gamma^j_{ij} = \frac{g^{jm}}{2} \left\{ \frac{\partial g_{mj}}{\partial y^i} + \frac{\partial g_{mi}}{\partial y^j} - \frac{\partial g_{ij}}{\partial y^m} \right\} = \frac{g^{jm}}{2} \frac{\partial g_{mj}}{\partial y^i} \quad , \tag{53}$$

where the last two sums cancelled upon an interchange of the dummy indices m and j in the last sum. By Cramer's rule, the inverse metric is given by $g^{jm} = \Delta^{jm}/g$ where Δ^{jm} is the $(j,m)^{th}$ cofactor of the matrix of metrics (g_{ik}). The cofactor Δ^{jm} also appears in the expansion by minors about the j^{th} row which is written as $g = g_{j1}\Delta^{1j} + \ldots + g_{in}\Delta^{nj}$. Since its coefficient g_{jm} appears no place else in the expansion, the cofactor is just the partial derivative $\partial g/\partial g_{jm}$. Hence, the inverse metric can be expressed in the form:

$$g^{jm} = \frac{1}{g} \frac{\partial g}{\partial g_{jm}} \quad . \tag{54}$$

When the inverse from Eq. 54 is substituted into Eq. 53, the sum of Christoffel symbols becomes

$$\Gamma^j_{ij} = \frac{1}{2g} \frac{\partial g}{\partial g_{jm}} \frac{\partial g_{jm}}{\partial y^i} = \frac{1}{2g} \frac{\partial g}{\partial y^i} = \frac{1}{\sqrt{g}} \frac{\partial \sqrt{g}}{\partial y^i} \quad . \tag{55}$$

Consequently, the divergence of the natural tangent field $\vec{e}_i$ is given by

$$\nabla \cdot \vec{e}_i = \frac{1}{J} \frac{\partial J}{\partial y^i} \quad , \tag{56}$$

when Eq. 11 is applied to yield $\sqrt{g} = \pm J$. Unlike the divergence of Cartesian bases elements $\hat{u}_i$, the natural tangents $\vec{e}_i$ have a nontrivial divergence unless J is independent of y^i. In continuation, to obtain the divergence of a vector field $\vec{\alpha} = \alpha^i \vec{e}_i$ the gradient given in Eq. 48 must be contracted by replacement of its tensor product with a dot product. The result becomes

$$\begin{aligned} \nabla \cdot \vec{\alpha} = \left(\frac{\partial \alpha^i}{\partial y^k} + \alpha^m \Gamma^i_{km} \right) \delta^k_i &= \frac{\partial \alpha^i}{\partial y^i} + \alpha^m \Gamma^i_{im} \\ &= \frac{\partial \alpha^i}{\partial y^i} + \alpha^i \Gamma^m_{im} \quad , \end{aligned} \tag{57}$$

where the last equality comes from an interchange of m and i and an application of the torsionless property (Eq. 29). From Eq. 55, the Christoffel symbol sum is replaced to yield

$$\nabla \cdot \vec{\alpha} = \frac{\partial \alpha^i}{\partial y^i} + \frac{\alpha^i}{\sqrt{g}} \frac{\partial}{\partial y^i}(\sqrt{g}) = \frac{1}{\sqrt{g}} \frac{\partial}{\partial y^i}(\alpha^i \sqrt{g}) \quad , \tag{58}$$

which reduces to Eq. 56 when $\alpha^j = \delta^j_i$ for a fixed i.

Similarly, the divergence of the dyadic $\alpha = \alpha^{ij} \vec{e}_i \otimes \vec{e}_j$ is obtained from the gradient given in Eq. 49. With the dot product replacement, it becomes

$$\begin{aligned}
\nabla \cdot \alpha &= \left\{ \frac{\partial \alpha^{ij}}{\partial y^k} + \alpha^{rj}\Gamma^i_{kr} + \alpha^{ir}\Gamma^j_{kr} \right\} \vec{e}^k \cdot \vec{e}_i \otimes \vec{e}_j \\
&= \left\{ \frac{\partial \alpha^{ij}}{\partial y^i} + \alpha^{rj}\Gamma^k_{rk} + \alpha^{ir}\Gamma^j_{ir} \right\} \vec{e}_j \\
&= \left\{ \frac{\partial \alpha^{ij}}{\partial y^i} + \frac{\alpha^{ij}}{\sqrt{g}} \frac{\partial}{\partial y^i} (\sqrt{g}) + \alpha^{ir}\Gamma^j_{ir} \right\} \vec{e}_j \\
&= \left\{ \frac{1}{\sqrt{g}} \frac{\partial}{\partial y^i} (\alpha^{ij}\sqrt{g}) + \alpha^{ir}\Gamma^j_{ir} \right\} \vec{e}_j \quad ,
\end{aligned} \tag{59}$$

where dummy indices have been interchanged, the torsionless property has been applied, and Eq. 55 has been used.

The Laplacian of a Tensor

When the divergence operator (Eq. 50) is applied to the gradient (Eq. 47) of some tensor (Eq. 26), the composed operator

$$\Delta = \nabla \cdot \nabla \tag{60}$$

which is applied to the tensor is known as the Laplacian, and on surfaces, as the Laplace-Beltrami operator. It is a simple matter to check (with Eqs. 45 and 51) that Eq. 60 reduces to the standard Laplacian when Cartesian coordinates are assumed. To examine the application of Eq. 60, the Laplacian of a function f shall be computed in curvilinear coordinates. From Eq. 46, the gradient is

$$\nabla f = g^{mi} \frac{\partial f}{\partial y^m} \vec{e}_i \quad , \tag{61}$$

where the metric was used to lower (Eq. 18a) the index of the basis vector field. With the vector field coefficients α^i taken from Eq. 61, the divergence obtained in Eq. 58 becomes the Laplacian

$$\Delta f = \frac{1}{\sqrt{g}} \frac{\partial}{\partial y^i} \left(g^{mi} \frac{\partial f}{\partial y^m} \sqrt{g} \right) , \tag{62}$$

in curvilinear coordinates. Further applications to higher rank tensors (i.e., rank greater than 0) follows the same pattern and need not be pursued here.

The Identity Dyadic

The identity is defined to be the tensor which leaves other tensors unchanged when a dot product on either side is taken. The dyadic

$$I = \vec{e}^r \otimes \vec{e}_r , \tag{63}$$

is the identity. For notational simplicity, consider the vector field $\vec{\alpha} = \alpha^i \vec{e}_i$. Then $\vec{\alpha} \cdot I = \alpha^i \vec{e}_i \cdot \vec{e}^r \otimes \vec{e}_r = \alpha^i \delta^r_i \vec{e}_r = \alpha^i \vec{e}_i = \vec{\alpha}$ and $I \cdot \vec{\alpha} = \vec{e}^r \otimes \vec{e}_r \cdot (\alpha^i \vec{e}_i) = \alpha^i g_{ri} \vec{e}^r = \alpha^i \vec{e}_i = \vec{\alpha}$ where Eq. 18b was used to lower the index. For higher rank tensors (Eq. 26) the dot products occur respectively on the first and last factors in the basis. Since the algebra is an exact parallel to the vector field case it need not be repeated to establish that Eq. 63 is the desired identity. By using Eq. 18 to raise and lower indices, the identity dyadic can also be expressed in the alternative forms

$$I = g^{ri} \vec{e}_i \otimes \vec{e}_r = \vec{e}_i \otimes \vec{e}^i = g_{im} \vec{e}^m \otimes \vec{e}^i . \tag{64}$$

The Cross Product

In three dimensions, the cross product of the Cartesian unit vectors is defined by

$$\hat{u}_i \times \hat{u}_j = \epsilon^{ijk}\hat{u}_k \quad , \tag{65}$$

where ϵ^{ijk} vanishes when (i,j,k) is not a permutation of $(1,2,3)$ and is otherwise equal to the sign of the permutation. From Eq. 30 and the inverse of Eq. 24, the Cartesian unit vectors can be expressed as

$$\hat{u}_\ell = \frac{\partial y^j}{\partial x^\ell}\vec{e}_j = \frac{\partial x^\ell}{\partial y^i}\vec{e}^{\,i} \quad . \tag{66}$$

By substitution into Eq. 65, we have

$$\left(\frac{\partial x^i}{\partial y^m}\vec{e}^{\,m}\right) \times \left(\frac{\partial x^j}{\partial y^r}\vec{e}^{\,r}\right) = \epsilon^{ijk}\left(\frac{\partial y^\ell}{\partial x^k}\vec{e}_\ell\right) \quad ,$$

or

$$\frac{\partial x^i}{\partial y^m}\frac{\partial x^j}{\partial y^r}\vec{e}^{\,m} \times \vec{e}^{\,r} = \epsilon^{ijk}\frac{\partial y^\ell}{\partial x^k}\vec{e}_\ell \quad , \tag{67}$$

by linearity of cross product. When each side of Eq. 67 is multiplied by $(\partial y^p/\partial x^i)(\partial y^q/\partial x^j)$ and summed over i and j, the equation becomes

$$\delta^p_m\delta^q_r\vec{e}^{\,m} \times \vec{e}^{\,r} = \epsilon^{ijk}\frac{\partial y^p}{\partial x^i}\frac{\partial y^q}{\partial x^j}\frac{\partial y^\ell}{\partial x^k}\vec{e}_\ell \quad ,$$

or

$$\vec{e}^{\,p} \times \vec{e}^{\,q} = \frac{\epsilon^{pq\ell}}{\sqrt{g}}\vec{e}_\ell \quad , \tag{68}$$

from the definition of a determinant applied to A^{-1} in Eqs. 11 and 22. To interchange covariant and contravariant basis elements, Eq. 18 is applied

to yield

$$\vec{e}_i \times \vec{e}_j = g_{ip}g_{jq}\,\vec{e}^p \times \vec{e}^q = g_{ip}g_{jq}\,\frac{\varepsilon^{pq\ell}}{\sqrt{g}}\,\vec{e}_\ell = g_{ip}g_{jq}g_{\ell k}\,\frac{\varepsilon^{pq\ell}}{\sqrt{g}}\,\vec{e}^k \quad , \tag{69}$$

which motivates us to define $\varepsilon^{pq\ell}$ as a tensor with indices which can be raised and lowered with the metric. Then Eq. 69 becomes

$$\vec{e}_i \times \vec{e}_j = \frac{\varepsilon_{ijk}}{\sqrt{g}}\,\vec{e}^k \quad , \tag{70}$$

where $\varepsilon_{ijk} \equiv g_{ip}g_{jq}g_{k\ell}\varepsilon^{pq\ell} = g\,\varepsilon^{ijk}$ from the definition of determinants.

The Curl of a Vector Field

In three dimensions, the curl of a vector field $\vec{\alpha} = \alpha_j\vec{e}^j$ is obtained from the gradient

$$\nabla\vec{\alpha} = \left(\frac{\partial\alpha_j}{\partial y^i} - \alpha_k\Gamma^k_{ij}\right)\vec{e}^i \otimes \vec{e}^j \quad , \tag{71}$$

when the tensor product is replaced by a cross product. To indicate the replacement, the curl is denoted by $\nabla \times \vec{\alpha}$. Upon substitution from Eq. 68, it is given by

$$\nabla\times\vec{\alpha} = \frac{\varepsilon^{ijm}}{\sqrt{g}}\left(\frac{\partial\alpha_j}{\partial y^i} - \alpha_k\Gamma^k_{ij}\right)\vec{e}_m = \frac{\varepsilon^{ijm}}{\sqrt{g}}\,\frac{\partial\alpha_j}{\partial y^i}\,\vec{e}_m \quad , \tag{72}$$

where the Christoffel symbols vanished due to the antisymmetry for i and j in ε^{ijk} and the torsionless property (Eq. 29) of symmetric subscripts. In Eq. 72, the metric can be used to raise the subscript (Eq. 20) should the vector field have been given initially as $\vec{\alpha} = \alpha^r\vec{e}_r$. In addition, it is a simple matter to check that the curl given in curvilinear coordinates reduces to the usual Cartesian expression when Cartesian coordinates are inserted.

FORMS FOR THE EQUATIONS OF MOTION

In vector analytic notation, the equations of motion for a viscous compressible, heat conducting gas (c.f. [3]) are given by

$$\frac{\partial \rho}{\partial t} + \nabla\cdot(\rho\vec{v}) = 0 \quad . \tag{73a}$$

$$\frac{\partial E}{\partial t} + \nabla\cdot\{E\vec{v} - K\nabla T + \tau\cdot\vec{v}\} = 0 \quad . \tag{73b}$$

$$\frac{\partial}{\partial t}(\rho\vec{v}) + \nabla\cdot\{\rho\vec{v} \otimes \vec{v} + \tau\} = 0 \quad , \tag{73c}$$

where t is time, ρ is mass density, v is velocity, E is total energy per unit volume, $T = T(\rho,E,v)$ is temperature, K is thermal conductivity, and τ is the stress tensor. Respectively, the equations are mathematical statements for the conservation of mass, energy, and momentum where the first equation (Eq. 73a) is usually called the continuity equation. To complete the system, the stress tensor is given by

$$\tau = (p + \tfrac{2}{3}\mu\nabla\cdot\vec{v})I - 2\mu D \quad , \tag{74}$$

where $p = p(\rho,E)$ is the pressure, μ is the viscosity, I is the identity tensor, and D is the deformation tensor which is defined to be the symmetric part of the velocity gradiant. Alternative formulations arise, for example when the energy variable is changed or when turbulence is modeled either algebraically or with the addition of equations ([4] - [10]). However, to examine various forms of the equations for computational purposes, it is sufficient to consider the formulation just given since the pattern of operations on other formulations would be the same.

Contravariant Form

When the Navier-Stokes equations given in Eq. 73 are directly expressed in curvilinear coordinates with velocity $\vec{v} = v^i \vec{e}_i$, the form of the system is called contravariant to indicate the contravariant variables v^i. With the contravariant form, the equations are determined entirely by the metric which can be either depend or not depend upon time. The metric description is a determination in terms of physical distances and angles in the coordinate system which upon discretization for numerical computations translates into distances and angles for a coordinate mesh. In the case with a time independent metric, the vector analytic expressions in curvilinear coordinates are used directly. The continuity equation (Eq.73a) becomes

$$\frac{\partial}{\partial t}(\rho\sqrt{g}) + \frac{\partial}{\partial y^i}(\rho v^i \sqrt{g}) = 0 \quad , \tag{75}$$

from the divergence formula of Eq. 58 and a multiplication by $\sqrt{g}$. In the energy equation, Eq. 46 is applied to yield the temperature gradient $\nabla T = g^{ij}(\partial T/\partial y^j)\vec{e}_i$ where Eq. 18a was used to lower the basis index. When the dot product in the stress term is computed in the covariant basis (Eq. 26), the product expression becomes $\tau \cdot \vec{v} = (\tau^{ij}\vec{e}_i \otimes \vec{e}_j) : (v^r \vec{e}_r) = g_{rj}\tau^{ij} v^r \vec{e}_i$. Then the sum of $Ev^i\vec{e}_i$, the temperature gradiant term, and the dot product term is just the expression under the divergence in the energy equation (Eq. 73b) and is given by

$$\{Ev^i - g^{ij}K\frac{\partial T}{\partial y^j} + g_{rj}\tau^{ij}v^r\}\vec{e}_i \quad . \tag{76}$$

From the divergence formula of Eq. 58 and a multiplication by $\sqrt{g}$, the energy equation then becomes

$$\frac{\partial}{\partial t}(E\sqrt{g}) + \frac{\partial}{\partial y^i}\left\{\left(Ev^i - g^{ij}K\frac{\partial T}{\partial y^j} + g_{rj}\tau^{ij}v^r\right)\sqrt{g}\right\} = 0 \quad . \qquad (77)$$

In contrast to the continuity and energy equations, the divergence of a dyadic must be computed for the momentum equation. From the linearity properties (Eq. 25) of the tensor product, the dyadic becomes $\rho\vec{v}\otimes\vec{v} + \tau = \rho(v^i\vec{e}_i)\otimes(v^j\vec{e}_j) + \tau^{ij}\vec{e}_i\otimes\vec{e}_j = (\rho v^i v^j + \tau^{ij})\vec{e}_i\otimes\vec{e}_j$. When the formula (Eq. 59) for the divergence of a dyadic is applied, the momentum equation becomes

$$\left\{\frac{\partial}{\partial t}(\rho v^j\sqrt{g}) + \frac{\partial}{\partial y^i}\left[(\rho v^i v^j + \tau^{ij})\sqrt{g}\right] + (\rho v^i v^r + \tau^{ir})\sqrt{g}\Gamma^j_{ir}\right\}\vec{e}_j = 0, \quad (78)$$

after a multiplication by $\sqrt{g}$.

To complete the specification of both the energy and momentum equations, the stress tensor must be expanded in the covariant tensor product basis to obtain its coefficients τ^{ij}. With the exception of the deformation tensor D, all parts of the expansion have been obtained previously. The deformation tensor is defined to be the symmetric part of velocity gradiant which is obtained by an application of Eq. 48 and which is a dyadic. The dyadic is written as a linear combination of tensor products of vector fields. Each tensor product of vector fields $\vec{\alpha}\otimes\vec{\beta}$ can, however, be decomposed into a symmetric part $\frac{1}{2}[\vec{\alpha}\otimes\vec{\beta} + \vec{\beta}\otimes\vec{\alpha}]$ and an antisymmetric part $\frac{1}{2}[\vec{\alpha}\otimes\vec{\beta} - \vec{\beta}\otimes\vec{\alpha}]$ by a direct application of the linearity properties (Eq. 25). When the velocity gradient is obtained from Eq. 48 and when the symmetric part is taken on a term by term basis, the deformation tensor is given by

$$D = \tfrac{1}{2} g^{kr}\left(\frac{\partial v^i}{\partial y^k} + v^m \Gamma^i_{km}\right)\left(\vec{e}_r \otimes \vec{e}_i + \vec{e}_i \otimes \vec{e}_r\right)$$

$$= \tfrac{1}{2}\left\{g^{ki}\left(\frac{\partial v^r}{\partial y^k} + v^m \Gamma^r_{km}\right) + g^{kr}\left(\frac{\partial v^i}{\partial y^k} + v^m \Gamma^i_{km}\right)\right\} \vec{e}_i \otimes \vec{e}_r \quad , \tag{79}$$

where the second equality is the result of an interchange between the dummy indices of summation i and r. With interchange, the coefficients of the deformation tensor have symmetric indices. In general, when the symmetric part of any dyadic is taken in the given basis, the symmetry will become equivalent to a symmetry of indices. In particular, the identity dyadic (Eq. 64) is seen to be symmetric; hence, the stress tensor as a linear combination (Eq. 74) of symmetric tensors is also symmetric. From the identity in Eq. 64, the divergence formula of Eq. 58, and the deformation tensor in Eq. 79, the expansion of the stress tensor (Eq. 74) in the tensor product basis becomes

$$\tau = \tau^{ir}\, \vec{e}_i \otimes \vec{e}_r \quad , \tag{80a}$$

where

$$\tau^{ir} = g^{ir}\left\{p + \frac{2\mu}{3\sqrt{g}} \frac{\partial}{\partial y^k}(v^k \sqrt{g})\right\} - \mu\left\{g^{ki}\left(\frac{\partial v^r}{\partial y^k} + v^m \Gamma^r_{km}\right) + g^{kr}\left(\frac{\partial v^i}{\partial y^k} + v^m \Gamma^i_{km}\right)\right\}. \tag{80b}$$

When the tensor product in Eq. 80a is replaced by a dot product, the trace of the stress tensor is obtained. From Eq. 7, a Leibnitz rule, and Eq. 55, the trace is given by

$$\mathrm{tr}(\tau) = g_{ir}\tau^{ir} = \delta^r_r\left\{p + \tfrac{2}{3}\mu\left(\frac{\partial v^k}{\partial y^k} + v^k \Gamma^m_{km}\right)\right\} - 2\mu\delta^k_r\left(\frac{\partial v^r}{\partial y^k} + v^m \Gamma^r_{km}\right) = 3p, \tag{81}$$

where δ^r_r sums to 3 and the torsionless property (Eq. 29) has been used. The form of the trace is particularly simple and clearly has a physical interpretation.

When the stress tensor is to be applied in a numerical calculation, the form given in Eq. 80 is often not convenient since the solution variables are not separated in a concise manner. From an application of a Leibnitz rule and Eq. 55 to the velocity divergence in Eq. 80b and from Eq. 37 for the Christoffel symbols, the coefficients of the stress tensor become

$$\tau^{ir} = g^{ir}p + a^{ir}_k v^k + b^{ijr}_k \frac{\partial v^k}{\partial y^j} , \tag{82a}$$

where

$$a^{ir}_k = \mu\left(\frac{2}{3} g^{ir}\Gamma^m_{km} + \frac{\partial g^{ir}}{\partial y^k}\right) , \tag{82b}$$

and

$$b^{ijr}_k = \mu\left(\frac{2}{3} g^{ir}\delta^j_k - g^{ij}\delta^r_k - g^{rj}\delta^i_k\right) , \tag{82c}$$

after some algebraic manipulations. The form given here can then be directly coded into a computer algorithm by the conversion of the summation indices into computer loops. Moreover, the equations of motion in contravariant form can be constructed on the computer with the stress given in Eq. 82 in a term by term fashion with the index conversions. By an examination of the equations, the construction depends only upon the metric; hence, a general code can be made which accepts the metric data as input which is derived from a particular choice of coordinate system for a particular problem.

When time-dependent problems are considered, fixed spatial coordinates can be used only for cases where the boundaries of the flow region do not move in time. In cases where the region is rigidly moved such as in a rotating cascade of airfoils or more generally where the region is also continually changing shape, the fixed coordinates must be replaced by coordinates which are time-dependent. Relative to a Cartesian space-time frame $\hat{u}_0,\ldots,\hat{u}_n$, the time-dependent coordinates can be expressed in the form

$$\vec{x} = x^i(y^0,\ldots,y^n)\hat{u}_i \quad , \tag{83}$$

which is an extension of Eq. 2 obtained by the inclusion of time coordinates x^0 and y^0 and a corresponding increase in the range of summation i to go from 0 to the number of spatial dimensions, n. To obtain the contravariant form of the equations of motion for the time-dependent coordinates (Eq. 83), a time-dependent metric formulation must be used. Unlike the positive definite Cartesian formulation for Euclidian distance given in Eq. 13, the time-dependent metric comes from the Cartesian formulation for distance measured in terms of the Lorentz frame from special relativity ([11] - [13]) and is given by

$$(ds)^2 = c^2(dx^0)^2 - (dx^1)^2 - (dx^2)^2 - (dx^3)^2 \quad , \tag{84}$$

where c is the velocity of light in free space. With the metric coefficients g_{ij} derived from Eq. 84, the continuity and momentum equations can be obtained from a divergenceless stree-energy tensor which is given by

$$T = T_i^{\ k}\, \vec{e}^{\,i} \otimes \vec{e}_k \, , \tag{85a}$$

where

$$T_i^{\ k} = \rho v_i v^k + (p + \tfrac{2}{3}\mu \nabla \cdot \vec{v})\delta_i^k - \mu g^{mk}[(D_m \vec{v})_i + (D_i \vec{v})_m] \quad , \qquad (85b)$$

and indices, including summation convention indices, all start at 0. Since the metric derived from Eq. 84 depends upon the velocity of light and since the velocities in classical mechanics are much less, the Navier-Stokes equations can be retrieved as an approximation to the equations

$$\nabla \cdot T = 0 \quad , \qquad (86)$$

when terms of order c^{-2} relative to unity are discarded. The approximation to the 0th equation of the system of Eq. 86 is just the continuity equation which has the same form as Eq. 75; the remaining equations are the momentum equations in the respective coordinate directions. The advantage inherent in the approximation of the special relativistic equation (Eq. 86) is that the Navier-Stokes equations are expressed in a manner independent of any space-time coordinate system and are given a metric structure induced from the relativistic structure. The metric structure contains the classical Coriolis and centrifugal force effects in a clean and concise manner. That is, in addition to spatial changes, the metric contains all of the time-dependent variations of the cooridnate transformtions. The details of the approximation were presented in McVittie [14] for inviscid flows and in Walkden [15] for viscous flows, including an energy equation. When the equations are fully expanded with the intent of a direct conversion of indices into a computer algorithm as in the time independent case, the system of equations contains a large number of terms. Neither the derivation nor even the expression [16] shall be reproduced here.

Differential Forms

When a flow field with shock waves is to be numerically simulated, a conservation law form for the governing equations (Eq. 73) is often useful, especially in cases where the mesh is adapted to a shock wave; for then, the jump conditions can be satisfied merely by mesh alignments. Before methods are developed to cast the governing equations into a conservation law form, we shall develop the theory of differential forms which appear in the integral formulation for the conservation of fluid dynamic quantities. The simplest nontrivial differential form is given by the differential df of a function f and is called a differential 1-form or simply a 1-form. In any system of coordinates $\vec{y}$, the 1-form can be expanded to yield

$$df = \frac{\partial f}{\partial y^i} dy^i \quad , \tag{87}$$

by an application of a chain rule at any given point of the underlying space. The expansion can also be interpreted as the expression of the 1-form df in the space of 1-forms which has a basis composed of the coordinate 1-forms $dy^1,\ldots,dy^n$. From another viewpoint, the space of 1-forms is obtained by the application of an operator d to functions f which can be considered as 0-forms. In continuation, it would then remain to define the operator on successively higher order forms. At each stage the operator would increase the order by one, and the result of any application would lie in a space of differential forms constructed with a sufficient number of products of 1-forms. The products are known as exterior products and are chosen to model the orientations of the differential area elements which appear in integration. Since the needed linearity properties are already preserved with tensor products (Eq. 25), the exterior product is obtained as a modification in a manner that is similar to the construction of tensor products from cross

products. In particular, the tensor product $\otimes$ is replaced by the exterior product $\wedge$ which, in addition, allows the order of factors to be interchanged with changes in sign. For any two vectors $\vec{u}$ and $\vec{v}$, the interchange is given by the rule

$$\vec{u} \wedge \vec{v} = -\vec{v} \wedge \vec{u} \quad , \tag{88}$$

which is extended to higher order products by successive applications. From the rule, any product with repeated factors must clearly vanish. Consequently, for a space of dimension n, there can be at most n factors since an $(n+1)$st factor could be expressed as a linear combination of the first n. Moreover, with n linearity independent factors, a reordered product would differ from the original by the sign of the permutation that resulted. An important application of reordered products is in the definition of determinants. Suppose that a linear transformation is given by $\vec{z}_i = A_i^j \vec{w}_j$ for bases $\vec{z}_1,\ldots,\vec{z}_n$ and $\vec{w}_1,\ldots,\vec{w}_n$ related by the matrix (A_i^j). Then, by linearity and by successive applications of Eq. 88 we have

$$\begin{aligned} \vec{z}_1 \wedge \ldots \wedge \vec{z}_n &= \left(A_1^{j_1}\vec{w}_{j_1}\right) \wedge \ldots \wedge \left(A_n^{j_n} w_{j_n}\right) = \left[A_1^{j_1}\ldots A_n^{j_n}\right] \vec{w}_{j_1} \wedge \ldots \wedge \vec{w}_{j_n} \\ &= \operatorname{sgn}(j_1,\ldots,j_n)\left[A_1^{j_1}\ldots A_n^{j_n}\right] \vec{w}_1 \wedge \ldots \wedge \vec{w}_n = \det(A_i^j)\ \vec{w}_1 \wedge \ldots \wedge \vec{w}_n \ , \end{aligned} \tag{89}$$

where $\operatorname{sgn}(j_1,\ldots,j_n)$ is the sign of the permutation of $j_1,\ldots j_n$ from the ordering $1,\ldots,n$ and the last equality comes from the definition of a determinant (c.f. [17], [18]). When f in Eq. 87 is successively taken to be $x^1,\ldots,x^n$, there is a linear transformation between the bases of 1-forms. The relation between volume elements is then obtained from Eq. 89 and is

given by

$$dx^1 \wedge \ldots \wedge dx^n = \det\left(\frac{\partial x^i}{\partial y^j}\right) dy^1 \wedge \ldots \wedge dy^n = J\, dy^1 \wedge \ldots \wedge dy^n, \quad (90)$$

where J is the Jacobian from Eq. 5 which appears in volume integrals when coordinates are changed. From the relation, the volume elements are observed to comprise the one-dimensional space of n-forms. Since the exterior product with any more than n-factors would vanish, the space of n-forms is also the last non-trivial space in a sequence of spaces starting with 0-forms. Let A denote the space of 0-forms which can be taken as the collection of all infinitely differentiable functions over the underlying n-dimensional space. Let E denote the n-dimensional space of 1-forms which can be locally generated from a basis of coordinate 1-forms $dy^1,\ldots,dy^n$ with coefficients from A. In continuation, let $\Lambda^p E$ denote the space of p-forms which can be generated from a basis obtained by the formation of all possible p*th* degree exterior products of a basis for E. For example, when $p = 2$ and when the coordinate 1-forms dy^i are used, the basis for $\Lambda^2 E$ is given by $dy^i \wedge dy^j$ for $1 \leq i < j \leq n$. For uniformity of notation, p can be taken to start at 0 so that $\Lambda^0 E = A$ and $\Lambda^1 E = E$.

With the spaces of differential forms $\Lambda^p E$, the differential operator $d : \Lambda^0 E \to \Lambda^1 E$ defined in Eq. 87 can be extended to an operator $d : \Lambda^p E \to \Lambda^{p+1} E$ which is valid for $p = 0,1,2,\ldots$ and which satisfies the conditions

$$
\begin{aligned}
&\text{(i)} \qquad df = \frac{\partial f}{\partial y^i}\, dy^i \quad , \\
&\text{(ii)} \quad d(\alpha+\beta) = d\alpha + d\beta \quad \text{for } p = q \quad , \\
&\text{(iii)} \quad d(d\alpha) = 0 \quad , \\
&\text{(iv)} \quad d(\alpha \wedge \beta) = d\alpha \wedge \beta + (-1)^p \alpha \wedge d\beta \quad ,
\end{aligned}
\tag{91}
$$

for f in $\Lambda^0 E$, α in $\Lambda^p E$, and β in $\Lambda^q E$. The differential operator which operates on the exterior product spaces $\Lambda^p E$ and is defined by Eq. 91 is known as the exterior derivative [19]. The motivation for the definition can be seen from an application in terms of the arbitrary coordinates y^i where $\alpha = a_{i_1 \cdots i_p}\, dy^{i_1} \wedge \cdots \wedge dy^{i_p}$ and $\beta = b_{j_1 \cdots j_q}\, dy^{j_1} \wedge \cdots \wedge dy^{j_q}$. Both (i) and (ii) of Eq. 91 are clear. In (iii) if d vanishes on differntials, then

$$
d\alpha = \frac{\partial \alpha_{i_1 \cdots i_p}}{\partial y^k}\, dy^k \wedge dy^{i_1} \wedge \cdots \wedge dy^{i_p} \quad ,
$$

and

$$
\begin{aligned}
d(d\alpha) &= \frac{\partial^2 a_{i_1 \cdots i_p}}{\partial y^k \partial y^j}\, dy^j \wedge dy^k \wedge dy^{i_1} \wedge \cdots \wedge dy^{i_p} \\
&= \sum_{j<k} \left\{ \frac{\partial^2 a_{i_1 \cdots i_p}}{\partial y^k \partial y^j} - \frac{\partial^2 a_{i_1 \cdots i_p}}{\partial y^j \partial y^k} \right\} dy^j \wedge dy^k \wedge dy^{i_1} \wedge \cdots \wedge dy^{i_p},
\end{aligned}
\tag{92}
$$

which vanishes since the order of differentiation in the second derivatives is interchangeable. For condition (iv),

$$
\begin{aligned}
d(\alpha \wedge \beta) &= d\left(a_{i_1 \cdots i_p} b_{j_1 \cdots j_q} dy^{i_1} \wedge \cdots \wedge dy^{i_p} \wedge dy^{j_1} \wedge \cdots \wedge dy^{j_q}\right) \\
&= \left\{\frac{\partial a_{i_1 \cdots i_p}}{\partial y^k} b_{j_1 \cdots j_q} + a_{i_1 \cdots i_p} \frac{\partial b_{j_1 \cdots j_q}}{\partial y^k}\right\} dy^k \wedge dy^{i_1} \wedge \cdots \wedge dy^{j_q} \\
&= \left(\frac{\partial a_{i_1 \cdots i_p}}{\partial y^k} dy^k \wedge dy^{i_1} \wedge \cdots \wedge dy^{i_p}\right) \wedge \left(b_{j_1 \cdots j_q} dy^{j_1} \wedge \cdots \wedge dy^{j_q}\right) \\
&\quad + dy^k \wedge \left(a_{i_1 \cdots i_p} dy^{i_1} \wedge \cdots \wedge dy^{i_p}\right) \wedge \left(\frac{\partial b_{j_1 \cdots j_q}}{\partial y^k} dy^{j_1} \wedge \cdots \wedge dy^{j_q}\right) \\
&= d\alpha \wedge \beta + (-1)^p \alpha \wedge d\beta \quad ,
\end{aligned}
\tag{93}
$$

where the $(-1)^p$ is the result of the p interchanges required to bring dy^k through $dy^{i_1} \wedge \cdots \wedge dy^{i_p}$. On examination of the applications in terms of coordinates, it is evident that the chain rule can be used to prove that the exterior derivative is independent of coordinates. A rigorous discussion is given by Flanders [19] where, in addition, the exterior derivative is also presented over surfaces.

In three-dimensional Euclidian space with Cartesian coordinates (x^1, x^2, x^3), the curl of a vector field (A_1, A_2, A_3) is obtained from the exterior derivative of the 1-form

$$\alpha = A_1 dx^1 + A_2 dx^2 + A_3 dx^3 \quad , \tag{94a}$$

and is given by

$$d\alpha = \left(\frac{\partial A_3}{\partial x^2} - \frac{\partial A_2}{\partial x^3}\right) dx^2 \wedge dx^3 + \left(\frac{\partial A_1}{\partial x^3} - \frac{\partial A_3}{\partial x^1}\right) dx^3 \wedge dx^1 + \left(\frac{\partial A_2}{\partial x^1} - \frac{\partial A_1}{\partial x^2}\right) dx^1 \wedge dx^2 . \quad (94b)$$

Similarly, the divergence is obtained from the exterior derivative of the 2-form

$$\alpha = A_1 dx^2 \wedge dx^3 + A_2 dx^3 \wedge dx^1 + A_3 dx^1 \wedge dx^2 \quad , \quad (95a)$$

and is given by

$$d\alpha = \left(\frac{\partial A_1}{\partial x^1} + \frac{\partial A_2}{\partial x^2} + \frac{\partial A_3}{\partial x^3}\right) dx^1 \wedge dx^2 \wedge dx^3 \quad . \quad (95b)$$

In vector analysis, the curl and divergence given in the above form appeared when boundary integrals were converted to volume integrals by means of theorems under the names of Green, Divergence, and Stokes. In continuation with differential forms, there is one theorem which supercedes the vector analytic versions and is known as the generalized Stokes theorem. For a p-dimensional surface M and a $(p-1)$-form α, the theorem is given by

$$\int_{\partial M} \alpha = \int_M d\alpha \quad , \quad (96)$$

where ∂M is the boundary of M. From the generalized Stokes theorem, the boundary operator ∂ is clearly realted to the exterior derivative d. Since the boundary operator is only applied to surfaces such as M above, it is an entirely topological operator as opposed to d which operates on forms. The relationship, however, comes form the existence of a parallel

theory for ∂ under an extension that is similar to the development of d. The parallel theories are of precisely the same form but with different objects. This remarkable similarity is stated more precisely in the deRham theorem [19], [20].

Another parallel development of a simpler nature can also be used to relate differential forms to the covariant and contravariant basis elements considered in tensor analysis. In particular, the vector field of natural tangents $\vec{e}_j$ to coordinate curves in the y^j variable can be expressed as the differential operator

$$\vec{e}_j = \frac{\partial}{\partial y^j} \quad , \tag{97}$$

rather than its application to any arbitrary position vector as originally given in Eq. 3. For coordinates on non-Euclidian surfaces, the operator form is essential since position vectors cannot be readily defined. Moreover, any vector field is a first order operator since it is a linear combination of the operators given in Eq. 97. With the vector fields in operator form, the differential 1-forms can be defined by means of an inner product $< \ , \ >$. For any vector field W and any function f, let

$$< df, \vec{W} > \ \equiv \ \vec{W}(f) \quad .$$

In the case when $\vec{W} = \vec{e}_j$ and $f = y^i$ the inner product becomes

$$< dy^i \ , \frac{\partial}{\partial y^j} > \ = \ \frac{\partial y^i}{\partial y^j} = \delta^i_j \quad , \tag{99}$$

which is a duality statement similar to Eq. 17, establishing a parallel between the 1-forms dy^i and the contravariant basis elements $\vec{e}^i$.

Conservation Law Form

In a fixed region M of n-dimensional Euclidian space a quantity U is conserved as a function of time if the rate of change of U in M is equal to the negative sum of the flux ω of quantity U across the boundary ∂M. In the language of differential forms the conservation of U is expressed as

$$\frac{\partial}{\partial t}\int_M U \otimes dV = -\int_{\partial M} \omega \quad , \tag{100}$$

for an n-form dV as a volume element on M and for some (n-1)-form ω which is some function of U that describes the U-flux through ∂M. If $x^1, x^2, \ldots x^n$ are Cartesian coordinates ordered in such a way that $dV = dx^1 \wedge \ldots \wedge dx^n$ and is positive, then the flux can be expressed as

$$\omega = \sum_{i=1}^{n} (-1)^{i+1} F^i(U) \otimes dx^1 \wedge \ldots \wedge dx^{i-1} \wedge dx^{i+1} \wedge \ldots \wedge dx^n \quad , \tag{101}$$

where F^i denotes the flux in the direction x^i. When U is a vector quantity, the functions F^i are vectors in the same space and the form ω is known as a vector (n-1)-form. As an illustration, consider the two-dimensional case where the flux reduces to the 1-form

$$\begin{aligned} \omega &= (-1)^{1+1} F_1 \otimes dx^2 + (-1)^{1+2} F_2 \otimes dx^1 \\ &= F_1 \otimes dx^2 - F_2 \otimes dx^1 \quad . \end{aligned} \tag{102}$$

In Figure 5, a differential volume element is displayed with vertices A, B, C, and D. In going from A to B, $dx^2 = 0$ and dx^1 is positive which implies that the flux $\omega = -F_2 \otimes dx^1$ points in the negative x^2-direction for positive components of F_2. Along BC, $dx^1 = 0$, dx^2 is positive; and hence, the flux $\omega = F_1 \otimes dx^2$ points in the positive x^1-direction for positive components of F_1. In both cases, the flux is directed out of the volume element when it has positive components. A similar argument for CD and DA with negative values for dx^1 and dx^2 respectively leads to

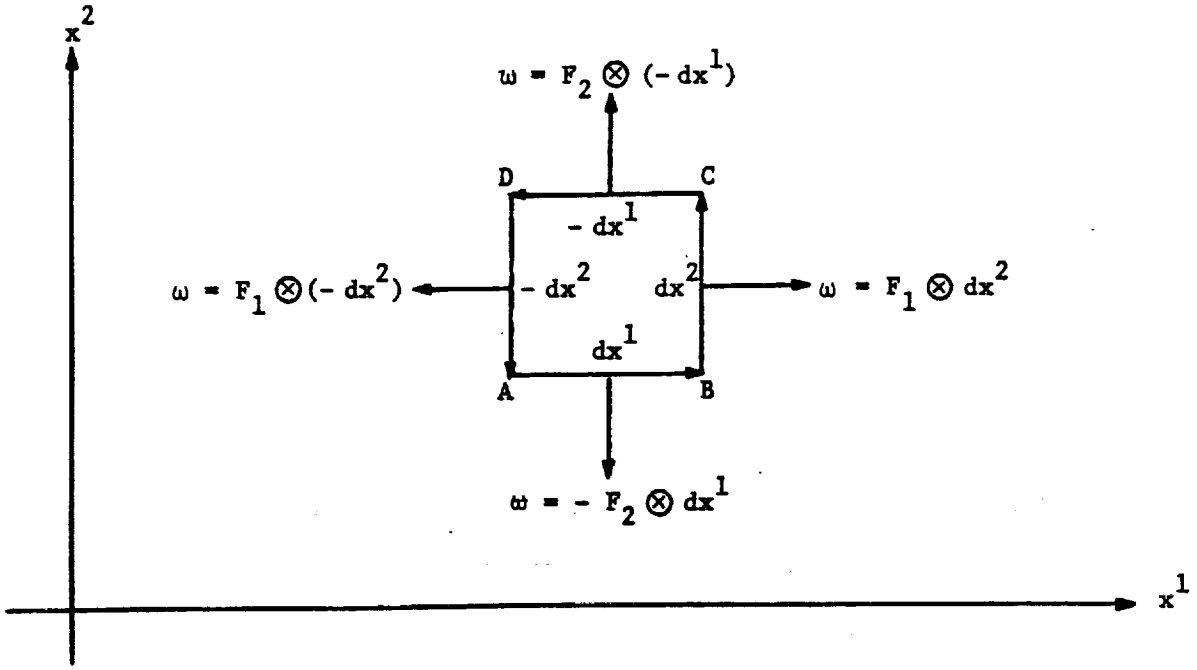

Figure 5. The flux through a differential volume element in two-dimensions

the same conclusion so that positive components of the F_i are always directed outward. With the general flux given in Eq. 101, an application of the general Stokes Theorem (Eq. 96) to the time conservation of U stated in Eq. 100 yields

$$\int_M \frac{\partial U}{\partial t} \otimes dV = \frac{\partial}{\partial t} \int_M U \otimes dV = -\int_{\partial M} \omega = -\int_M d\omega = -\int_M \sum_{i=1}^{n} \frac{\partial F^i}{\partial x^i} \otimes dV \quad , \qquad (103)$$

where the first equality follows from the time independence of M; the last, from an application of the exterior derivative in which the factor $(-1)^{i+1}$ accounted for the required interchanges to retrieve the volume element $dx^1 \wedge \ldots \wedge dx^n$ for each term. By allowing M to be arbitrary, we obtain

$$\frac{\partial U}{\partial t} + \sum_{i=1}^{n} \frac{\partial F^i}{\partial x^i} = 0 \quad , \qquad (104)$$

which is referred to as a system of conservation laws expressed in conservation law form. The termonology is clearly reasonable since each flux F^i appears under a derivative in its respective direction $\partial/\partial x^i$. An integration with respect to x^i then yields the exact differential dF^i which upon integration over the range of x^i reduces to a difference between boundary values. A number of numerical methods (e.g. [21], [22]) are adapted to conservation law forms so that the integration in x^i for F^i reduces to the same boundary values as in the differential case by means of a cross cancellation process such as a telescopic collapse of the flux terms.

Conservation Law Form from the Contravariant Equations

Since the stated governing equations for fluid dynamics (Eq. 73) are conservation laws for mass, energy, and momentum, it should be possible to express them in conservation law form for any system of coordinates. In the contravariant form with coordinates fixed in time, only the conservation of momentum (Eq. 78) is not in conservation law form (Eq. 104) since it has terms that are not differentiated. Such terms could be viewed as source terms in comparison to the remaining terms which appear in conservation form. The source terms, however, are due to spatially non-constant natural tangents $\vec{e}_i$ which arise from nonlinear coordinate curves and non-uniform rates of travel along coordinate curves even if they are linear. Otherwise, covariant derivaties of the $\vec{e}_i$ would vanish; as a result, Christoffel symbols would also vanish (Eq. 27); and consequently, the momentum equations would reduce to conservation law form. With nontrivial curvilinear coordinates, the nonvanishing source terms can be absorbed into a conservation law form obtained by a natural set of integrating factors. To observe which set is natural, the Christoffel symbols in the momentum equation (Eq. 78) are replaced by their coordinate expression in Eq. 32 to obtain

$$\left[\frac{\partial}{\partial t}\,(\rho v^j\sqrt{g}) + \frac{\partial \sigma^{ij}}{\partial y^i} + \sigma^{ir}\,\frac{\partial y^j}{\partial x^k}\,\frac{\partial^2 x^k}{\partial y^r \partial y^i}\right]\vec{e}_j = 0 \quad , \tag{105}$$

where $\sigma^{ij} = (\rho v^i v^j + \tau^{ij})\sqrt{g}$ for notational simplicity. By examination, the inverse Jacobian transformation is the natural integrating factor since the first order part of the last term would be removed and a Leibnitz form would result for spatial derivatives. The inverse Jacobian also corresponds with a change of basis from the curvilinear directions $\vec{e}_j$ to the Cartesian directions $\hat{u}_m$. From an application of Eq. 4, the result is given by

$$\left[\frac{\partial}{\partial t}\left(\rho v^j \sqrt{g}\,\frac{\partial x^m}{\partial y^j}\right)+\frac{\partial x^m}{\partial y^j}\,\frac{\partial \sigma^{ij}}{\partial y^i}+\sigma^{ir}\delta^m_k\,\frac{\partial^2 x^k}{\partial y^r \partial y^i}\right]\hat{u}_m = 0 \quad . \tag{106}$$

In the last term, the effect of the Kronecker symbol δ^m_k is to replace k by m. When, in addition, the dummy index r is replaced by j, the equation becomes

$$\left[\frac{\partial}{\partial t}\left(\rho v^j \sqrt{g}\,\frac{\partial x^m}{\partial y^j}\right)+\frac{\partial x^m}{\partial y^j}\,\frac{\partial \sigma^{ij}}{\partial y^i}+\sigma^{ij}\,\frac{\partial}{\partial y^i}\left(\frac{\partial x^m}{\partial y^j}\right)\right]\hat{u}_m = 0 \quad , \tag{107}$$

which, in component form, reduces to the system

$$\frac{\partial}{\partial t}\left(\rho v^j \sqrt{g}\,\frac{\partial x^m}{\partial y^j}\right)+\frac{\partial}{\partial y^i}\left(\sigma^{ij}\,\frac{\partial x^m}{\partial y^j}\right) = 0 \quad , \tag{108}$$

that is in conservation law form.

Conservation Law Form Relative to a Fixed Frame

An alternative method to obtain conservation law form for fixed coordinates is to use a fixed frame of reference. As can be noted, derivatives of a fixed frame vanish, and consequently, Christoffel symbols can be selectively removed to yield a conservation law form. In general, the nonconservative terms appear when the divergence is computed for a tensor of rank two or higher. On examination of the divergence operator given in Eq. 50, only the first tensor factor need not be expressed in the fixed frame. Let each covariant basis element $\vec{e}_i$ and each contravariant basis element $\vec{e}^k$ be expressed in terms of a fixed frame $\vec{f}_1, \vec{f}_2, \ldots, \vec{f}_n$ by the respective linear combinations $\vec{e}_i = A_i{}^j \vec{f}_j$ and $\vec{e}^k = A^{kj}\vec{f}_j$ which result since the fixed frame is a basis for R^n. Since $\vec{e}^k = g^{ki}\vec{e}_i = g^{ki}A_i{}^j\vec{f}_j = A^{kj}\vec{f}_j$, the coefficients

are related by $A^{kj} = g^{ki}A_i^{\ j}$ which implies that the rules for raising and lowering indices are followed; hence, we are justified in using the same sybmol, A, for both covariant and contravariant expressions. When the last $p+q-1$ factors of the general tensor in Eq. 26 are transformed into the fixed frame, the tensor is expressed in the form

$$\alpha = B^{ik_2\ldots k_p r_1\ldots r_q} \vec{e}_i \otimes \beta_{k_2\ldots k_p r_1\ldots r_q} , \qquad (109a)$$

where

$$B^{ik_2\ldots k_p r_1\ldots r_q} = \alpha^{ii_2\ldots i_p}_{\quad j_1\ldots j_q} A_{i_2}^{\ k_2}\ldots A_{i_p}^{\ k_p} A^{j_1 r_1}\ldots A^{j_q r_q} , \qquad (109b)$$

for coefficients and

$$\beta_{k_2\ldots k_p r_1\ldots r_q} = \vec{f}_{k_2} \otimes \ldots \otimes \vec{f}_{k_p} \otimes \vec{f}_{r_1} \otimes \ldots \otimes \vec{f}_{r_q} , \qquad (109c)$$

for the fixed tensor. Since the derivative of the fixed tensor (Eq. 109c) vanishes, the divergence is an exact parallel to the divergence of a vector field (Eqs. 52 - 58). In particular, the divergence is given by

$$
\begin{aligned}
\nabla \cdot \alpha &= \vec{e}^{m} \cdot D_m \left(B^{ik_2 \ldots r_q} \vec{e}_i \otimes \beta_{k_2 \ldots r_q} \right) \\
&= \vec{e}^{m} \cdot \left\{ \frac{\partial B^{ik_2 \ldots r_q}}{\partial y^m} \vec{e}_i + B^{ik_2 \ldots r_q} \Gamma^j_{mi} \vec{e}_j \right\} \otimes \beta_{k_2 \ldots r_q} \\
&= \left\{ \frac{\partial B^{ik_2 \ldots r_q}}{\partial y^m} \delta^m_i + B^{ik_2 \ldots r_q} \Gamma^j_{mi} \delta^m_j \right\} \otimes \beta_{k_2 \ldots r_q} \qquad (110) \\
&= \left\{ \frac{\partial B^{ik_2 \ldots r_q}}{\partial y^i} + B^{ik_2 \ldots r_q} \Gamma^j_{ji} \right\} \otimes \beta_{k_2 \ldots r_q} \\
&= \frac{1}{\sqrt{g}} \frac{\partial}{\partial y^i} \left(B^{ik_2 \ldots r_q} \sqrt{g} \right) \otimes \beta_{k_2 \ldots r_q} \; .
\end{aligned}
$$

On substitution into expressions for conserved quantities, conservation law form can be readily obtained, provided that $\sqrt{g}$ is independent of time and thus can be brought through any existing derivatives with respect to time. An example is given by a substitution into the momentum equation (Eq. 73c) to yield the conservation law form

$$
\left\{ \frac{\partial}{\partial t} \left(\rho v^i A_i^{\ k} \sqrt{g} \right) + \frac{\partial}{\partial y^i} \left[\left(\rho v^i v^j + \tau^{ij} \right) A_j^{\ k} \sqrt{g} \right] \right\} \vec{f}_k = 0 \; . \qquad (111)
$$

When the fixed frame is chosen to be the basis of natural tangent vectors to coordinate curves at some fixed point in space, the momentum equation in Eq. 111 reduces to the form derived by Vinokur [23] for application to each point on a coordinate mesh. About a mesh point $\vec{P}$, the functions $A_j^{\ k}$ need only be applied along coordinate curves, even though they should exist throughout the volume element surrounding $\vec{P}$. For $\vec{P} = (P^1, P^2, \ldots P^n)$, let $\vec{Q}_i = (P^1, \ldots, P^{i+1}, y^i, P^{i+1}, \ldots, P^n)$ be the variation only in the y^i coordinate direction for $i = 1,2,\ldots,n$. Then about $\vec{P}$ we have

$$\vec{e}_j(\vec{Q}_i) = A_j{}^k(\vec{Q}_i)\vec{e}_k(\vec{P}) \quad , \tag{112}$$

where $A_j{}^k(\vec{Q}_i)$ is a function of y^i which reduces to δ_j^k when $y^i = P^i$. Along the coordinate curve in the y^i variable, the covariant derivative can be expressed in terms of the $A_j{}^k$ by a substitution of Eq. 112 into its definition as a limit of difference quotients. With the substitution, the covariant derivative D_i of $\vec{e}_j$ is given by

$$\begin{aligned}(D_i\vec{e}_j)(\vec{P}) &= \lim_{\vec{Q}_i \to \vec{P}} \frac{\vec{e}_j(\vec{Q}_i) - \vec{e}_j(\vec{P})}{y^i - P^i} \\ &= \lim_{\vec{Q}_i \to \vec{P}} \left[\frac{A_j{}^k(\vec{Q}_i) - A_j{}^k(\vec{P})}{y^i - P^i}\right]\vec{e}_k(\vec{P}) \qquad (113) \\ &= \frac{\partial A_j{}^k}{\partial y^i}\vec{e}_k(\vec{P}) \quad .\end{aligned}$$

When the expression for the covariant derivative in Eq. 27 is evaluated at $\vec{P}$ and is inserted into Eq. 113, we have

$$\Gamma_{ij}^k = \frac{\partial A_j{}^k}{\partial y^i} \quad , \tag{114}$$

by linear independence. The point of evaluation $\vec{P}$ can be omitted from Eq. 114 since $\vec{P}$ can be an arbitrary point. In an anticipated numerical simulation with Eq. 112, there would be distinct conservation laws (Eq. 111) in correspondance with distinct mesh points. Consequently, such an application would be better suited to explicit numerical methods in order to avoid simultaneous multiple representations of the governing equations at each mesh point.

A Conservation Law Form Preserving Transformation Rule from Differential Forms

A more direct method to obtain conservation law form for physical conservation laws is to use differential forms rather than to modify the tensor form in the previous manners. In addition, to include time variations in both the solution variables and the coordinates, the flux of Eq. 101 is replaced by the n-form

$$\omega = \sum_{k=0}^{n} (-1)^k F^k(U) \otimes dx^0 \wedge \ldots \wedge \widehat{dx^k} \wedge \ldots \wedge dx^n \quad , \tag{115}$$

over (n+1)-dimensional space-time where x^0 denotes time, and for notational simplicity, the symbol $\widehat{dx^k}$ means that dx^k is deleted from the exterior product. For an arbitrary region M in space-time, the conservation of a quantity is equivalent to its flux through the boundary ∂M summing up to zero. From the general Stokes theorem (Eq. 96) we obtain

$$0 = \int_{\partial M} \omega = \int_M d\omega = \int_M \left(\sum_{i=0}^{n} \frac{\partial F^i}{\partial x^i} \right) \otimes dV \quad , \tag{116}$$

and the conservation law form

$$\sum_{i=0}^{n} \frac{\partial F^i}{\partial x^i} = 0 \quad , \tag{117}$$

since M was arbitrary. Since differential forms are independent of coordinates, the conservation law form in Eq. 117 can be obtained for different coordinate representations of ω and $d\omega$ by a mere application of the transformation rules for differential forms and exterior derivatives. When coordinates are changed to $y^0, y^1, \ldots, y^n$ the flux (Eq. 115) becomes

$$\omega = \sum_{k=0}^{n} (-1)^k F_k \otimes \left(\frac{\partial x^0}{\partial y^{j_0}} dy^{j_0}\right) \wedge \cdots \wedge \widehat{\left(\frac{\partial x^k}{\partial y^{j_k}} dy^{j_k}\right)} \wedge \cdots \wedge \left(\frac{\partial x^n}{\partial y^{j_n}} dy^{j_n}\right)$$

$$= \sum_{k=0}^{n} (-1)^k \left\{F_k \frac{\partial x^0}{\partial y^{j_0}} \cdots \widehat{\frac{\partial x^k}{\partial y^{j_k}}} \cdots \frac{\partial x^n}{\partial y^{j_n}}\right\} \otimes dy^{j_0} \wedge \cdots \wedge \widehat{dy^{j_k}} \wedge \cdots \wedge dy^{j_n} ,$$

(118)

which is in the original form of Eq. 115 but with extra indices summation, each of which goes from 0 to n. An application of the exterior derivative then yields

$$d\omega = \sum_{k=0}^{n} (-1)^k \frac{\partial}{\partial y^{j_k}} \left\{F_k \frac{\partial x^0}{\partial y^{j_0}} \cdots \widehat{\frac{\partial x^k}{\partial y^{j_k}}} \cdots \frac{\partial x^n}{\partial y^{j_n}}\right\} \otimes dy^{j_k} \wedge dy^{j_0} \wedge \cdots \wedge \widehat{dy^{j_k}} \wedge \cdots \wedge dy^{j_n}$$

$$= \sum_{k=0}^{n} \frac{\partial}{\partial y^{j_k}} \left\{F_k \frac{\partial x^0}{\partial y^{j_0}} \cdots \widehat{\frac{\partial x^k}{\partial y^{j_k}}} \cdots \frac{\partial x^n}{\partial y^{j_n}}\right\} \otimes dy^{j_0} \wedge \cdots \wedge dy^{j_n}$$

$$= \sum_{k=0}^{n} \frac{\partial}{\partial y^{j_k}} \left\{F_k \, \mathrm{sgn}(j_0,\ldots j_n) \frac{\partial x^0}{\partial y^{j_0}} \cdots \widehat{\frac{\partial x^k}{\partial y^{j_k}}} \cdots \frac{\partial x^n}{\partial y^{j_n}}\right\} \otimes dy^0 \wedge \cdots \wedge dy^n ,$$

(119)

where $\mathrm{sgn}(j_0,\ldots j_n)$ is the sign of the permutation of $j_0, j_1, \ldots, j_n$ from the ordering $0,1,\ldots,n$. To simplify the exterior derivative we note that

$$\mathrm{sgn}(j_0,\ldots j_n) \frac{\partial x^0}{\partial y^{j_0}} \cdots \widehat{\frac{\partial x^k}{\partial y^{j_k}}} \cdots \frac{\partial x^n}{\partial y^{j_n}} , \qquad (120)$$

is just the cofactor of the matrix $(\partial x^m/\partial y^\ell)$ at the k*th* row and j_k*th* column for fixed k and j_k. One way to see this fact is to note that the expression is the determinant of the full $(n+1) \times (n+1)$ matrix with unity in the (k,j_k)*th* position and zeros for the remaining positions in the k*th* row and j_k*th* column. By Cramer's rule [17], the expression then reduces to $(\partial y^{j_k}/\partial x^k)J$ where J is the Jacobian, $\det((\partial x^\ell/\partial y^m))$. On substitution, Eq. 119 becomes

$$d\omega = \frac{\partial}{\partial y^{j_k}} \left\{ F_k \frac{\partial y^{j_k}}{\partial x^k} J \right\} \otimes dy^0 \wedge \ldots \wedge dy^n \quad , \tag{121}$$

which leads to the simple conservation law form

$$\frac{\partial}{\partial y^i} \left\{ F_k \frac{\partial y^i}{\partial x^k} J \right\} = 0 \quad , \tag{122}$$

where the dummy index of summation j_k was replaced by i. If $z^m = z^m(y^0,\ldots,y^n)$ is another transformation but with a Jacobian H, then the same derivation leads to the conservation law form

$$\frac{\partial}{\partial z^m} \left\{ \left(F_k \frac{\partial y^i}{\partial x^k} J \right) \frac{\partial z^m}{\partial y^i} H \right\} = 0 \quad , \tag{123}$$

which reduces to

$$\frac{\partial}{\partial z^m} \left\{ F_k \frac{\partial z^m}{\partial x^k} (JH) \right\} = 0 \quad , \tag{124}$$

where JH is the Jacobian of the composed transformation. Thus, as would be expected from the coordinate invariant formulations from differential

forms, the result is a transformation rule which preserves conservation law form. From another point of view, Eq. 122 can also be derived directly from manipulations with calculus on a case by case basis. One example is given in Viviand [24] where Eq. 122 was derived in two-dimensions with x^i as Cartesian coordinates and y^i as curvilinear coordinates. With the coordinate invariant formulation in terms of differential forms and the resulting transformation rule, the remaining question is whether or not conservation laws exist in a given system. This topic has been examined by Eiseman and Stone [25] - [27] for both local and global conservation laws in spaces which can be more general than Euclidian spaces.

Frame Field Formulations

In a collective sense, a basis of vector fields is referred to as a frame field. For curvilinear coordinates, the fundamental frame field is the basis of natural tangents (Eq. 3) to coordinate curves since it determines the coordinate metric (Eq. 7). As the frame field which contains the basic metric information for the coordinates, we shall call it the coordinate frame. When curvilinear coordinates are used to obtain a discrete mesh for the numerical simulation of a flow field, the coordinate frame is also the frame which is properly aligned with the discretization. Consequently, in a discrete analysis, any other frame fields would have to be related to the coordinate frame. From this vantage point, the contravariant formulation would then be the most natural one to select since the coordinate frame is used for the velocity vector, the derivative directions, and the stress tensor. In the course of a numerical solution, however, the geometric properties of the coordinate mesh may not bear any relation to the physical properties of the

flow. For example, if a mesh for a constant uniform flow is chosen to be rectilinear, to be aligned with the flow, and to expand in the flow direction, then the natural tangents would also expand in length. As a result, a trivial flow field ($\vec{v}$ = const.) is computed with nontrivial variables (v^i). If, in addition, the coordinates were curved and not aligned with the flow, then the example would be even more complicated. In the example of uniform or locally uniform flow, the errors are clearly caused by the mesh geometry in the given region. To minimize the errors due to such an inconsistency between the geometric properties of the mesh and the physical properties of the flow, frame fields other than the coordinate frame should be used. In the case with the rectilinear mesh that expanded in the direction of alignment with a uniform flow, the coordinate frame can be replaced by a normalized coordinate frame in the equations of motion. The normalized frame is given by the unit vector fields $\vec{e}_i/\sqrt{g_{ii}}$ for each coordinate direction y^i. Relative to the frame, the velocity field is given by solution components which are actual velocity magnitudes in the respective coordinate directions. Since discrete representations of derivatives will vanish for constants, the uniform flow field will then be reproduced without an error from the mesh geometry. In the more complex case where a fully curvilinear mesh is used, the normalization of the coordinate frame, however, will not remove the geometric error from the mesh. To remove the geometric error, the velocity should be expanded relative to an orthonormal frame where one of its constituent vector fields is aligned with the uniform flow. As before, the velocity coefficients then become actual velocity magnitudes in the respective directions and the

uniform flow is again retrieved. In flows past isolated airfoils, the flow approaches uniformity away from the airfoil. For moderate angle of attack, the approach can be rather rapid. Consequently, the orthonormal frame for velocity components can be expected to yield accurate results. Numerical evidence ([28] - [29]) supports the expectations. In the numerical studies, the choice of orthonormal frame was referred to as the application of Cartesian directions since only a Cartesian coordinate discription of velocity was used. Form the more general viewpoint, the frame field formulation was introduced in [30] and the previous Cartesian frame was called a particular case of a solution frame since the velocity or momentum components are solution variables and since more general frame fields are needed for alignment with flows which undergo a change in direction. Such directional changes commonly occur with cascades of compressor or turbine blades. Within the context of frame fields [30], there are also derivative and approximation frames. In a number of special cases, a frame field has been selected to align solution variables, derivatives, or equations with a given direction of interest. In Jameson's [31] generalization of the type-dependent differencing due to Murman and Cole [32], a specific derivative frame was employed. This frame, known as the Frenet frame [1], consisted of vector fields that are tangent, normal, and binormal to the streamlines. The result was called the "rotated difference molecule". This same frame was also used for both a derivative and a solution frame by Lakshminarayana and Horlock [33] - [34] who applied it to the vorticity equation (for both stationary and rotating systems). Their analysis consisted of successive application of dot products and differentiation rules for the frame field; the differentiation rules consisted of the Frenet formulas along with

other formulas for the normal and binormal directions. The results were a sequence of interesting generalizations of the previous formulations for secondary flow.

To illustrate the application of frame fields for the numerical simulation of turbomachinery flow fields, a two-dimensional cascade of turbine blades, depicted in Figure 6, shall be considered.

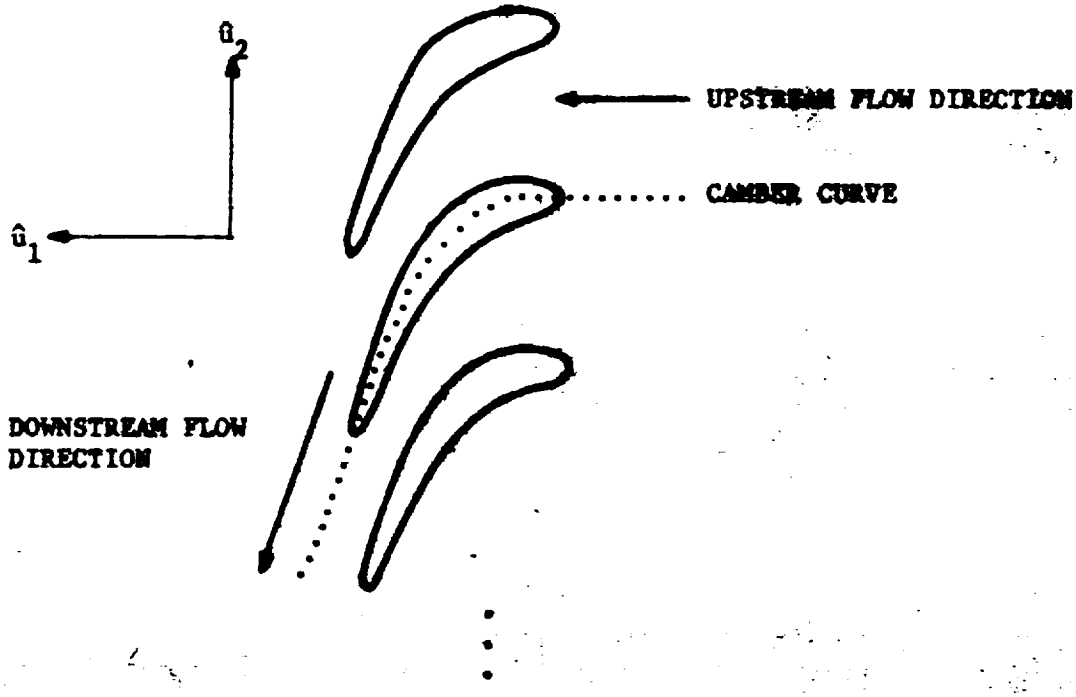

Figure 6: A Typical Cascade of Turbine Blades

In the figure, a camber curve, denoted by the dotted curve, is illustrated as an extension of the turbine blade camber line into both upstream and downstream directions as a smooth curve. In a parallel to the case with isolated airfoils, the cascade flow field directions should be roughly aligned with the camber curve tangent for each given x^1 location.

Consequently, the field of orthonormal frames consisting of unit normals and tangents to the camber curve can be expected to increase the accuracy of a numerical flow field simulation. If the camber curve is given in the form $x^2 = h(x^1)$ for some function h, then the unit tangent and normal are given by

$$\hat{f}_1(x^1) = A\left\{\hat{u}_1 + \frac{dh}{dx^1}\,\hat{u}_2\right\} \quad , \tag{125a}$$

and

$$\hat{f}_2(x^1) = A\left\{-\frac{dh}{dx^1}\,\hat{u}_1 + \hat{u}_2\right\} \, , \tag{125b}$$

respectively for all x^2 values and for the normalization factor

$$A = \left\{1 + \left(\frac{dh}{dx^1}\right)^2\right\}^{-\frac{1}{2}} \quad . \tag{125c}$$

Of the two possible choices for the normal vector (Eq. 125b) corresponding to the two sides of the camber curve h, the upward pointing one was selected as can be observed from the positive contribution in the $\hat{u}_2$ direction. In the compact summation convention notation, the frame field attached to the camber curve can be written in the form $\hat{f}_m = f_m^k \hat{u}_k$ where the coefficients f_m^k are taken from Eq. 125. To relate the frame field to the coordinate frame, Eq. 30 is applied to yield

$$\hat{f}_m = f_m^k \frac{\partial y^j}{\partial x^k}\,\vec{e}_j \quad . \tag{126}$$

The inverse expression is obtained from the inverse $\hat{u}_i = B_i^k \hat{f}_k$ to Eq. 125 where the coefficients are found by Cramer's rule to be $B_1^1 = B_2^2 = 1$ and $B_2^1 = -B_1^2 = dh/dx^1$. From an application of the successive inverse $(\partial x^i/\partial y^r)B_i^m$ to Eq. 126, we obtain

$$\vec{e}_r = \frac{\partial x^i}{\partial y^r} B_i^m \hat{f}_m \quad , \tag{127}$$

by use of the inverse relationships $B_i^m f_m^k = \delta_i^k$ and $(\partial x^i/\partial y^r)(\partial y^j/\partial x^i) = \delta_r^j$. With the transformation rule for the frames given by Eqs. 126 and 127, there is also a transformation for the velocity components in each frame. The velocity is given by $\vec{v} = v^r \vec{e}_r$ for contravariant components v^r and by $\vec{v} = w^m \hat{f}_m$ for camber frame components w^m. A substitution from Eq. 127 then leads to

$$w^m = v^r \frac{\partial x^i}{\partial y^r} B_i^m \quad , \tag{128a}$$

by linear independence; a substitution from Eq. 126, to

$$v^j = w^m f_m^k \frac{\partial y^j}{\partial x^k} \quad . \tag{128b}$$

By successive applications of Eq. 128b, the velocity components in the contravariant form of the equations of motion can be expressed in camber frame components w^m which are roughly aligned with the flow by construction. Since the solution variables are coefficients relative to the camber frame, the camber frame is being used as a solution frame in the resultant expressions. To convert back to the coordinate frame, successive applications of Eq. 128a

would be required. In the above case, only the solution variables are given relative to the camber frame; the derivatives, however, are still in the coordinate frame as can be observed from the operator form of the natural tangents (Eq. 97). The derivative frame can also be changed to the camber frame or any other convenient frame. When the change is into the camber frame, Eq. 127 is converted into the operator form

$$\frac{\partial}{\partial y^r} = \frac{\partial x^i}{\partial y^r} B_i^m \frac{\partial}{\partial z^m} \quad , \tag{129}$$

where z^m are local coordinates about any fixed point which has the camber frame as its coordinate frame. By substitutions from Eq. 129, all derivatives can be expressed in camber frame directions in all possible equations. When the substitutions are made, a conservation law form

$$\frac{\partial G_k}{\partial y^k} = 0 \quad , \tag{130}$$

is preserved only when the conservation law preserving transformation rule (Eq. 122) is applied to yield

$$\frac{\partial}{\partial z^i}\left\{ G_k \frac{\partial z^i}{\partial y^k} H \right\} = 0 \quad , \tag{131a}$$

where

$$H = \det\left(\frac{\partial y^j}{\partial z^m}\right) = \det\left(f_m^k \frac{\partial y^j}{\partial x^k}\right) \quad , \tag{131b}$$

the last equality of which comes form the operator form of Eq. 126. When the transformation rule is originally applied to preserve conservation law

form (Eq. 117) for a change from Cartesian coordinates x^i into curvilinear coordinates y^j, the fluxes in Eq. 130 are given by

$$G_k = F_j \frac{\partial y^k}{\partial x^j} J \quad , \tag{132a}$$

where

$$J = \det\left(\frac{\partial x^i}{\partial y^j}\right) \quad , \tag{132b}$$

from an observation of Eq. 122. On substitution, the conservation law form then becomes

$$\frac{\partial}{\partial z^i}\left\{\left(F_j \frac{\partial y^k}{\partial x^j} J\right)\frac{\partial z^i}{\partial y^k} H\right\} = 0 \quad , \tag{133}$$

or

$$\frac{\partial}{\partial z^i}\left\{F_j \frac{\partial z^i}{\partial x^j} JH\right\} = 0 \quad . \tag{134}$$

A simplification can be obtained from the product rule for determinants which on application to the product in Eq. 134 yields

$$JH = \det\left(\frac{\partial x^i}{\partial y^j} f_m^k \frac{\partial y^j}{\partial x^k}\right) = \det\left(\delta_k^i f_m^k\right) = \det\left(f_m^i\right) = 1 \quad ,$$

where the last equality follows from Eq. 125. From the operator form of Eq. 127, the derivative of z^i in Eq. 133 is given by

$$\frac{\partial z^i}{\partial y^k} = \frac{\partial x^r}{\partial y^k} B_r^i \tag{136}$$

with a change of indices. By substitution

$$\frac{\partial z^i}{\partial x^j} = \frac{\partial y^k}{\partial x^j}\frac{\partial z^i}{\partial y^k} = \frac{\partial y^k}{\partial x^j}\frac{\partial x^r}{\partial y^k}B^i_r = \delta^r_j B^i_r = B^i_j \quad . \tag{137}$$

When the expressions from Eqs. 135 and 137 are inserted into Eq. 134, the conservative form reduces to

$$\frac{\partial}{\partial z^i}\left\{F_j B^j_i\right\} = 0 \quad , \tag{138}$$

where the derivative with respect to z^i is related to the operator form of Eq. 126 which, for completeness, is given by

$$\frac{\partial}{\partial z^i} = f^k_i \frac{\partial y^m}{\partial x^k}\frac{\partial}{\partial y^m} = f^k_i \frac{\partial}{\partial x^k} \quad , \tag{139}$$

with an interchange of the dummy indices i and m for the first equality and an application of the chain rule for the second. On examination of Eqs. 138 and 139, the conservation law form preserving transformation rule of Eq. 122 could have been established for frame fields and applied directly. In the case just considered, the transformation between two orthonormal frames had a determinant of unity (Eq. 135), as could be expected for such transformations which are either just ivolutions or rotations.

The Approximation Frame

In addition to the solution and deirvative frames, an approximation frame has been derived [30] to unify the class of unidirectional flow approximations which lead to spatial marching algorithms for the Navier-Stokes equations. The class of approximations had developed over the past decade [35] - [47] as a means to study three-dimensional steady-state flows (incompressible, compressible, subsonic supersonic, etc.) in cases where the flow was assumed to be unidirectional. A motivation for this assumption was derived from the experimentally observable fact that without abrupt changes in geometry a high Reynolds number flow is dominated by only upstream conditions. Here, small disturbances in the primary direction tend to decay quickly. Consequently, a suitable approximation can and has been assumed to produce a well-posed system of governing equations from which a stepwise integration can successfully be applied to a given set of initial conditions. The rate of success with numerical computations tends to support this assumption. As in boundary layer theory, the approximations prior to the approximation frame were obtained by an examination of the relative order of magnitude of each term on an equation by equation basis. Unlike boundary layer theory, these estimates only neglected the diffusive flux in the assumed primary direction. The net result was that the approximate governing equations contained the information which was necessary to accurately model secondary flow phenomena. In addition the approximations, although similar in concept, were each different; the primary differences came from the chosen system of conservation laws (e.g., the transport of momentum, vorticity, energy, etc.) and from the geometric properties associated with each particular problem.

These differences also pointed to the fact that each of the order of magnitude approximations were too specialized to obtain an approximation which was valid for all cases where a primary flow direction exists.

The physical properties, associated with a primary flow direction, depend upon the fundamental constitutive relationship of a fluid. For this reason, the approximation presented in [30] was a direct approximation of the stress tensor which was clearly a statement about the constitution of the fluid. Consequently, such an approximation is independent of the choice of basic conservation laws governing transport phenomena. Moreover, the approximation is performed in a manner which preserves the tensor character of the stress. Consequently, the approximation is also independent of coordinates. In this manner, the limitations of the order of magnitude approximations are overcome. With the added generality, it should be noted that some terms of negligible size are retained. However, benefits from the added generality can outweigh by far the expense of including these terms. Such benefits are reflected in the wider range of applicability for a specific algorithm and in the quality of an approximation which can easily be increased because of the added flexibility.

To suitably approximate the stress tensor, only the viscous part will be considered since it is the diffusive fluxes which are to be approximated. For subsonic cases, the remaining part of the stress tensor (the pressure field) must be treated carefully. This includes cases where there are both subsonic and supersonic regions. On the viscous stress, the approximation frame is used to determine which parts are to be removed; hence, which parts should contribute little to a flow with an assumed primary direction. To start the construction, this direction is assumed to be given in the form of

of a vector field $\vec{\alpha}_3$ which identifies a primary direction at each spatial point. Then $\vec{\alpha}_3$ can be extended to an orthogonal triple of vectors $\vec{\alpha}_1$, $\vec{\alpha}_2$, $\vec{\alpha}_3$ to form a frame at each spatial point. This extension must be accomplished in a smooth enough fashion over the whole flow field so that at least one continuous derivative can be taken. The required differentiability occurs because of the requirement to differentiate the components of the stress tensor as they would occur in the conservation laws for momentum, vorticity, or energy. From the construction, a smooth field of orthogonal frames is obtained such that $\vec{\alpha}_3$ is aligned with the assumed primary flow direction and $\vec{\alpha}_1$, $\vec{\alpha}_2$ span orthogonal transverse planes. Altogether, this is the desired approximation frame in which a differential viscous stress cube can be formed at each spatial point. An illustration is given in Figure 7 where the tensor components $\vec{\sigma}^{ij} = \sigma^{ij}\, \vec{\alpha}_i \otimes \vec{\alpha}_j$ are displayed for the viscous part of the stress tensor σ which is given by

$$\sigma = \sigma^{ij}\, \vec{\alpha}_i \otimes \vec{\alpha}_j \tag{140}$$

in the approximation frame tensor product basis. The resulting components of viscous stress on a cube surface are either aligned with or are orthogonal to the primary direction. Consequently, the force balances represented by the Navier-Stokes equations are effectively separated into three mutually exclusive directions so that approximations in any given direction do not directly affect other directions. That is, a force in any one of the directions does not project nontrivially onto the other two remaining directions. If the equations of motion were written for the isolated cube, then the stress components would only contribute to the force balance in their respective

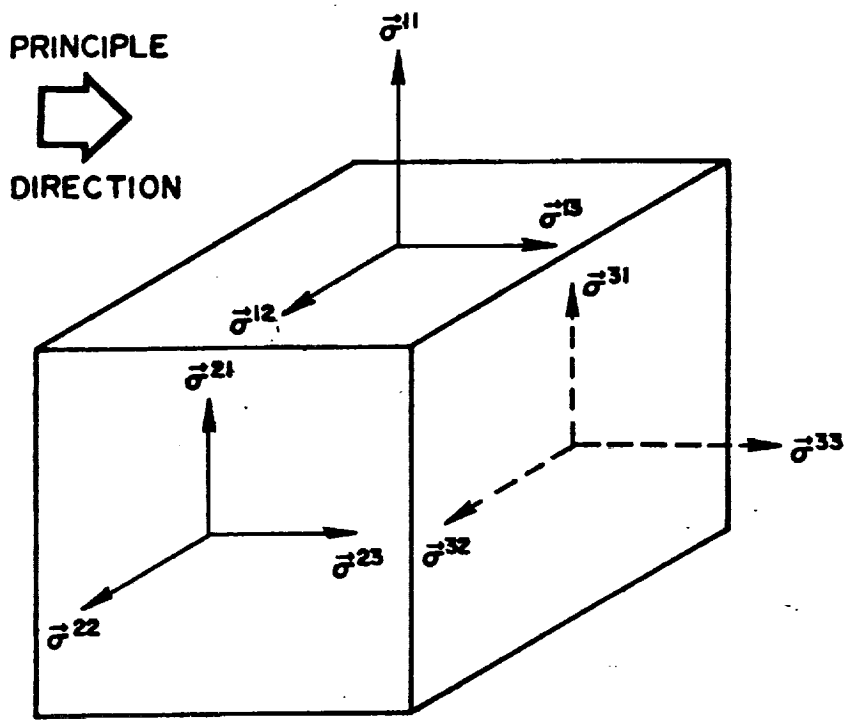

$$\vec{\sigma}^{ij} = \sigma^{ij}\vec{\alpha}_i \otimes \vec{\alpha}_j$$

Approximation = $\vec{\sigma}^{3i} = 0$ for $i = 1, 2, 3$

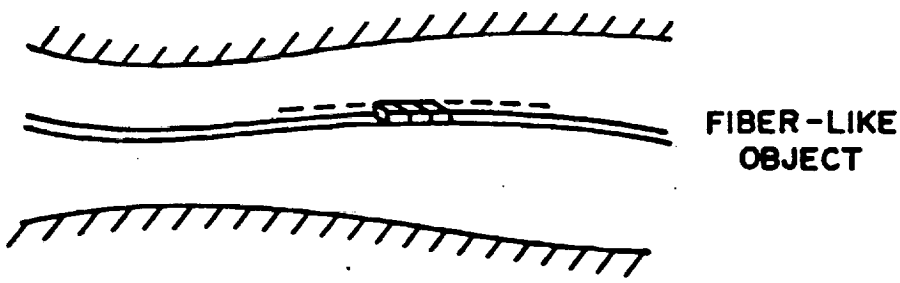

Figure 7. Viscous Stress Cube. The resulting tensor is non-symmetric and the effective differential element is a fiber-like object.

directions. However, in the primary direction $\vec{\alpha}_3$, the viscous contribution σ^{33} is expected to add little to the strong convective forces; hence, this contribution is ignored, and as a result, the α_3-direction momentum balance is not elliptic in character. In addition, for the $\vec{\alpha}_1$ and $\vec{\alpha}_2$ directions the contribution of the viscous shearing stresses σ^{31} and σ^{32} are also small relative to convective forces; hence, they also are ignored, and as a result, the respective momentum balances each are not elliptic in character. By contrast, the symmetric counterparts σ^{13} and σ^{23} each add to the force balance in the primary direction, and since they are the primary mechanism for the viscous retardation of the flow they are significant; hence, they cannot be neglected. Due to the orthogonality of the approximation frame, the force balances are mutually exclusive. Moreover, by joining existing cubes along transverse faces, effectively longer and longer viscous stress cubes can be formed. On a differential level, this is possible since the total assumption is that viscous forces on transverse faces are negligible. As a conceptual device, these forces can be considered on a fiberlike object which is aligned with the assumed primary direction. From this viewpoint, only internal viscous forces within the fiber are neglected. That is, the fiber has no stiffness; therefore, the only balance against the convective forces is due to the shearing stress along its boundary. This is particularly appropriate when the fiber is in the boundary layer since a no-slip condition causes the fluid to decelerate from viscous forces and come to rest at the walls (see Fig. 7).

In the approximation frame, the approximation of the viscous part of the stress tensor is given by the assumption that the components σ^{3j} are

negligible relative to the convective forces for $j = 1,2,3$. When the assumption is applied, the approximate stress tensor $\tilde{\sigma}$ is expressed by

$$\tilde{\sigma} = \tilde{\sigma}^{ij} \vec{\alpha}_i \otimes \vec{\alpha}_j = (1 - \delta_i^3)\sigma^{ij} \vec{\alpha}_i \otimes \vec{\alpha}_j \quad . \tag{141}$$

Unlike the original viscous stress (Eq. 140), the approximation (Eq. 141) is not symmetric, as could be expected from the directional bias. When the approximate stress is used in place of the original stress, unidirectional viscous approximations are obtained for the conservation of momentum, energy, and vorticity. A unidirectional system of governing equations, obtained from the approximate stress, is not elliptic and can be solved by a forward marching procedure. In cases involving subsonic flow, the elliptic character which has been removed must be replaced. The replacement can be in the form of viscous perturbation pressure field for a known marching direction pressure gradient (e.g. [39]) or in the form of an iterative cycle where a simple elliptic potential equation is solved by some efficient elliptic solver and the viscous unidirectional equations are spatially marched (e.g. [42], [43]). In the latter case, the velocity is split into rotational and irrotational parts and the pressure is defined solely in terms of the irrotational part. In the former case, the known pressure gradient is often taken from secondary flow theory [33] - [34].

Before the approximation as presented in Eq. 141 can be applied, it must be put into a form which is consistent with the chosen system of conservation laws governing the transport phenomena. Within the conservation laws, the stress tensor is usually expressed in component form where the components

are the coefficients of the stress in a tensor product basis determined by some frame field $\vec{\beta}_1, \vec{\beta}_2, \vec{\beta}_3$. This frame field would probably be the solution frame to be compatible with other parts of the momentum balance. To achieve the desired consistency, the stress components must be taken from the β-frame, transformed into the α-frame, approximated in the α-frame by Eq. 141, and then transformed back into the β-frame so that the results can be used. For notation, let w^{ij} be the coefficients of the viscous part of the stress tensor in the β-frame, let $\vec{\alpha}_j = F_j^i \vec{\beta}_i$ be the transformation into the α-frame, and let $\vec{\beta}_i = G_i^k \vec{\alpha}_k$ be the inverse transformation back into the β-frame. With the given notation, the transformation into the α-frame is given by

$$w^{km} \vec{\beta}_k \otimes \vec{\beta}_m = w^{km} G_k^i G_m^i \vec{\alpha}_i \otimes \vec{\alpha}_j \quad , \tag{142}$$

from the linearity properties of the tensor product (Eq. 25). An application of the approximation from Eq. 141 with $\sigma^{ij} = w^{km} G_k^i G_m^j$ then yields

$$\tilde{\sigma} = (1 - \delta_i^3) w^{km} G_k^i G_m^j \vec{\alpha}_i \otimes \vec{\alpha}_i = \sum_{i=1}^{2} w^{km} G_k^i G_m^j \vec{\alpha}_i \otimes \vec{\alpha}_j \quad . \tag{143}$$

When the transformation back into the β-frame is applied, the approximate stress becomes

$$\begin{aligned} \tilde{\sigma} &= \sum_{i=1}^{2} w^{km} G_k^i F_i^r G_m^j F_j^s \vec{\beta}_r \otimes \vec{\beta}_s = \sum_{i=1}^{2} w^{km} G_k^i F_i^r \delta_m^s \vec{\beta}_r \otimes \vec{\beta}_s \\ &= \sum_{i=1}^{2} w^{ks} G_k^i F_i^r \vec{\beta}_r \otimes \vec{\beta}_s = (\delta_k^r - G_k^3 F_3^r) w^{ks} \vec{\beta}_r \otimes \vec{\beta}_s \quad . \end{aligned} \tag{144}$$

An illustration of the approximation procedure is given in Figure 8 where the basic approximation is seen to be performed in a lifted space.

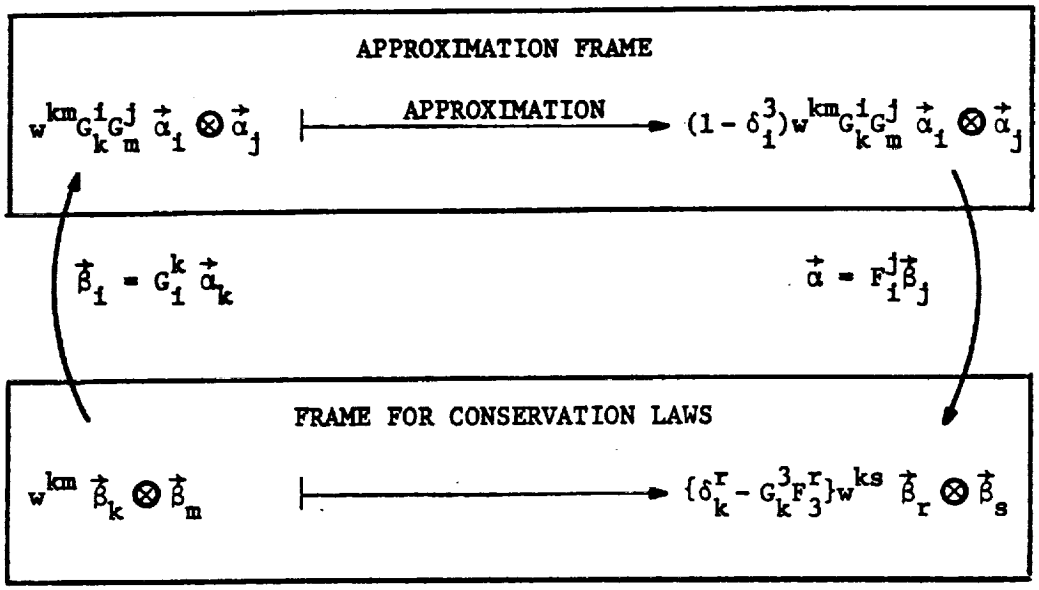

Figure 8. The Unidirectional Approximation to the Viscous Stress

The coefficient from the last equality in Eq. 144 is the viscous stress approximation in a form that can be directly inserted into a governing system of fluid dynamic equations to obtain a unidirectional approximation. For example, if the β-frame is just the coordinate frame, then the unidirectional approximation to the contravariant conservative form of the momentum equation (Eq. 108) is given by

$$\frac{\partial}{\partial y^i}\left\{\left[\rho v^i v^j + g^{ij}p + (\delta^i_k - G^3_kF^i_3)w^{kj}\right]\frac{\partial x^m}{\partial y^j}\sqrt{g}\right\} = 0 \quad , \tag{145}$$

for a suitable choice of vector field $\vec{\alpha}_3$ that defines the primary flow direction.

Several applications of the approximation can be mentioned. In each case the central part is the selection of a vector field which adequately defines a primary flow direction. Since the most accurate approximation would result from the velocity field itself, this is a natural selection. One procedure would be to directly use the Frenet frame for the streamlines. This is also the closest approach to the secondary flow equations as presented by Lakshminarayana and Horlock [33]. However, the Frenet frame is not always well-defined. Certainly problems would arise when the streamlines inflect or have local regions of uniform flow. Each of these possibilities would cause the Frenet frame to suddenly change orientation or lose the distinction between unique normal and binormal directions. As a result, the desired continuity of the frame would be lost in such cases. Consequently, a preferable method would be to use the velocity field and to construct a differentiable orthogonal frame around it. This could be chosen to coincide with the Frent frame in certain regions. Alternatively, the priamry direction vector field could be selected as some approximation to the viscous velocity field. For example, the directions from an inviscid potential flow solution could be used. Often the potential flow directions are just the tangent vectors to the steamline family of coordinate curves in a potential flow coordinate system. Moreover, other primary directions can be selected as tangent vectors to some given family of coordinate curves in some other system of coordinates. When this is done, the approximation is independent of the remaining directions. In particular, a transverse face of the stress cube is not aligned with the tangent plane to the transverse coordinate

directions, unless the system is orthogonal. Since only one family of coordinate curves could be used, a more general approach would be to generate a suitable family of curves that are aligned or approximately aligned with the flow direction. When vertically translated versions of the camber curve (Fig. 6) are considered, an approximate alignment is obtained for cascade flow fields when they are viewed as channel flows with a third slab symmetric dimension. In the cascade example, the approximation frame would be given by

$$\vec{\alpha}_3 = \hat{f}_1 \quad ,$$

$$\vec{\alpha}_1 = \hat{f}_2 \quad , \tag{146}$$

$$\vec{\alpha}_2 = \hat{f}_1 \times \hat{f}_2 \quad ,$$

where $\hat{f}_1$ and $\hat{f}_2$ are given in Eq. 125 and $\vec{\alpha}_3$ is the approximate primary flow direction.

NUMERICAL METHODS

Overview

When the form of the governing fluid dynamic equations is selected for a given problem, the next step in the process of numerical flow field simulation is to select a suitable numerical method which in turn may depend upon the form of the equations. The choices that are available extend over a broad range. There are explicit and implicit finite difference methods, finite element [48] and finite volume ([49] - [53]) methods, collocation piecewise

polynomial methods ([54] - [56]), spectral collocation and Galerkin methods [57], box [58] and higher order box [59] methods, operator compact implicit methods [60], flux corrected transport methods ([61] - [63], monotone methods ([64] - [65]), random choice methods ([66] - [67]) type-dependent methods ([31], [32], [51]), artificial compressibility methods ([68] - [69]) inflation and continuation methods ([70], [71]), approximate equation coefficient methods with locally exact solutions ([72] - [73]), adaptive methods with and without a fixed number of mesh points ([74] - [82]), multi-grid methods ([83] - [89]), asymptotic methods ([90] - [92]) and other methods which are usually variants or combinations (e.g. [93] - [95]) of the methods listed. For general references, a survey of many of the methods can be obtained from an examination of the recent proceedings for the AIAA Computational Fluid Dynamics Conferences, the International Conferences on Numerical Methods in Fluid Dynamics, and the von Karman Institute Short Courses on Computational Fluid Dynamics.

Rather than a comparative presentation of the various methods, our discussion will be limited to a specific class of techniques which are useful for many of the turbomachinery problems where Mach number ranges usually extend only into the low supersonic region. Turbomachinery flow fields, as internal flows, are non-trivially bounded above and below by solid objects. Specifically, for cascades of airfoils, the flow region is multi-connected which is more complex than the channel flows which are sometimes used as an approximation to avoid leading and trailing edge analyses for each airfoil or blade shape. Along the solid boundaries for the internal flow problems of turbomachinery, no-slip boundary conditions must be applied whenever a numerical simulation of a viscous flow field is attempted. As a consequence, there is a singular perturbation problem for

the boundary layer which is especially acute for high Reynolds number flow. When the flow region is discretized, the boundary layer must be resolved with a finely spaced mesh, for otherwise, accuracy is lost. The finely spaced mesh, however, causes the CFL stability limit for explicit finite difference methods to be overly restrictive on the permissable time-steps. Such a restriction is particularly troublesome when time-dependent equations are solved with the intent of converging upon the steady state flow field as rapidly as possible. The time-step restriction means that the steady state solution can only be obtained from a large number of time-steps which implies that a large amount of computation must be done. Vector computers, however, are most efficient with explicit numerical methods, can rapidly perform a large number of computations, and thus, would tend to offset to some degree the effect of the stability restricted time-step. In addition, the development of multigrid techniques would be helpful since the aggregate amount of computational work would be limited by shifting to coarser grids when finer grids would not substantially improve the solution. The saved work comes from the use of a sequence of coarse grids which have substantially smaller numbers of mesh points on which computations are executed. Most successful applications of the multigrid methods, however, have been in cases where the grid sequence is composed of Cartesian grids. Such a sequence can be used for curved boundaries when boundary interpolations are applied to local coordinates. To avoid the complex organization and manipulation of the data, a sequence of grids derived from curvilinear coordinates would be helpful. Some successful results have been obtained [89], however, the general combination of multigrid methods and curvilinear coordinates needs further development. For the complex geometric

configurations which occur in turbomachinery problems, the application of curvilinear coordinates is essential to obtain a well-ordered numerical algorithm which can match the geometry and the solution gradients. To avoid the explicit stability restriction, implicit methods were developed. With implicit methods, the numerical solution can be stably computed for a much larger time-step at a price of more computation and storage per step. When an alternating-direction-implicit (ADI) splitting is applied, computational efficiency per step is increased beyond that for a pure implicit method. Relative to explicit methods, the ADI methods will more rapidly converge to a steady state flow field. Consequently, our discussion will primarily be centered upon ADI methods. Since the motion of a viscous fluid is described by nonlinear equations, a key part of an implicit method is the treatment of the nonlinear properties of the equations. The earliest treatments involved an iteration cycle which was costly. Later, Lindemuth and Killeen [96] discovered that temporal accuracy did not deteriorate with a linearization, and consequently, they devised a non-iterative algorithm. Subsequently, the non-iterative technique was applied by Briley and McDonald [97], was mathematically analyzed and extended by Beam and Warming ([22], [98], [99]), and was applied to isolated airfoil problems by Steger [29]. In addition, MacCormack included an implicit step to devise a rapid solver [100] and Ballhaus, Jameson, and Albert [101] and Holst [102] each considered extensions to transonic flow.

The General Initial Value Form

All of the initial value formulations for viscous gas dynamic problems can be written in the general form

$$\frac{\partial H_i}{\partial t} = F_i \quad , \tag{147a}$$

where t is a time or time-like variable (as in spatial maching techniques) and where H_i and F_i independently depend on t, the spatial coordinates, the solution vector, and derivatives of the solution vector. In a compact notation, the functional dependence is given by

$$\begin{aligned} H_i &= H_i(\tau, y^j, p_r^k) \\ F_i &= F_i(\tau, y^j, p_r^k) \\ \tau &= t \end{aligned} \tag{147b}$$

where the indices j,k are assumed to vary over their respective ranges and where r is assumed to be the multi-index $(r_1, r_2, \ldots, r_n)$ which corresponds to

$$p_r^k = \left(\frac{\partial}{\partial y^1}\right)^{r_1} \left(\frac{\partial}{\partial y^2}\right)^{r_2} \cdots \left(\frac{\partial}{\partial y^n}\right)^{r_n} u^k \quad , \tag{147c}$$

for the solution variable u^k when $r_1 = r_2 = \ldots = r_n = 0$ and $(r_1 + r_2 + \ldots + r_n)th$ order derivatives when one or more of the indices $r_j \geq 0$ is strictly positive. In anticipation of chain rule expansions, the partial derivative of Eq. 147c with respect to a solution variable u^m is given by the differential operator

$$\frac{\partial p_r^k}{\partial u^m} = \delta_m^k \left(\frac{\partial}{\partial y^1}\right)^{r_1} \left(\frac{\partial}{\partial y^2}\right)^{r_2} \cdots \left(\frac{\partial}{\partial y^n}\right)^{r_n} \quad . \tag{148}$$

To see how this occurs, the time-like derivative of Eq. 147c is directly computed to be

$$\frac{\partial p_r^k}{\partial t} = \frac{\partial}{\partial t}\left(\frac{\partial}{\partial y^1}\right)^{r_1} \cdots \left(\frac{\partial}{\partial y^n}\right)^{r_n} u^k = \left(\frac{\partial}{\partial y^1}\right)^{r_1} \cdots \left(\frac{\partial}{\partial y^n}\right)^{r_n} \frac{\partial u^k}{\partial t}$$

$$= \delta_m^k \left(\frac{\partial}{\partial y^1}\right)^{r_1} \cdots \left(\frac{\partial}{\partial y^n}\right)^{r_n} \frac{\partial u^m}{\partial t} = \frac{\partial p_r^k}{\partial u^m} \frac{\partial u^m}{\partial t} \quad . \tag{149}$$

where the second equality is due to an interchange of the order of differentiation; the third, the definition of the Kronecker delta; and the fourth, the operator from Eq. 148. Unlike most forms of the chain rule, the order of the factors in the result of Eq. 149 is important since the operator of Eq. 148 must be applied to the second factor for each m as m is summed over its range.

From the chain rule, the general system of Eq. 147 can be rewritten so that the time or time-like derivative is explicitly applied to the solution variables u^m. In the explicit form, the system becomes

$$\frac{\partial H_i}{\partial u^m} \frac{\partial u^m}{\partial t} = F_i - \frac{\partial H_i}{\partial t} \quad , \tag{150a}$$

where

$$\frac{\partial H_i}{\partial u^m} = \frac{\partial H_i}{\partial p_r^k} \frac{\partial p_r^k}{\partial u^m} \quad . \tag{150b}$$

is the Jacobian of operators and where the partial derivative of H_i with respect to t comes from the t-dependent solution independent parameters that, for example, can arise from t-dependent geometry. If the Jacobian is nonsingular as a linear transformation, then the time-like derivatives of the entire solution vector can be obtained by a direct solution. Otherwise, a constrained system of lower rank must be considered. Under a change of basis, the explicit form of Eq. 150 can often be rewritten in an equivalent form where the Jacobian (Eq. 150b) is represented by an operator matrix with M linearly independent rows and $N-M$ rows of zeros where M is the rank of the Jacobian and N is the total number of rows (and columns). The last $N-M$ rows of transformed equations correspond to the nullity of the Jacobian and hence involve no time-like derivatives. Consequently, the last $N-M$ rows are viewed as a set of constraints which can be used to eliminate the last $N-M$ components of the solution vector in the first M equations. The constraints are in the form of Eq. 150a with a vanishing left hand side. When the equivalent form exists with constraints, the original system of N equations in N unknowns has been reduced to another equivalent system of M equations in M unknowns. Such an original system can be called a reducible system in correspondence with the matrix terminology [103] which is a direct parallel since a discretization of the system would lead to reducible matrices. If the system is reducible at each point $(t,y^1,\ldots,y^n)$ by a sufficiently smooth basis transformation, then the system can be called a solvable system. Only solvable systems shall be considered; moreover, without loss of generality, we can assume that the Jacobian (Eq. 150b) is nonsingular, for otherwise, the reduced system would

just produce a smaller equivalent system that is nonsingular and could be solved in the same manner. With the assumption of solvability, an inversion then yields

$$D^k \equiv \frac{\partial u^k}{\partial t} = A^{ki}\left\{F_i - \frac{\partial H_i}{\partial t}\right\} \quad , \tag{151}$$

where the matrix (A^{ki}) is the inverse Jacobian and the notation D^k is introduced to denote the value of the t-derivative of the k*th* solution vector component that is directly determined by the system of partial differential equations.

Linearization in the Time-like Variable

When the system of partial differential equations (Eq. 147) is to be solved by a non-iterative numerical method, the equations must be linearized in some fashion. Moreover, on examination of various linearization strategies, corresponding numerical methods can be derived by direct integration and by finite differences to yield both implicit and explicit algorithms. To simplify the notation in our examination of linearization, at least initially, consider the scalar ordinary differential equation

$$\frac{du}{dt} = f(u) \quad , \tag{152}$$

where the only possible nonlinearity occurs in f and where a solution $u(t)$ is desired when $u_n = u(t_n)$ is given and $t > t_n$. From the first two terms of the Taylor series expansion of f, Eq. 152 can be approximated by

$$\left(\frac{du}{dt}\right) = f_n + \left(\frac{df}{dt}\right)_n (t - t_n) = f_n + \left(\frac{df}{du}\right)_n \left(\frac{du}{dt}\right)_n (t - t_n) \quad , \tag{153}$$

where the subscripts n denote evaluations at t_n, and the error of approximation is of order $(t - t_n)^2$. When the derivative of u at n is expanded in the forward difference form

$$\left(\frac{du}{dt}\right)_n = \frac{u - u_n}{t - t_n} + 0((t - t_n)) \quad , \tag{154}$$

and second order terms in $(t - t_n)$ are neglected, we obtain the implicit approximation

$$\frac{du}{dt} = f_n + \left(\frac{df}{du}\right)_n (u - u_n) \quad , \tag{155}$$

which still deviates from Eq. 152 by only second order terms. If, in addition, the remaining derivative of u were to be replaced by the backward difference $(u - u_n)/(t - t_n)$, then the resultant equation would be observed from Eq. 154 to deviate from Eq. 152 by first order rather than second order terms. However, without a decrease in accuracy, a direct integration of the implicit linearization of Eq. 155 is always possible and the result is given by

$$u = u_n + \left[e^{A(t - t_n)} - 1\right] A^{-1} f_n \quad , \tag{156}$$

where

$$A = \left(\frac{df}{du}\right)_n \quad .$$

Moreover, in the special case when f is linear, the solution is also the exact solution of the original equation (Eq. 152). The special linear case is also easily seen to include constant coefficient linear systems by a parallel development. In the general nonlinear cases, the exponential character is clearly contained in the integral (Eq. 156) of the implicit linearization and thus, the scheme is well-aligned with the local solution growth. By contrast, the exponential character is only evident in an approximate sense for explicit forms. A second order explicit approximation is obtained from a substitution of the original equation (Eq. 152) at time t_n into the Taylor expansion of Eq. 153 to yield the linearization

$$\frac{du}{dt} = f_n + \left(\frac{df}{du}\right)_n f_n(t - t_n) \quad , \tag{157}$$

which upon integration becomes

$$\begin{aligned} u &= u_n + \left[(t - t_n) + \left(\frac{df}{du}\right)_n \frac{(t - t_n)^2}{2!}\right] f_n \\ &= u_n + \left[A(t - t_n) + \frac{A^2(t - t_n)^2}{2!}\right] A^{-1} f_n \quad . \end{aligned} \tag{158}$$

By comparison, the bracketed expression in the second equality is just a third order approximate of the exponential character in the implicit form of Eq. 156. Unlike the implicit form, the explicit scheme does not reproduce exact solutions to linear constant coefficient equations; but instead, it gives approximations where the error is of order $(t - t_n)^3$.

In continuation, higher order linearizations can be obtained by the inclusion of more terms in the Taylor series expansion of f and as a result, higher order explicit and implicit schemes can be systematically developed. As the terms are added, however, there is an increase in the number of possible schemes at each accuracy level since there is an increase in the number of choices for and between finite difference and equation evaluations (from Eq. 152) for substitutions into the Taylor expansion of f. To illustrate the development, consider the third order accurate approximate equation

$$\frac{du}{dt} = f_n + \left(\frac{df}{du}\right)_n \left(\frac{du}{dt}\right)_n (t - t_n) + \left[\frac{d^2 f}{du^2}\left(\frac{du}{dt}\right)^2 + \frac{df}{du}\frac{d^2 u}{dt^2}\right]_n \frac{(t - t_n)^2}{2!} . \quad (159)$$

When implicit forms are desired, the substitutions are constrained by the requirement that linearity must be maintained at the implicit level. In Eq. 159, the disallowed substitution is a forward difference for both factors in $(du/dt)^2$ which would then produce a squared implicit quantity. The allowable choices are then selected from all other combinations of forward and backward differences and evaluations of Eq. 152 which upon substitution maintain the third order accuracy of Eq. 159. The required accuracy here, is only first order since the term in question already contains the factor $(t - t_n)^2$. Also to maintain accuracy, $(du/dt)_n$ in the $(t - t_n)$-term must be evaluated from Eq. 152 or be approximated with a second order finite difference. With these considerations, fourth order implicit schemes can be obtained. With the same accuracy considerations, fourth order explicit schemes can also be obtained. As an example, consider the explicit scheme derived from only direct substitutions of Eq. 152 into

Eq. 159. From Eq. 152, we have

$$\frac{d^2u}{dt^2} = \frac{df}{dt} = \frac{df}{du}\frac{du}{dt} = \frac{df}{du} f \quad , \tag{160}$$

which, along with Eq. 152, is inserted into Eq. 159 to yield

$$\frac{du}{dt} = f_n + \left(\frac{df}{du} f\right)_n (t - t_n) + \left[\frac{d^2f}{du^2} f^2 + \left(\frac{df}{du}\right)^2 f\right]_n \frac{(t - t_n)^2}{2} \quad . \tag{161}$$

A direct integration then yields the scheme

$$u = u_n + \left\{ (t - t_n) + \left(\frac{df}{du}\right)_n \frac{(t - t_n)^2}{2} + \left[\frac{d^2f}{du^2} f + \left(\frac{df}{du}\right)^2\right]_n \frac{(t - t_n)^3}{6.} \right\} f_n \quad . \tag{162}$$

When $f = \alpha u$ for some constant α, the scheme of Eq. 162 becomes

$$u = \left\{ 1 + \alpha(t - t_n) + \frac{\alpha^2 (t - t_n)^2}{2} + \frac{\alpha^3 (t - t_n)^3}{6} \right\} u_n \quad , \tag{163}$$

which is just the first four terms in the Taylor series expansion of the analytic solution $u_n e^{\alpha(t - t_n)}$ of the original equation (Eq. 152). When $f = 1 + u^2$, the original equation is nonlinear and the scheme of Eq. 162 becomes

$$u = u_n + \left\{ (t - t_n) + u_n (t - t_n)^2 + (u_n^2 + \tfrac{1}{3})(t - t_n)^3 \right\} (1 + u_n^2) \quad . \tag{164}$$

For $t_n = 0$ and $u_n = 0$, Eq. 164 is easily recognized as the first four terms in the Taylor series of the known solution $u(t) = \tan(t)$ when the initial condition $u(0) = 0$ is applied to Eq. 152. In each case and in

general, the explicit scheme of Eq. 162 would deviate from analytic solutions to Eq. 152 by a fourth order term. To evaluate Eq. 162, or indeed any of the schemes generated from linearization strategies, a stability analysis would be required in each case. For linear cases, complex exponentials are inserted into the schemes so that an amplification factor can be bounded (often leading to step size limits) and examined for both dissipation and phase errors (as plotted in [22], for example). In nonlinear cases, there is usually an intuitive extrapolation from the linear analysis applied to a local linearization. Alternatively, energy methods can be applied (e.g. [104]) when the analysis is tractable. Altogether however, the stability analyses can be very complicated and, for nonlinear problems, often produce limited information. As a coarse rule of thumb, implicit methods are usually more stable than explicit methods. As a consequence the methods of linearization considered on the scalar equation (Eq. 152) will be applied to the general system of Eq. 147 to develop a general Crank-Nicolson scheme. Other schemes could also be obtained in parallel to the scalar case but will not be pursued here.

A Crank-Nicolson Scheme

The numerical scheme that is developed here is an extension of the classical Crank-Nicolson scheme to cover the general equation form given by Eq. 147 and to still maintain second order accuracy. In the well-centered framework of Crank-Nicolson we have the second order accurate scheme

$$\frac{(H_i)_{n+1} - (H_i)_n}{h} = (F_i)_{n+\frac{1}{2}} \quad , \tag{165}$$

where $h = t_{n+1} - t_n$ and the subscripts involving n will denote levels of t rather than a spatial dimension as in Eq. 147. No confusion will result, however, since spatial dimensions are implicit in the summation convention and do not appear explicitly. To extract the solution vector and to develop the noniterative implicit scheme, a sequence of linearizations must be applied to both sides of the Crank-Nicolson statement (Eq. 165). The same considerations as in the scalar case of the previous section will apply. From a Taylor expansion of the right hand side about level n, we maintain accuracy by setting

$$(F_i)_{n+\frac{1}{2}} = (F_i)_n + \left\{ \frac{\partial F_i}{\partial \tau} + \frac{\partial F_i}{\partial p_r^k} \frac{\partial p_r^k}{\partial u^m} \frac{\partial u^m}{\partial t} \right\}_n \frac{h}{2} \quad , \tag{166}$$

where the chain rule (including Eq. 149) has been applied. The n-level evaluations in the first order piece are straight forward with the exception of the quantity $(\partial u^m/\partial t)_n$. This can be evaluated either by a finite difference or directly from the differential equations with D^k of Eq. 151. If the latter approach is taken, then the fundamental implicit part of the basic Crank-Nicolson scheme is lost. Thus, a finite difference shall be used. Since the term itself is first order, the simple first order forward difference is sufficient, and the expression becomes

$$(F_i)_{n+\frac{1}{2}} = (F_i)_n + \left(\frac{\partial F_i}{\partial \tau} \right)_n \frac{h}{2} + \left(\frac{\partial F_i}{\partial p_r^k} \frac{\partial p_r^k}{\partial u^m} \right)_n (u_{n+1}^m - u_n^m) \quad , \tag{167}$$

where the order of the factors in the last term is important since $(\partial p_r^k/\partial u^m)_n$ is a differential operator (Eq. 148) acting upon the solution vectors.

On the left hand side of the Crank-Nicolson scheme, a difference quotient of fluxes must be evaluated with a maintenance of second order accuracy. To initially avoid the explicit appearance of differential operators, the chain rule expansion of Eq. 149 will be reserved until a Taylor expansion of the difference quotient has been completed. The expansion with second order errors is given by

$$\frac{(H_i)_{n+1} - (H_i)_n}{h} \simeq \left(\frac{\partial H_i}{\partial t}\right)_{n+\frac{1}{2}} \simeq \left(\frac{\partial H_i}{\partial \tau} + \frac{\partial H_i}{\partial p_r^k}\frac{\partial p_r^k}{\partial t}\right)_{n+\frac{1}{2}}$$

$$\simeq \left\{\frac{\partial H_i}{\partial \tau} + \frac{h}{2}\frac{\partial^2 H_i}{\partial \tau \partial t}\right\}_n + \left\{\frac{\partial H}{\partial p_r^k} + \frac{h}{2}\frac{\partial^2 H_i}{\partial p_r^k \partial t}\right\}_n \left(\frac{\partial p_r^k}{\partial t}\right)_{n+\frac{1}{2}}$$

$$\simeq \left\{\frac{\partial H_i}{\partial \tau} + \frac{h}{2}\left[\frac{\partial^2 H_i}{\partial \tau^2} + \frac{\partial^2 H_i}{\partial \tau \partial p_s^\ell}\frac{\partial p_s^\ell}{\partial t}\right]\right\}_n$$

$$+ \left\{\frac{\partial H_i}{\partial p_r^k} + \frac{h}{2}\left[\frac{\partial^2 H_i}{\partial p_r^k \partial \tau} + \frac{\partial^2 H_i}{\partial p_r^k \partial p_s^\ell}\frac{\partial p_s^\ell}{\partial t}\right]\right\}_n \left(\frac{\partial p_r^k}{\partial t}\right)_{n+\frac{1}{2}} \qquad (168)$$

$$\simeq \left(\frac{\partial H_i}{\partial \tau} + \frac{h}{2}\frac{\partial^2 H_i}{\partial \tau^2}\right)_n + \left(\frac{h}{2}\frac{\partial^2 H_i}{\partial \tau \partial p_s^\ell}\right)_n \left(\frac{\partial p_s^\ell}{\partial t}\right)_n$$

$$+ \left(\frac{\partial H_i}{\partial p_r^k} + \frac{h}{2}\frac{\partial^2 H_i}{\partial p_r^k \partial \tau}\right)_n \left(\frac{\partial p_r^k}{\partial t}\right)_{n+\frac{1}{2}} + \left(\frac{h}{2}\frac{\partial^2 H_i}{\partial p_r^k \partial p_s^\ell}\right)_n \left(\frac{\partial p_s^\ell}{\partial t}\right)_n \left(\frac{\partial p_r^k}{\partial t}\right)_{n+\frac{1}{2}}$$

$$\simeq \left(a_i\right)_n + \left(b_{i\ell}^s\right)_n \left(\frac{\partial p_s^\ell}{\partial t}\right)_n + \left(c_{ik}^r\right)_n \left(\frac{\partial p_r^k}{\partial t}\right)_{n+\frac{1}{2}} + \left(d_{i\ell k}^{sr}\right)_n \left(\frac{\partial p_s^\ell}{\partial t}\right)_n \left(\frac{\partial p_r^k}{\partial t}\right)_{n+\frac{1}{2}}$$

where, for notational convenience,

$$a_i = \frac{\partial H_i}{\partial \tau} + \frac{h}{2}\frac{\partial^2 H_i}{\partial \tau^2}$$

$$b^s_{i\ell} = \frac{h}{2}\frac{\partial^2 H_i}{\partial \tau \partial p^\ell_s} \qquad (169)$$

$$c^r_{ik} = \frac{\partial H_i}{\partial p^k_r} + \frac{h}{2}\frac{\partial^2 H_i}{\partial p^k_r \partial \tau}$$

and

$$d^{sr}_{i\ell k} = \frac{h}{2}\frac{\partial^2 H_i}{\partial p^k_r \partial p^\ell_s}$$

The time-like dependence of solution independent parameters outwardly enters the scheme through the derivatives with respect to τ which was used in place of t to separate the dependence in question from the general t dependence. Such parameters, we recall, can come from t-dependent geometry which leads to t-dependent metric data (eg., Eqs. 85-86) or equivalent data (eg., Eqs. 122 and 138). The derivatives with respect to τ occur only in the coefficients a_i, $b^s_{i\ell}$, and c^r_{ik}. When the t-dependence occurs only in u^m, the coefficients a_i and $b^s_{i\ell}$ both vanish and c^r_{ik} reduces to the Jacobian transformation of H_i with respect to p^k_r. The expression of $d^{sr}_{i\ell k}$ is independent of τ-derivatives and is easily identified as the Hessian of H_i with respect to both p^k_r and p^ℓ_s which is scaled by $h/2$.

A direct evaluation of the $(n+\frac{1}{2})$-level derivatives in Eq. 168 from D^k in Eq. 151 would lead in general to a nonlinearity at the implicit level. The nonlinearity is clearly avoided, however, with the finite difference formulation

$$\left(\frac{\partial p^k_r}{\partial t}\right)_{n+\frac{1}{2}} = \left(\frac{\partial p^k_r}{\partial u^m}\right)_n \left(\frac{\partial u^m}{\partial t}\right)_{n+\frac{1}{2}} \simeq \left(\frac{\partial p^k_r}{\partial u^m}\right)_n \left(\frac{u^m_{n+1} - u^m_n}{h}\right) , \qquad (170)$$

which is second order in h because of the central difference. The first factor is now a differential operator (Eq. 148) acting upon the difference quotient. Upon substitution, Eq. 168 becomes

$$\frac{(H_i)_{n+1} - (H_i)_n}{h} = \left(a_i\right)_n + \left(b^s_{i\ell}\right)_n \left(\frac{\partial p^\ell_s}{\partial t}\right)_n + \left[\left(c^r_{ik} + d^{sr}_{i\ell k}\,\frac{\partial p^\ell_s}{\partial t}\right)\frac{\partial p^k_r}{\partial u^m}\right]_n \left(\frac{u^m_{n+1} - u^m_n}{h}\right) \tag{171}$$

where it remains to determine the n-level t-derivatives in a manner which preserves second order accuracy.

Since both $b^s_{i\ell}$ and $d^{sr}_{i\ell k}$ are first order in h, the evaluation of the respective derivatives need only be first order accurate. While the choice for the $b^s_{i\ell}$ has no further constraints, the choice in the $d^{sr}_{i\ell k}$ term must also be restricted to explicit evaluations, for otherwise, a nonlinearity would result. With a forward difference, the nonlinearity would occur in the form of quadratic terms in the solution variable which is the same problem that occurred in the discussion of Eq. 159. Consequently, the simplest options are either to use a backward difference to time level (n-1) or to directly replace the derivative with an evaluation from Eq. 151. To avoid the extra storage that would result from a three-level scheme, the second option will be used. When, in addition, a forward difference formulation (Eq. 170) is used for the $b^s_{i\ell}$ -term, Eq. 171 becomes

$$\frac{(H_i)_{n+1} - (H_i)_n}{h} = (a_i)_n + (b^r_{ik} + c^r_{ik} + d^{sr}_{i\ell k} Q^\ell_s)_n \frac{\partial p^k_r}{\partial u^m} \left(\frac{u^m_{n+1} - u^m_n}{h}\right), \quad (172)$$

where

$$Q^\ell_s = \frac{\partial p^\ell_s}{\partial u^j} D^j \quad ,$$

is not a differential operator but is instead a function determined by the application of the differential operator represented by its first factor (Eq. 148) to the jth solution derivative D^j obtained from Eq. 151.

On re-examination of the $b^s_{i\ell}$-terms, we observed that there was some degree of choice in the evaluation of the t-derivative. This degree of freedom can be used to advantage. For any coefficient operator e_{im} that

is first order in h, we have second order relation

$$(e_{im})_n \left[(D^m)_n - \left(\frac{u^m_{n+1} - u^m_n}{h} \right) \right] \simeq 0 \quad , \tag{173}$$

which can be added to Eq. 172 without a change of order. From the addition the difference quotient in H_i is then given by the expression

$$(a_i)_n + (e_{im} D^m)_n + \left[(b^r_{ik} + c^r_{ik} + d^{sr}_{i\ell k} Q^\ell_s) \frac{\partial p^k_r}{\partial u^m} - e_{im} \right]_n \left(\frac{u^m_{n+1} - u^m_n}{h} \right) . \tag{174}$$

When $e_{im} = 0$, the effect is to represent b^r_{ik} - terms with finite differences; when $e_{im} = b^r_{ik}(\partial p^k_r / \partial u^m)$, the representation is entirely an explicit evaluation. Moreover, the selections for e_{im} can be used to shift any number of terms between implicit and explicit levels. The reasons for such a shift can arise from some favorable stability or matrix inversion property or from some simplification in the solution procedure. The effect of the shifts is to be viewed within the context of the extended Crank-Nicolson scheme which on combination of Eqs. 165, 167, and 174 is given by

$$\left[\left(b^r_{ik} + c^r_{ik} + d^{sr}_{i\ell k} Q^\ell_s - \frac{h}{2} \frac{\partial F_i}{\partial p^k_r} \right) \frac{\partial p^k_r}{\partial u^m} - e_{im} \right]_n (u^m_{n+1} - u^m_n)$$

$$= h \left[F_i + \frac{h}{2} \frac{\partial F_i}{\partial \tau} - a_i - e_{im} D^m \right]_n \quad . \tag{175}$$

On examination of the coefficients (Eq. 169) for the scheme, the shifts cannot be used to eliminate the implicit level Jacobian transformation operator $(\partial H_i / \partial u^m)$ since it is independent of h while e_{im} is first order in h. For the same reason, the t-derivatives of parameters $(\partial H_i / \partial \tau)$ also cannot

be shifted. When there is no shift between implicit and explicit levels and when H_i and F_i depend upon t only through (p_r^k), the general Crank-Nicolson scheme reduces to

$$\left\{\frac{\partial H_i}{\partial u^m} + \frac{h}{2}\left[D^\ell \frac{\partial^2 H_i}{\partial u^m \partial u^\ell} - \frac{\partial F_i}{\partial p_r^k}\frac{\partial p_r^k}{\partial u^m}\right]\right\}_n (u_{n+1}^m - u_n^m) = h(F_i)_n \ . \qquad (176)$$

Moreover, when $H_i = u^i$, we have

$$\left\{\delta_m^i - \frac{h}{2}\frac{\partial F_i}{\partial p_r^k}\frac{\partial p_r^k}{\partial u^m}\right\}_n (u_{n+1}^m - u_n^m) = h(F_i)_n \ , \qquad (177)$$

which is the standard form of the Crank-Nicolson scheme. In a parallel manner, the same formalism can be applied to obtain a wide variety of schemes for the treatment of the t-dependence. In particular, when the Crank-Nicolson centering is replaced by a variable balance between levels n and $n+1$, as in [105], the same derivation will work simultaneously for a group of schemes.

To implement the schemes, the spatial derivatives must be evaluated in some fashion. The simplest evaluation is accomplished with the use of central differences for interior points and one-sided differences for boundary points. For any function $f(t,\vec{y})$ and for a constant mesh increment Δy^j; let E_k^j be the operator which replaces the component y^j by $y^j + k\Delta y^j$ in the evaluation of f. Since mesh data is assumed only at integral values of k, half point evaluation operators will be taken as averages so that, for example, $E_{\frac{1}{2}}^j = (E_1^j + E_0^j)/2$. Now let Δ^j be a difference operator that is defined on the entire mesh by the central difference

$$\Delta^j|_{\vec{y}} = \frac{E^j_{\frac{1}{2}} - E^j_{-\frac{1}{2}}}{\Delta y^j} \quad , \tag{178a}$$

when $\vec{y}$ is an interior mesh point and by

$$\Delta^j|_{\vec{y}} = \frac{-E^j_0 + 4E^j_1 - E^j_2}{2\Delta y^j} \quad , \tag{178b}$$

and

$$\Delta^j|_{\vec{y}} = \frac{3E^j_0 - 4E^j_{-1} + E^j_{-2}}{2\Delta y^j} \quad , \tag{178c}$$

when $\vec{y}$ corresponds respectively to the mesh points with the smallest and largest values of y^j which defines the lower and upper boundaries of constant y^j. A replacement of each differential operator $(\partial/\partial y^j)$ by Δ^j in Eq. 148 then yields a second order accurate finite difference operator which upon substitution into the general Crank-Nicolson scheme (Eq. 175) leads to a second order difference scheme when boundary conditions are inserted. Alternative forms for discretization include higher order differences, Padé formulas [103], box schemes [59], and variable difference operators [22]. With collocation or Galerkin methods, both piecewise polynomial ([54] - [56], [95], [48]) and spectral methods [57] can be used to represent the solution u^m_n rather than the operators.

Alternating-Direction-Implicit Methods

On discretization, the general numerical scheme (Eq. 175) reduces to a linear algebraic system of the form

$$\{A + h\,B\}\vec{\psi}_{n+1} = \vec{S} \quad , \tag{179}$$

where A and B are linear transformations derived respectively from the discretization of the zero*th* and first order parts of the implicit operator and where $\vec{S}$ is the discretization of the source vector which is the explicit part. The solution vector $\vec{\psi}$ corresponds with the discretization of $(u^1 - u_n^1, u^2 - u_n^2, \ldots, u^N - u_n^N)$. This form has been called the delta form [105]. When B can be expressed as a sum of linear transformations, each of which leads to an easily solved system when used in place of B, then Eq. 179 can be solved up to second order accuracy by a successive solution corresponding to each part of the sum. Such a decomposition into a sequence of easily solved parts was examined in the general formulation of alternating-direction implicit methods due to Douglas and Gunn [106]. For simplicity, suppose that $B = B_1 + B_2$ where B_1 and and B_2 each yield easily solved systems. For two-dimensional applications without mixed derivatives, B_1 and B_2 are usually taken to be the transformations corresponding respectively to derivative discretizations grouped in the given directions. That is, y^1-derivatives are contained in B_1; y^2-derivatives, in B_2. With the sum, Eq. 179 becomes

$$\{A + h(B_1 + B_2)\}\vec{\psi}_{n+1} = \vec{S} \quad . \tag{180}$$

By the addition of $h^2 B_1 A^{-1} B_2$ to the implicit side, the second order accuracy of the system does not change and we get the factored form

$$(A + h B_1) A^{-1} (A + h B_2) = \vec{S} \quad , \tag{181}$$

which can be split into

$$(A + h B_1)\,\vec{\psi}_* = \vec{S} \quad , \tag{182a}$$

and

$$(A + h B_2)\,\vec{\psi}_{n+1} = A\vec{\psi}_* \quad . \tag{182b}$$

When only first and second derivatives appear and are approximated by the difference operators of Eq. 178, the split system of equations is solved as a sequence of block tridiagonal or nearly block tridiagonal systems. If the boundary conditions are periodic or extend inward by more than two mesh points, the deviation from a pure block tridiagonal form occurs. For block tridiagonal systems, the inversion is efficiently done with Gaussian elimination by means of the Thomas algorithm. The slight deviations from pure block tridiagonal forms do not cause much additional work. Thus, in each case, Eq. 182a is efficiently solved as a sequence of one dimensional (block tridiagonal) problems corresponding to each mesh line in the y^1-direction. Upon completion, ψ_* is defined over the entire mesh which means that Eq. 182b is then formulated over the entire mesh. The solution of Eq. 182b is performed, as in the first step, as a sequence of one dimensional problems corresponding to mesh lines in the y^2-direction. The y^2-direction sweeps through the mesh then completes the calculation for the solution increment $\vec{\psi}_{n+1}$. The solution vector in the calculation is given at each mesh point by $(u^1,\ldots,u^n) = \vec{\psi} + (u_n^1,\ldots,u_n^N)$ which is evaluated for both * and n+1 values. An evaluation at the n-level yields $\vec{\psi}_n = 0$ which is consistent with the definition of $\vec{\psi}$ as the difference of solution values from the n-level.

As a result, Eq. 182a can be rewritten as

$$A\vec{\psi}_* + hB_1\vec{\psi}_* + hB_2\vec{\psi}_n = \vec{S} \quad , \tag{183}$$

which deviates from the original linear algebraic system of equations only in the evaluations of $\vec{\psi}$ at $*$ and n rather than uniformly at $n+1$. Since the form of the original system is retained, the boundary conditions for the solution at $*$ can be obtained from the original system. The implication for fluid dynamics problems is that the boundary conditions at $*$ can be given a physical meaning. A similar form and argument can be given applied for the solution at $n+1$ (in Eq. 182b) for the second sweep. When Eq. 182a is added to Eq. 182b, and subsequently, when $A\vec{\psi}_*$ is subtracted from both sides, we have

$$A\vec{\psi}_{n+1} + hB_1\vec{\psi}_* + hB_2\vec{\psi}_{n+1} = \vec{S} \quad , \tag{184}$$

which again retains the original form of the system and which again can have boundary conditions derived from the original system. Taken together, the two sweeps corresponding to the two alternating direction implicit (ADI) directions are said to be consistent [106].

In the Douglas-Gunn formulation, the ADI "directions" correspond to the operators B_i which sum to the operator B, which yield simply solved systems, and which need not be associated with any particular coordinate direction. As an example, consider a uniform mesh central difference (Eq. 178) approximation (Eq. 179) to an initial value problem (Eq. 147 with initial conditions) without second derivatives but with any number of spatial dimensions. Rather than spatial directions, the operator directions can be taken as forward and backward difference directions respectively, as in the LU decompositions studied by Jameson and Turkel [107]. Specifically, the central difference operator of Eq. 178a can be written in the form

$\Delta_+^j + \Delta_-^j$ where

$$\Delta_+^j = \frac{E_1^j - E_0^j}{\Delta y^j} \quad , \tag{185}$$

and

$$\Delta_-^j = \frac{E_0^j - E_{-1}^j}{\Delta y^j} \quad ,$$

are the forward and backward differences. When all terms are then grouped into forward and backward differences, the operator B is decomposed correspondingly into operators B_1 and B_2. Moreover, the forward difference operator B_1 could be directly written by using only forward differences in the original derivation of Eq. 179, and similarly for B_2 with backward differences. From this stage, the consistent Douglas-Gunn splitting (Eqs. 180 - 184) applies as in the case with actual coordinate directions. However, by contrast, only two factors are needed for any number of spatial dimensions and an LU decomposition, as in [103], results. Matrix elements for the decomposition are matrix blocks in correspondence with the number of equations and solution variables. To insure a stable matrix inversion by Gaussian elimination without pivoting, Jameson and Turkel [107] added a third derivative term to the original system and considered coefficient choices to enforce diagonal dominance for both upper and lower triangular factors. The same type of manipulation should also come from a specification of e_{im} in Eq. 175. The extension to cases with second derivatives follows the same format and again results in an LU decomposition. The additional mesh point dependence required for second derivatives translates, here, into an upper triangular factor

U and a lower triangular factor L with a larger band width than in the pure first derivative cases. With further increases in band width, cases with higher derivatives can be considered. In any case, when Douglas-Gunn splitting is applied to decompositions into forward and backward differences, an implicit analogue to the original MacCormack method [21] is obtained. A further LU decomposition is given in Steger and Warming [108] where the splitting is between positive and negative eigenvalues.

In addition to splitting between forward and backward differences, there are also variants for ADI methods when the implicit directions are aligned with coordinate directions. The alternating-direction Galerkin method of Douglas and Dupont [107] is one example. Their development is based on a tensor product structure for both operators and function spaces. Further examples can also be conceived when the splitting is viewed as a succession of two-point boundary value problems which upon assembly yield a solution at a given time level, provided that there is stability and convergence to the correct solution. The motivation is to obtain a high order of accuracy so that fewer points are needed to compute a solution to within a given tolerance. Some cases are the ADI spline collocation of Rubin and Koshla [54] at natural knots, the application of collocation at Gaussian knots from deBoor and Schwartz [56], and the splined local solutions of approximate coefficient systems studied by Pruess [73].

Solutions on a Composite Mesh

When a flow through a multiconnected region is to be simulated numerically, it is advantageous to use a discretization which is obtained by the application of one or more coordinate transformations in a composite fashion. The composite is obtained when transformations are smoothly joined together along parts of their boundaries, even if one transformation is just joined to itself along different parts of its boundary. In the case with one transformation, the junctures are either branch cuts or periodicity conditions as in the case with cascades of airfoils. Also with cascades, upstream and/or downstream grid resolution can be achieved with separate coordinate systems. A composite mesh for a cascade of airfoils is illustrated in Figure 9 where the upstream resolution is obtained by a Cartesian system; the downstream, by a branch cut off of a cusped trailing edge. In the figure, the Cartesian system covers the rectangular region with (oriented) boundary A B C X Y Z C B A H A. The other coordinate system has an outer boundary G F E D X Y Z D E F G, a downstream boundary G I J P G, and an inner boundary J K O L M N O K J consisting of an airfoil contour O L M N O with an attached branch cut that precedes the airfoil in the orientation of J K O and follows it in the orientation O K J. Both coordinate systems are bounded from above and below by a periodic boundary A B C D E F G where each system is joined to itself, as in the case with the branch cut from the airfoil. The juncture between the systems is given by X Y Z.

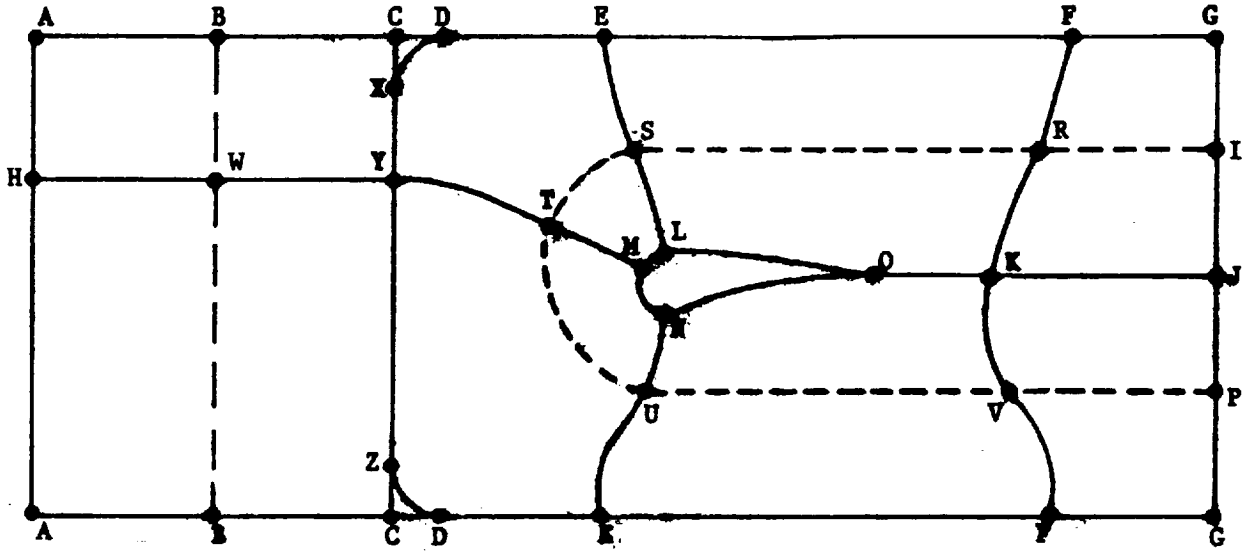

Figure 9. The Mesh Topology for a Cascade of Airfoils with a Branch Cut from a Cusped Trailing Edge and with a Cartesian Extension Upstream.

With a suitable mesh generation algorithm, the junctures can be done smoothly so that no special numerical approximations are needed for the derivatives at coordinate system junctures. Given two well-defined coordinate systems, almost the entire region will be covered. The uncovered portions are given by the two curved triangular regions XCD and ZCD which for purposes of resolution should be made small enough to be on the order of a mesh size in the local region. It is important to note that the uncovered regions are the result of the mesh topology and are not coordinate singularities to be associated with either coordinate system. A coordinate singularity would yield a degenerate metric (Eq. 11) and degenerate equations (eg., Eqs. 75 - 82) which indeed is not necessarily the case for the coordinate systems which border the uncovered regions. Schematics of typical coordinate curves are

depicted with solid curves to designate one ADI-direction and dashed curves for the other. If there are n dashed curves of the form BWB and m of the form IRSTUVP in correspondence with each coordinate system, then the three types of solid curves MTYWH, LSEUN, and KRFVK respectively contain $m+n$, $2m$, and $2m$ mesh points. When there are p mesh points along XYZ, q mesh points along DEFG, and no mesh points internal to the sides of the uncovered regions XCD and ZCD, the dashed curve IRSTUVP contains $p+2q$ mesh points and the dashed curve BWB contains $p+2$ points counting two periodic segments ABC in correspondence with the top and bottom of the Cartesian system. As the m dashed curves IRSTUVP are taken to vary from inner to outer boundaries, the coordinate mesh around the airfoil and branch cut is generated with a total of $(p+2q)m$ mesh points. From the $(p+2)n$ Cartesian mesh points in the upstream extension, the p juncture points common to both systems must be deducted to yield a total of $(p+2)n - p$ distinct points and a grand total of $(p+2)n + (p+2q)m - p$ for the entire mesh. Among the possible choices for m, n, p, q, only the choice of p will cause a change in the number of mesh points simultaneously for both systems. With the other choices, the number of mesh points is controlled entirely within the given coordinate system. Consequently, another advantage with the use of more than one coordinate system is that a local resolution for a given region can often be accomplished with the addition of mesh points in a local coordinate system while there is no increase in the number of mesh points in the other systems. As an example, a resolution of an airfoil boundary layer and wake can be accomplished with both a redistribution and an increase in the number (m) of dashed

coordinate curves IRSTUVP without an increase in the number of mesh points for the upstream extension. In the ADI splitting along dashed and solid curves respectively, the lengths of the resultant one-dimensional parts will vary within each ADI direction. Along the dashed curves, the lengths will be $p+2$ and $p+2q$ as the type is varied from BWB to IRSTUVP. Along the solid curves, the lengths are $m+n$ and $2m$ which are respectively the longest lengths obtained when periodicity is applied. An illustration of the computational mesh with periodicity indicated by point labels is given in Figure 10. In the rectilinear computational space, the primed letters are used to denote points in correspondence with the physical space in Figure 9. The dashed and solid curves are also matching with Figure 9.

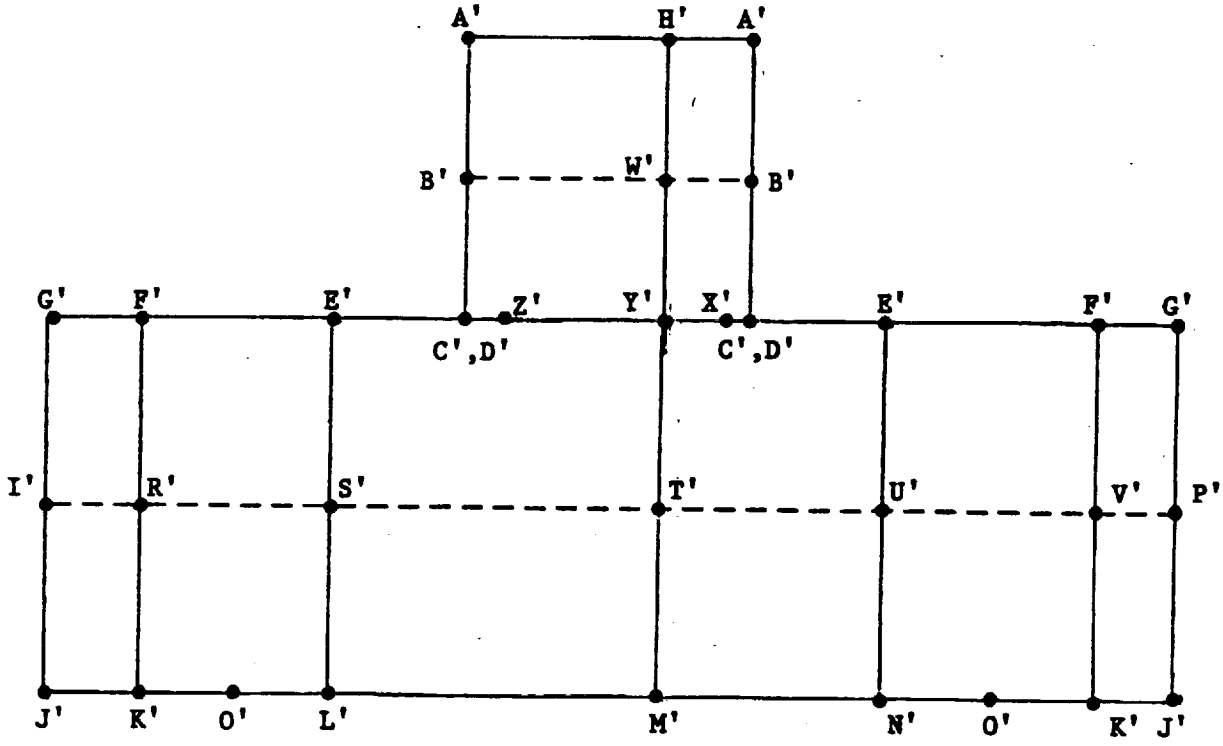

Figure 10: The Computational Space for the Cascade Depicted in Figure 9.

With the assumption that X, Z, C, and D are the only mesh points on the boundaries of the uncovered regions, C' and D' appear as the same computational point but are distinguished by the association of C' only with the upstream extension and D' only with the other system. In cases with such complicated computational spaces, the theory of ADI splitting is not very well developed and we must rely more on computational experience. Such experience has been gained on L-shaped regions where, for example, a flow over a rearward facing step has been computed. Also, some theory has been indicated in [110].

BOUNDARY CONDITION

Given a general form for the equations of motion and a numerical method for their solution, general boundary conditions must be obtained in order to develop a general algorithm for the numerical simulation of a flow field over any region which is described by one or more coordinate transformations. In addition to boundary conditions in coordinate directions, there must be the more general capability to specify boundary conditions as linear combinations of functions and derivatives which are taken in any direction and are applied to any scalar or vector quantity. For most fluid mechanics problems, only derivatives of order two or less need be considered. To form the necessary boundary conditions, expressions must be derived for generally directed derivatives and for a decomposition of the velocity vector into specified directions. With an assumed discretization from one or more coordinate systems, the coordinate frame (all $\vec{e}_j$ from Eq. 3) will be taken as a frame of reference since the geometric boundaries of objects in a flow field are fit with coordinate surfaces.

As a result, the Cartesian frame will not be needed as it was for the discussion on camber frames (Eqs. 125-129). Given the contravariant expansion of the velocity vector field $\vec{v} = v^i \vec{e}_i$ and a frame field of unit vector fields $\hat{f}_1, \hat{f}_2, \ldots, \hat{f}_n$, the projection of the velocity vector onto each frame field direction $\hat{f}_j$ is given by $(\vec{v} \cdot \hat{f}_j)\hat{f}_j = v^i(\vec{e}_i \cdot \hat{f}_j)\hat{f}_j$ and the sum of all projections yields the velocity decomposition into the specified frame field directions which is given by

$$\vec{v} = v^i(\vec{e}_i \cdot \hat{f}_j)\hat{f}_j \quad . \tag{186}$$

As an example, suppose that a two-dimensional physical boundary is described by a coordinate curve in the y^1-variable for some constant value of y^2 and that a velocity decomposition into normal and tangential directions is needed for the boundary conditions. The tangential direction is clearly determined by $\vec{e}_1$; the normal direction, by $\vec{e}^2$, as can be observed from the definition of contravariant vector fields (Eq. 17) which are illustrated in Figure 4. Upon normalization with Eqs. 7 and 21, the unit frame field along the bounding curve is defined by the unit tangents $\hat{f}_1 = \vec{e}_1/\sqrt{g_{11}}$ and the unit normals $\hat{f}_2 = \vec{e}^2/\sqrt{g^{22}}$. Again with Eqs. 7, 17, and 21, the dot products $\vec{e}_i \cdot \hat{f}_j$ are obtained and the results are inserted into Eq. 186 to give

$$\vec{v} = \left(v^1\sqrt{g_{11}} + v^2 \frac{g_{12}}{\sqrt{g_{11}}}\right)\hat{f}_1 + \frac{v^2}{\sqrt{g^{22}}}\hat{f}_2 \quad , \tag{187}$$

for the tangent-normal decomposition which is directly applicable when the solution frame is the coordinate frame. For other solution frames, the

coefficients must first be transformed into the coordinate frame to obtain the contravariant components v^i for Eq. 187 in a manner such as given in Eq. 128 where $\hat{f}_i$ represents a different frame. The transformation between solution and coordinate frames, as illustrated in the example, also carries over in general to both decompositions and derivative expressions that are given in contravariant components.

Derivative expressions along a boundary and in arbitrary directions can be obtained from the dot product of an arbitrarily specified unit vector field $\hat{f}$ and the gradient operator defined in Eq. 47. When the vector field directions $\hat{f}$ are locally integrated, a local coordinate z is determined in a neighborhood of the boundary by the condition that $\hat{f}$ is the field of natural tangents (Eq. 3) to the coordinates in the z-variable at points on the boundary. Since the natural tangets are of unit length, z is an arc length variable (Eq. 9). Consequently, the $\hat{f}$-direction derivative operator with respect to arc length z is given by

$$\frac{\partial}{\partial z} = \hat{f} \cdot \nabla \quad . \tag{188}$$

For a function a, an application yields the z-derivative

$$\frac{\partial a}{\partial z} = (\hat{f} \cdot \vec{e}^i) \frac{\partial a}{\partial y^i} \quad . \tag{189}$$

By an application to the velocity vector, the z-derivative of velocity becomes

$$\frac{\partial \vec{v}}{\partial z} = \hat{f} \cdot \nabla \vec{v}$$

$$= \hat{f} \cdot \left(\frac{\partial v^i}{\partial y^k} + v^m \Gamma^i_{km} \right) \vec{e}^k \otimes \vec{e}_i \qquad (190)$$

$$= (\hat{f} \cdot \vec{e}^k) \left(\frac{\partial v^i}{\partial y^k} + v^m \Gamma^i_{km} \right) \vec{e}_i \quad ,$$

where the second equality follows from Eq. 48. For second derivatives, consider another possibly different vector field of unit vectors $\hat{h}$ and its associated local arc length coordinate w in the boundary region. The general second derivative is then given by

$$\frac{\partial}{\partial w} \frac{\partial}{\partial z} = \hat{h} \cdot \nabla \, \hat{f} \cdot \nabla \quad , \qquad (191)$$

which is a repeated derivative in the same direction if $\hat{h} = \hat{f}$ and otherwise is a mixed derivative. For a function a, we have

$$\frac{\partial}{\partial w} \frac{\partial a}{\partial z} = (\hat{h} \cdot \vec{e}^i) \frac{\partial}{\partial y^i} \left[(\hat{f} \cdot \vec{e}^j) \frac{\partial a}{\partial y^j} \right] \quad , \qquad (192)$$

and for velocity,

$$\frac{\partial}{\partial w} \frac{\partial \vec{v}}{\partial z} = (\hat{h} \cdot \vec{e}^k) \left(\frac{\partial \beta^i}{\partial y^k} + \beta^m \Gamma^i_{km} \right) \vec{e}_i \quad , \qquad (193a)$$

where

$$\beta^i = (\hat{f} \cdot \vec{e}^j) \left(\frac{\partial v^i}{\partial y^j} + v^\ell \Gamma^i_{j\ell} \right) \quad . \qquad (193b)$$

As an example, suppose that normal derivatives are needed at a bounding surface described by curvilinear coordinates $y^2, \ldots, y^n$ for some constant value of y^1 in Eq. 2. In a parallel manner to the velocity decomposition example, the unit normal vector field is obtained from the contravariant basis field $\vec{e}^1$ which by definition (Eq. 17) is perpendicular to the basis

of boundary tangents $\vec{e}_2,\ldots,\vec{e}_n$. Upon division by its magnitude $\sqrt{g^{11}}$ from Eq. 21, the unit normal vector fields are given by

$$\hat{f} = \hat{n} = \frac{\vec{e}^1}{\sqrt{g^{11}}} \quad . \tag{194}$$

By substitution, the normal derivatives with respect to arc length z are given by

$$\frac{\partial a}{\partial z} = \frac{g^{1i}}{\sqrt{g^{11}}} \frac{\partial a}{\partial y^i} \quad , \tag{195a}$$

and

$$\frac{\partial^2 a}{\partial z^2} = \frac{g^{1i}}{\sqrt{g^{11}}} \frac{\partial}{\partial y^i} \left(\frac{g^{1j}}{\sqrt{g^{11}}} \frac{\partial a}{\partial y^j} \right) \quad , \tag{195b}$$

for a function a, and by

$$\frac{\partial \vec{v}}{\partial z} = \frac{g^{1k}}{\sqrt{g^{11}}} \left(\frac{\partial v^i}{\partial y^k} + v^m \Gamma^i_{km} \right) \vec{e}_i \quad , \tag{196a}$$

and

$$\frac{\partial^2 \vec{v}}{\partial z^2} = \frac{g^{1k}}{\sqrt{g^{11}}} \left(\frac{\partial \beta^i}{\partial y^k} + \beta^m \Gamma^i_{km} \right) \vec{e}_i \quad , \tag{196b}$$

where

$$\beta^i = \frac{g^{1j}}{\sqrt{g^{11}}} \left(\frac{\partial v^i}{\partial y^j} + v^\ell \Gamma^i_{j\ell} \right) \quad , \tag{196c}$$

for velocity.

With the derivative expressions, extrapolation boundary conditions can be directly specified in any direction by setting a derivative to zero in the

specified direction. When the unit vector field $\hat{f}$ defines the specified direction and z is the associated curve arc length, the extrapolation function is a polynomial in z of degree one less than the order of the vanishing derivative. For linear extrapolation to a boundary, the second derivative is set equal to zero at the boundary by use of Eq. 192 for scalars and Eq. 193 for vectors, where in each equation, $\hat{h} = \hat{f}$. The coordinate derivatives which appear in each equation must then be approximated to at least second order accuracy. With finite difference methods, one-sided differences would be used in from the boundary while central differences could be used for the other coordinate directions. For a skewed extrapolation, central differences would cause mesh points to appear on either side of the boundary mesh point where the derivative vanishing condition is applied. When ADI methods are applied along coordinate directions, an implicit boundary condition is usually applied for stability reasons, and as a consequence, points on either side of the given boundary point must be evaluated at the explicit level to avoid a lateral implicit coupling along and near the boundary which in turn would defeat the purpose of the ADI splitting. A skewed extrapolation will generally result when the direction of extrapolation is a characteristic direction which is used to avoid artificial numerical reflections from a transmissive boundary. As an example, a shock wave impinging upon a free stream transmissive boundary should not be reflected off of it, but instead, should pass through undisturbed. With the free stream Mach number, the shock angle can be computed relative to the velocity vector and the resultant direction can be used for extrapolation. From numerical experiments [111] with a 45° shock angle, extrapolations were taken separately in directions along the shock and normal to a transmissive boundary

intersecting the shock at 45°. Solutions were spatially marched in a direction along the transmissive boundary and the only disturbance in the flow was the shock wave of moderate strength. In the experiments, the only nonreflecting boundary condition occured when there was an alignment with the shock wave.

The extrapolation process given for first degree polynomials in z carries over to polynomials of an arbitrary degree j when the coordinate derivatives are suitably approximated. In general, the coordinate derivatives appear in the vanishing condition for the $(j+1)\delta t$ z-derivative of a quantity which defines the j*th* degree polynomial in z for the quantity. The $(j+1)\delta t$ z-derivative is obtained by $(j+1)$ successive applications of $\partial/\partial z$ defined in Eq. 188 as $\hat{f} \cdot \nabla$ and illustrated for general second derivatives in Eq. 191. In the case of zero*th* degree extrapolation in the $\hat{f}$ direction, $j = 0$ and the coordinate direction derivatives appear only up to first order as can be observed from Eqs. 189 and 190 and should be approximated to first order accuracy. In continuation, the first degree (above) and higher degree extrapolations will contain coordinate derivatives of order up to that of the vanishing z-direction derivative, each of which must be approximated to an accuracy consistent with the polynomial degree in z.

Extrapolation boundary conditions of the various degrees are useful in a variety of situations where boundary quantities can be approximated entirely from an assumed solution smoothness in a given direction. Typical cases occur with transmissive boundaries where disturbances must exit without reflection since the boundary locations are arbitrarily chosen to delete a part of the physical domain. Barring junctures between coordinate systems

(as in X Y Z of Figure 9), the remaining transmissive boundaries are an approximation of infinite distance where free stream conditions can be assumed as known. As a consequence, even the specification (using Eq. 186) of freestream values (Dirichlet conditions) along the transmissive boundaries can be viewed as a zeroth degree extrapolation from values at infinity. When the transmissive boundaries are placed in close proximity to the object under study, the approximation to infinite conditions will usually not be accurate unless further information about the solution is used. For example, in the study of Engquist and Majda [112] a linear two-dimensional scalar wave equation is considered where the general solution is a superposition of simple waves which is used to derive a pseudo-differential operator (that contains a square root of differential operators) as a nonreflecting boundary condition which in turn is approximated to obtain differential operator boundary conditions for successive levels of accuracy. In continuation, they applied their technique to the shallow water equation and were able to reduce reflections at the transmissive boundaries. However, when viscous compressible flows are considered, the desired information about the solution is usually not complete enough to directly use the methods of Engquist and Majda. Another method has been considered by Hedstrom [113] and extended by Rudy and Strikwerda [114] and [115] to obtain non-reflecting subsonic downstream boundary conditions for pressure. The conditions increase the convergence rate to a steady state in cases where a constant static pressure p_∞ can be assumed for the steady state flow on the downstream transmissive boundary. Transmissive boundaries have been investigated from a number of viewpoints ([116] - [124]) and further research on this subject is needed, especially when the boundaries are close to solid objects in the flow. By

comparison, with supersonic transmissive boundaries, no specifications are needed and an extrapolation of characteristic variables (c. f. [118]) in characteristic directions could be expected to give successful results in a number of cases for both implicit and explicit boundary conditions.

At solid boundaries to a viscous flow, the physical no-slip boundary conditions are used with the specification of zero velocity or some close approximation to it. It then remains to determine the density or pressure and the energy. Choices have varied from extrapolation to an application of the equations of motion such as a differentiated continuity equation (for doubly specifiably boundaries), a momentum equation, or a known approximate potential flow solution. For implicit conditions, a time-like linearization is necessary. In a parallel to boundary layer theory, boundary conditions for surface pressure can be obtained from the normal momentum equation as given by Steger [29]. From the frame field viewpoint, the normal momentum equation comes directly with the choice of a frame for derivatives where the normal direction is part of the frame.

Further types of boundaries include junctures between coordinate systems and surfaces about which a region is extended by use of reflective symmetry. The application of reflective conditions can be accomplished with a small band of reflected mesh points, with equations of motion, and with extrapolation where even functions such as scalars and odd functions such as normal velocity components are obtained from polynomials in a normal direction variable z which respectively contain only even or odd powers. Junctures

between a coordinate system or systems such as XYZ or the branch cut OKJ in Figure 9 are given by periodic conditions where in effect the boundary point is treated as if it were an interior point unless there is a lack of smoothness in the mesh; and hence, a need for special treatment as would occur with a derivative discontinuity which would require one-sided differencing for finite difference methods. When the juncture is an uncovered region caused by the mesh topology as in XCD of Figure 9, there is no required special treatment provided that the region is small enough to not disturb the flow field solution beyond normal truncation error and that no mesh lines dead end at the region. In the latter case, mesh lines which dead end can be directly treated by extrapolation or by one sided equations of motion.

With the general mesh topology that caused the uncovered regions, there is clearly the capability to resolve certain high gradient regions in a truely local sense and to still obtain a reasonable mesh in other regions such as the Cartesian upstream extension ABCXYZCBAHA in Figure 9. In general, the simultaneous application of several coordinate systems can be used to extend coordinate boundaries to approximate more closely far field condtions without a sacrifice in the basic mesh structure beyond and near the solid objects where steep gradients exist. As a consequence, there is a balance to be made between a composite mesh extension with simple far field boundary conditions and a single coordinate mesh of limited extent where the imposition of far field boundary conditions are more complex since severe flow irregularities would be shed from the solid boundaries, would probably not be dissipated when the close in transmissive boundary is reached, and would have to be passed out of the region without reflection.

MESH GENERATION FROM COORDINATE TRANSFORMATIONS

As the state of computational fluid dynamics has advanced, so has the desire to utilize these advances to perform complicated and extensive flow field simulations. Included in the simulations are those which involve the complex geometric boundaries and topologies which commonly appear in turbomachinery. As the trend continues, the critical importance of the mesh generation process has become evident. In the mesh problem a complicated region must be discretized in a suitable manner before the desired numerical simulation can even be attempted. The constraints placed upon the mesh will vary with the flow field properties and with the numerical method to be applied. The weakest constraints are associated with finite element methods since an integration by parts lowers the required level of smoothness (differentiability) and since the given region can be more generally discretized with triangles (with possibly one curved side, [48]) rather than by rectangles. The major restriction on the triangles is that they cannot become too distorted or else accuracy would suffer [48]. Besides the topological generality, the main advantage of the triangular decomposition is that certain regions of critical importance can be resolved in an area sense. By contrast, the unmodified application of a single coordinate transformation is restricted to a gridded structure in which the addition of coordinate curves for the resolution of a given area will also extend to other areas; thus, mesh points would be wasted. However, the problem of resolution in an area sense, as examined in Figure 9, can also be accomplished with a composite of coordinate transformations. A major advantage with the application of coordinate transformations, whether in an isolated sense or in a collective sense, is that the matrix inversion problem is generally

simplier than for triangular meshes. Typical matrix structures associated with coordinate transformations usually have a high degree of regularity (such as simple banded structures) rather than the more general sparse matrix which requires the application of special inversion techniques ([125] and [126]). For finite difference methods, the mesh must have a high degree of regularity and smoothness. Moreover, when a collection of sufficiently smooth coordinate transformations are smoothly joined together to generate a composite mesh, finite difference methods can be used to obtain solutions with the same topological and area resolution properties that were intrinsic to finite element methods. In between finite difference and finite element methods, there are finite volume methods ([49] and [51]) which also require the structural regularity from coordinate transformations but which require a lower level of smoothness since the governing equations are expressed by an integral rather than by a differential expression. In any case, no matter which numerical method is used, an examination of coordinate generation techniques is needed when a general algorithm for flow field simulation is constructed to accept regularly structured geometric data as input. In the previous sections, various equation formulations, numerical methods, and boundary conditions were presented in a manner from which such an algorithm can be constructed in a variety of ways for various classes of problems.

In the examination of coordinate generation techniques, various types of coordinates will be considered and evaluated in terms of the constraints that are needed to adequately discretize complicated regions for the purpose of flow field simulation. The constraints arise from fluid dynamic properties, solid boundaries and their arrangement, junctures between coordinate

systems, and a desired general level of coordinate simplicity. The creation of smooth junctures between coordinate systems and the minimization of mesh distortion throughout each system both lead to simplicity for the entire mesh which on a local level can be measured by the metric (Eq. 15). Simplicity is obtained relative to the collective application of all constraints, and as a result, metric simplicity will be limited by the constraints. In general, the broad classes of coordinate transformations in the order of increasing metric complexity are given by conformal, orthogonal, and nonorthogonal transformations. A similar ordering also can be given for general space-time transformations. To examine coordinate systems either on an individual basis or in a broad sense, the constraints above are considered in geometric terms and are separated into the categories of boundary specifications, uniformity specifications, and interanl specifications. Boundary specifications include the basic geometry of solid objects, the junctures between systems, the boundary coordinates or equivalently pointwise distributions, the angles of coordinate curves which enter a boundary, and the rates of entry for such coordinate curves. Uniformity specifications are applied to either local or global distributions of coordinate curves or points to form a basis from which the curves or points can be redistributed by an a priori specification of a distribution function or by a solution adaptive approach, both without distortion from the underlying transformation. Internal specifications are applicable when an interior shape is needed or when an interior mesh structure such as a Cartesian or Polar system is to be smoothly embedded within a global mesh to simplify a flow field simulation in the given region. When boundary geometry is specified without a required distribution of boundary points,

conformal transformations can be used. When the distribution of boundary points are also specified, conformal transformations are inadequate and must be replaced by either orthogonal or nonorthogonal systems. As further constraints are added, a greater degree of precision is required to control the mesh in order to satisfy the given specifications. The requirement for precise controls leads to the development of the general multisurface transformation. As a consequence, the discussion shall start with conformal methods, continue to orthogonal and nonorthogonal methods, and end with the multi-surface method.

Conformal Transformations

A conformal transformation is a mapping which preserves angles between any pair of intersecting curves. When a Cartesian system of curvilinear variables $(y^1,y^2,\ldots y^n)$ is mapped into the space under study by means of Eq. 2, the lines $\vec{\gamma}_j(t) = (y^1,\ldots,y^{j-1},y^j+t,y^{j+1},\ldots y^n)$ and their natural tangents $\hat{u}_j$ (which are obtained by differentiation with respect to t) are mapped respectively into curves $\vec{x} \circ \vec{\gamma}_j(t)$ and their natural tangents $\vec{e}_j$ given by Eq. 3. Under a conformal transformation, the orthogonality $(\hat{u}_i \cdot \hat{u}_j = \delta_{ij})$ between the curves $\vec{\gamma}_i$ and $\vec{\gamma}_j$ must be preserved with the image curves $\vec{x} \circ \vec{\gamma}_i$ and $\vec{x} \circ \vec{\gamma}_j$ which means that $g_{ij} = \vec{e}_i \cdot \vec{e}_j$ vanishes for $i \neq j$. Similarly, the orthogonality between the lines $\vec{\alpha}^c_{ij}(t) = (y^1,\ldots,y^{i-1},y^i+t,y^{i+1},\ldots,y^{j-1},y^j+ct,y^{j+1},\ldots,y^n)$ for $c = 1$ and -1 must also be preserved. Consequently, the natural tangents $\vec{e}_i + c\vec{e}_j$ corresponding to $c = 1$ and -1 must be orthogonal. Thus, $0 = (\vec{e}_i+\vec{e}_j) \cdot (\vec{e}_i-\vec{e}_j) = \vec{e}_i \cdot \vec{e}_i - \vec{e}_j \cdot \vec{e}_j = g_{ii} - g_{jj}$ for all i and j. As a result,

the matrix of metrics is diagonal with equal entries; hence it has a determinant $g = g_{11}^{n}$ and from Eq. 11 a Jacobian $J = (g_{11})^{n/2}$. In terms of the Jacobian, the metric (Eq. 15) for conformal transformations is given by

$$(ds)^2 = |J|^{2/n} \{(dy^1)^2 + (dy^2)^2 + \ldots + (dy^n)^2 \} , \qquad (197)$$

which in two-dimensions reduces to

$$(ds)^2 = |J| \{(dy^1)^2 + (dy^2)^2\} . \qquad (198)$$

Also in two-dimensions, functions of one complex variable can be applied to generate conformal mappings when the functions are analytic. For analytic functions, $f(y^1 + \sqrt{-1}\, y^2) = x^1 + \sqrt{-1}\, x^2$, the Cauchy-Riemann conditions are valid and are given by

$$\frac{\partial x^1}{\partial y^1} = \frac{\partial x^2}{\partial y^2}$$

and (199)

$$\frac{\partial x^1}{\partial y^2} = - \frac{\partial x^2}{\partial y^1}$$

which can be inserted into the definition of the Jacobian (Eq. 5) to yield

$$J = \begin{pmatrix} \frac{\partial x^1}{\partial y^1} & -\frac{\partial x^2}{\partial y^1} \\ \frac{\partial x^2}{\partial y^1} & \frac{\partial x^1}{\partial y^1} \end{pmatrix} = \left(\frac{\partial x^1}{\partial y^1}\right)^2 + \left(\frac{\partial x^2}{\partial y^1}\right)^2 = \left(\frac{\partial x^2}{\partial y^2}\right)^2 + \left(\frac{\partial x^1}{\partial y^2}\right)^2 , \quad (200)$$

where the last equality follows by another application of Eq. 199. The metric given in Eq. 198 can also be derived directly from the Cartesian arc length expansion (Eq. 13) with the aid of Eqs. 199 and 200 which develops in the manner

$$\begin{aligned} (ds)^2 = (dx^1)^2 + (dx^2)^2 &= \left(\frac{\partial x^1}{\partial y^k} dy^k\right)^2 + \left(\frac{\partial x^2}{\partial y^k} dy^k\right)^2 \\ &= J(dy^1)^2 + 2\left(\frac{\partial x^k}{\partial y^1}\frac{\partial x^k}{\partial y^2}\right)dy^1 dy^2 + J(dy^2)^2 \qquad (201) \\ &= J\left\{(dy^1)^2 + (dy^2)^2\right\} . \end{aligned}$$

With the two-dimensional conformal metric $g_{ij} = J\delta_{ij}$ from Eqs. 198 or 201, the Christoffel sysmbols from Eq. 37 become

$$\Gamma^1_{11} = \Gamma^2_{12} = -\Gamma^1_{22} = \frac{\partial}{\partial y^1}(\log \sqrt{J})$$

and (202)

$$\Gamma^2_{22} = \Gamma^1_{12} = -\Gamma^2_{11} = \frac{\partial}{\partial y^2}(\log \sqrt{J}) \quad .$$

The metric information including the resulting Christoffel symbols, can be used both to define a system of governing equations in the coordinates and to examine the coordinate structure. Since the metric is determined solely

in a scaled Cartesian sense with the Jacobian as the factor, the spatial variance in the coordinate structure is just a dilation. Upon discretization, the dilation can be observed in a mesh of approximate squares which very in size. For large or unbounded regions, the rate of dilation is often quite large which, for viscous flow anlyses, poses a problem of adequate resolution in upstream and downstream directions. In addition, the conformal structure imposes a distribution of points along the bounding contours, as can be observed from the analytic continuation arguments of complex variable theory. Although a bounding contour may then be adequately fit, the imposed distribution of points along the contour may also be inconsistent with the distribution of solution gradients which would appear with viscous flow problems. In contrast with the absence of control over mesh dilation and the distribution of boundary points, an advantage is the direct formulation of inviscid, incompressible potential flow information which in itself can be useful.

When boundaries of the flow region can be fit with analytically formulated transformations, when mesh dilation is of little concern, and when the distribution of boundary points is unimportant, conformal transformations are optimal in the sense of problem simplicity because of the metric structure (Eqs. 198 or 201) and the direct formulation. In a number of cases boundaries can be fit by means of a sequence of simple conformal transformations. However, in most cases of practical importance, the boundary shapes are too complicated; and consequently, cannot be simply fit as desired. Thus, approximate methods must be considered. For general airfoil shapes, the method of Theodorsen and Garrick [127] has been extended by Ives [128] and applied to both cascades [128] and two element airfoils [130] where, in each

case, the Fast Fourier Transform was used to gain computational efficiency in the generation process. Each of those techniques maps airfoils to near circles through a sequence of simple transformations which is followed by a Fourier type transformation to take the near circle into an exact one so that the overall transformation is conformal. For shapes that are more general than airfoils, Schwartz - Christoffel type transformations can be applied to approximately fit the contours. The first systematic Schwartz - Christoffel technique was developed by Anderson [131] who used the classical form with piecewise linear curves. This technique works best for simply connected regions where no branch cuts are needed. However, a basic limitation in this method is the poor representation of wall currature which can be partially resolved by rounding the corners in the manner discussed by Henrici [132]. In further work, Davis [133] applied the curved-sided formulation from Woods [134] to remove some more of the curvature problems. To alleviate the complexity that is often required to fit boundaries with conformal transformations, nearly conformal transformations have been used by Jameson [31] to remove the need for a Fourier analysis on airfoil contours and by Caughey [135] to remove the need for a precise fit with Schwartz - Christoffel transformations. In each case, easily formulated conformal transformations are used to obtain approximately the right shape which is then made into a precise fit by means of a simple shearing transformation. The result is a slightly nonorthogonal system of coordinates. If the shearing transformation is replaced by the multi-surface transformation [136] to be discussed in a following section, then orthogonality and even conformality can be retrieved on major portions of the region.

Orthogonal Transformations

When conformal mappings are not easily obtained or when more control over mesh distributions is needed, the slightly larger class of orthogonal transformations should be considered next since it will still yield a fairly simple metric structure. For orthogonal transformations, $g_{ij} = \vec{e}_i \cdot \vec{e}_j$ vanishes when $i \neq j$ which leaves only the diagonal entries g_{ii} in the metric which then is given in the form

$$(ds)^2 = g_{11}(dy^1)^2 + g_{22}(dy^2)^2 + \ldots + g_{nn}(dy^n)^2 \quad , \qquad (203)$$

where the coefficients may be unequal. To clarify the distinction between orthogonal and conformal transformations, consider a fixed point and the coordinates in a small neighborhood around it. In the neighborhood, the functions g_{ii} are nearly equal to their values at the point; thus, the measurement of distance (Eq. 203) along coordinate curves is very nearly given by distance measurements along the respective vectors $\vec{e}_i$ in the space of tangents attached to the point in question. When the functions g_{ii} are all equal, the distance measurement in the tangent space is merely a uniform dilation or contraction of the original Cartesian system. Consequently, length ratios, and hence, angles are preserved between the Cartesian sysem and the tangent space. But then the direction of a vector in the tangent space corresponds precisely with the curves which pass through the point and have the vector as a tangent. Hence, the transformation with equal diagonal entries preserves angles and is therefore conformal by the original definition. Moreover, since the implication of angle preservation from a metric form is a converse to the derivation of the metric form from

angle preservation, the metric form as given by Eq. 197 can be used as a definition for conformality. Consequently, as the length ratios $\sqrt{g_{ii}} / \sqrt{g_{jj}}$ for distinct i and j deviate from unity, the transformation smoothly deviates from conformality.

When two-dimensional conformal transformations are applied to obtain a rotationally symmetric system of three-dimensional coordinates, the resulting system is orthogonal but not conformal. In particular, such a transformation is given by

$$\begin{aligned} x^1 &= u \\ x^2 &= v \sin y^3 \\ x^4 &= v \cos y^3 \end{aligned} \tag{204}$$

where $f(y^1 + \sqrt{-1}\, y^2) = u + \sqrt{-1}\, v$ is analytic. For the angle $y^3 = \pi/2$, Eq. 204 reduces to the two-dimensional case where $u = x^1$ and $v = x^2$ and the Jacobian J is given by Eq. 200. With the aid of the Cauchy-Riemann conditions (Eq. 199 with $x^1 = u$, $x^2 = v$), the Jacobian H for Eq. 204 is given by

$$\begin{aligned} H &= \det \begin{bmatrix} \dfrac{\partial u}{\partial y^1} & \dfrac{\partial u}{\partial y^2} & 0 \\ \dfrac{\partial v}{\partial y^1} \sin y^3 & \dfrac{\partial v}{\partial y^2} \sin y^3 & v \cos y^3 \\ \dfrac{\partial v}{\partial y^1} \cos y^3 & \dfrac{\partial v}{\partial y^2} \cos y^3 & -v \sin y^3 \end{bmatrix} \\ &= \frac{\partial u}{\partial y^1}\left(-v \frac{\partial v}{\partial y^2}\right) - \frac{\partial u}{\partial y^2}\left(-v \frac{\partial v}{\partial y^1}\right) = -v\left[\left(\frac{\partial u}{\partial y^1}\right)^2 + \left(\frac{\partial v}{\partial y^1}\right)^2\right] = -v J \ , \end{aligned} \tag{205}$$

and the metric, by

$$
\begin{aligned}
(ds)^2 &= (dx^1)^2 + (dx^2)^2 + (dx^3)^2 \\
&= \left[\frac{\partial u}{\partial y^1}\, dy^1 + \frac{\partial u}{\partial y^2}\, dy^2\right]^2 \\
&\quad + \left[\frac{\partial v}{\partial y^1}(\sin y^3)\, dy^1 + \frac{\partial v}{\partial y^2}(\sin y^3)\, dy^2 + (v \cos y^3)\, dy^3\right]^2 \\
&\quad + \left[\frac{\partial v}{\partial y^1}(\cos y^3)\, dy^1 + \frac{\partial v}{\partial y^2}(\cos y^3)\, dy^2 - (v \sin y^3)\, dy^3\right]^2 \qquad (206) \\
&= \left[\left(\frac{\partial u}{\partial y^1}\right)^2 + \left(\frac{\partial v}{\partial y^1}\right)^2\right](dy^1)^2 + \left[\left(\frac{\partial u}{\partial y^2}\right)^2 + \left(\frac{\partial v}{\partial y^2}\right)^2\right](dy^2)^2 \\
&\quad + 2\left[\frac{\partial u}{\partial y^1}\frac{\partial u}{\partial y^2} + \frac{\partial v}{\partial y^1}\frac{\partial v}{\partial y^2}\right] dy^1 dy^2 + (v)^2 (dy^3)^2 \\
&= J(dy^1)^2 + J(dy^2)^2 + (v)^2 (dy^3)^2 \quad .
\end{aligned}
$$

On substitution of the metric coefficients $g_{11} = g_{22} = J$, $g_{33} = (v)^2$ into Eq. 37, the nonvanishing Christoffel symbols become

$$
\begin{aligned}
&\Gamma^1_{11} = \Gamma^2_{12} = -\Gamma^1_{22} = 2\Gamma^3_{13} = \frac{\partial}{\partial y^1} \log \sqrt{J} \\
&\Gamma^2_{22} = \Gamma^1_{12} = -\Gamma^2_{11} = 2\Gamma^3_{23} = \frac{\partial}{\partial y^2} \log \sqrt{J} \qquad (207) \\
&\Gamma^1_{33} = -\frac{v}{J}\frac{\partial v}{\partial y^1} \\
&\Gamma^2_{33} = -\frac{v}{J}\frac{\partial v}{\partial y^2} \, .
\end{aligned}
$$

When the two-dimensional conformal mapping f is taken as the identity mapping, the rotationally symmetric transformation of Eq. 204 reduces to cylindrical coordinates with metric data $g_{11} = g_{22} = 1$, $g_{33} = (y^2)^2$ and a nonzero Christoffel symbol $\Gamma^2_{33} = -y^2$.

To generate orthogonal coordinates, there are methods which simply compute orthogonal trajectories to a given family of surfaces and methods which come entirely from the solution to a system of parital differential equations. For orthogonal trajectories in two dimensions, a family of smooth non-intersecting curves is generated between two bounding surfaces and then, from a specified distribution of points on one boundary, the orthogonal trajectories are computed until the other boundary is reached. When the family is composed of a continuum of curves, a smooth field of normal vectors can be constructed and from each point on one boundary, a curve with its tangent field determined by the normal field can be analytically specified as an intgral which starts at the point and ends somewhere on the other boundary. When such integrals are computed for all points on the first boundary, the family of orthogonal trajectories is obtained which, on combination with the originally generated family, forms an orthogonal coordinate system. If the original family of curves is generated not as a continuum but instead as a finite collection which almost uniformly subdivides the region, then orthogonal trajectories must be numerically computed from curve to curve starting with the first boundary and continuing, as before, until the second boundary is reached. An algorithm to generate orthogonal trajectories to the finite family of curves was given by McNally [137]. In McNally's method each trajectory is advanced from curve to curve in three steps: first, a normal line is

is sent from the present curve to the succeeding curve; second, a normal line from the succeeding curve is sent back to the trajectory location on the present curve; and third, the trajectory is advanced as a line which is nearly half way between the previous two. The result is an approximate set of orthogonal trajectories which converges to analytically defined trajectories as the finite family converges to a continuum. Applications of McNally's method were given by Graves [138] to generate orthogonal coordinates from isolated objects to a surrounding far field boundary. In each case, the trajectories were started from a specified distribution of points on the object, progressed through the finite family of curves and ended upon the far field boundary. As in all orthogonal trajectory methods, the distribution of points on the final target boundary is not arbitrarily specified; but instead, is determined by both the initial distribution on the starting boundary and the choice of curves in the specified family. As a consequence, the pointwise distribution on the far field boundary was especially sensitive to the geometry of the isolated objects. Results were generally good for convex objects since the trajectories were mildly distributed which lead to minor deviations from an arc length distribution on the far field boundary. However, with concave objects, the trajectories became severely bunched; and by the time the far field boundary was reached, the distribution was severely distorted relative to arc length. To relieve the severe bunching of coordinate curves, Steger and Chaussee [139], in a preliminary study, considered the orthogonality relationship ($g_{12} = 0$) and a Jacobian specification (J in Eq. 5) as a pair of hyperbolic partial differential equations to be solved from the isolated object into the far field. On application to a highly concave object they were able to relieve

the bunching problem. In a similar manner, an initial value problem was also considered earlier by Stadius [140] who generated orthogonal coordinates from a different hyperbolic system with different specifications. In either study, the solution to the hyperbolic system not only determines the distribution of points on the outer boundary, but indeed also the boundary itself. For external flow problems over a single object, the precise form of the far field boundary is not particularly important so long as the geometric variations are mild. By contrast, however, the outer boundaries for internal flows must often meet precise specifications. One important example is an outer boundary where periodicity conditions are required as in the case with cascades of airfoils (eg. D E F G in Figure 9). For such cases, we must be able to precisely specify both inner and outer boundaries along with their pointwise distributions. In a preliminary study, the present author [141] has considered a linear elliptic system derived from a specified metric. Additional controls on general mesh clustering also exist within the system. However, the precise level of control that is needed to specify an internal mesh structure is not readily available in this context and for that purpose nonorthogonal coordinates must be considered. In particular, with the multi-surface coordinates [136] to be considered subsequently, such controls are available and can be applied, for example, to establish a uniform distribution of coordinate curves which can be redistributed without distortion by any distribution function.

Non-Orthogonal Transformations

The capability to prescribe mesh properties is only partially available with orthogonal systems and can more readily be obtained with the larger class of nonorthogonal systems. Among the first properties to be prescribed were the specifications of both the boundary geometry and the distribution of boundary points. As a generalization from the complex variable techniques for conformal mapping, Laplace equations for each Cartesian direction in the physical domain were solved in the rectilinear domain of curvilinear variables with the boundary geometry and pointwise distributions combined into a specification of boundary conditions [142]. The boundary conditions are needed to obtain the prescribed properties and are the cause of the deviation from conformality into a nonorthogonal system. As can be expected, this deviation is greatest near the physical boundaries where there is a forced distribution of mesh points, and then gradually, there is an approach to conformal conditions in going from the boundaries toward the interior of the region. In addition to the specification of boundary locations and pointwise distributions, periodic boundary conditions were also specified to obtain branch cuts of various sorts. The location of and the pointwise distribution along the cuts could not be given in advance since such properties were then determined by the solution of the system of partial differential equations. For applications to a cascade of airfoils, the periodic boundary then cannot be given by periodic boundary conditions since there would be no assurance that the intended periodic portions would even have the same shape. To obtain coordinate systems for cascades of airfoils or blade shapes without the need to solve elliptic partial differential equations, an algebraic approach was developed [143]. The

observation was made that the boundary geometry and the pointwise distribution along the boundary could be separated into an intrinsic parameter (in two-dimensions, usually arc length) discription of the boundary geometry and a choice of parameterization for the pointwise distribution which can be applied relative to the intrinsic parameterization. With a general parameterization $\vec{t}$, the algebraic transformation was given by the simple linear deformation

$$\vec{P}(r,\vec{t}) = \vec{P}_1(\vec{t}) + r[\vec{P}_2(\vec{t}) - \vec{P}_1(\vec{t})] \quad , \tag{208}$$

which fits the boundaries $\vec{P}_1(\vec{t})$ and $\vec{P}_2(\vec{t})$, respectively when $r = 0$ and 1. For the cascade of airfoils, $\vec{t}$ is a scalar t which parameterizes both the airfoil contour $\vec{P}_1$ and an outer boundary $\vec{P}_2$ where periodicity is applied on portions above and below the airfoil. The periodic alignment is obtained with the same shape specification for each portion and with a choice of parameterization that yields a precise matching of mesh points. An example is given in Figure 11 where three of the coordinate systems are stacked on top of each other to display the periodic alignment. In addition, the independent variable r was replaced by a distribution function $R(r)$ so that an attached boundary layer could be resolved. The distribution function [144] was chosen to be

$$R(r) = mr + (1-m)\left[1 - \frac{\tanh D(1-r)}{\tanh D}\right] . \tag{209}$$

Here, the ratio of hyerbolic tangents is a homotopy parameter in the linear deformation of the line $R = mr$ into the line $R = m(r-2) + 2$. The rate

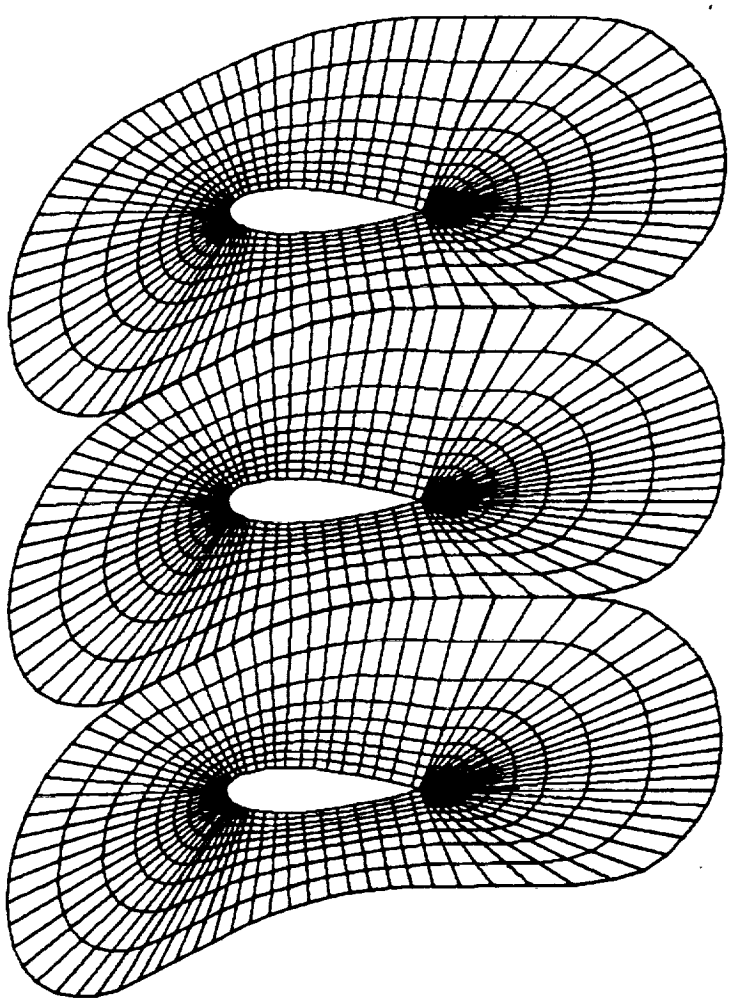

Figure 11. A Cascade of NACA 0024 Airfoils. The camber curve is bent so that the coordinate system can be aligned with an arbitrary upstream flow direction.

of deformation is controlled by a damping factor D; this determines the length of essential adherence to the line $R = mr$. The slope m is chosen so that the resulting line would yield a uniform mesh which is fine enough to resolve the given boundary layer region.

The distribution is, in fact, a generalization of the distribution due to Roberts [144]. For n mesh points and a constant $a > 0$, his distribution is given in inverse form as a map from a physical domain [-a, a] into a computational range [1,n]. From an inversion and a normalization of the range and domain to the interval [-1,1], his distribution reduces to a normalized hyperbolic tangent. A rigid translation then corresponds to the special case with $m = 0$. As a result, the damping factor is the only control on the shape of his distribution.

Cascade coordinates have also been obtained [145] with a generalization [146] of the earlier elliptic system [142] to one which is based on Poisson equations rather than Laplace equations. The source terms in the Poisson equations were used as forcing functions to push the coordinate curves around within the region. With the cascade coordinates [145], Dirichlet boundary conditions were required to impose periodicity; and the forcing functions were used to limit, to some degree, the mesh distortion. In both the algebraic and the partial differential equation approaches, however, the periodic mathcing was continuous but not differentiable. Slope discontinuities across the periodic boundary segments can be observed from Figure 11 and from the differential equation results when the latter is stacked in a similar fashion. As a consequence, we must not only specify the boundary geometry and its pointwise distribution, but also the direction and the rate for which coordinate curves enter the boundary. For higher order derivative continuity, even more specifications

must be added to the list. However, in many applications first derivative continuity is sufficient since higher order errors can be made small enough to be dissipated, for example, by finite differences where the errors are on the order of the truncation error. To obtain first order derivative continuity at the periodic cascade boundaries with the differential equation approach, either a higher order system with more specifiable boundary conditions or else a method to determine suitable forcing functions would be required. Since coordinate system nonsingularity depends upon a maximum principle [147] which would probably be lost with a higher order system (e.g., $x^2y + xy - xy^2$ is a solution to the biharmonic equation on $[-1,0] \times [0,1]$ which has a minimum at $(-1/3, 1/3)$), the determination of suitable forcing functions has the best chance of success. With a branch cut specified by Dirichlet conditions, some success over a previous case [147] has been obtained by an iteration on the forcing functions [148]. The iteration was necessary because the choice of forcing function is coupled to its affect only through the solution to the system of partial differential equations. By contrast to the partial differential equation approach, the multi-surface method [136] of coordinate generation can be directly used to obtain all of the desired specifications necessary to prescribe branch cuts to any fixed level of smoothness. Moreover, it is an algebraic approach which is computationally efficient and is multi-dimensional [149]. On computation, the efficiency comes about since the constructive process is done as a short sequence of lower dimensional problems. In addition, precise local controls are available for the precise specification of mesh forms anywhere within the region under consideration. Unlike the forcing functions of the differential equation approach, the local con-

trols are applied to a local region outside of which the mesh is not altered. The difference is that the forcing functions are clustering controls which can be applied locally but which change the mesh as a whole due to the ellipticity of the mesh generating system.

The Multi-Surface Transformation

When curvilinear coordinator are employed in the numerical solution of a boundary value problem, constraints must often be placed upon the coordinates, in addition to the basic requirement that the bounding surfaces are coordinate surfaces of one or more coordinate systems. The locations of the constraints can occur anywhere in the problem domain. On the boundaries, a particular pointwise distribution may be needed; in regions near boundaries, a particular coordinate form may be advantageous; and away from the boundaries, an internal coordinate specification may also be required. Typically, the constraints will arise either to resolve regions with large solution gradients or to cause some simplification in the problem formulation and solution.

In conjunction with the demand for constraints, the general multi-surface transformation [136] must be examined. The multi-surface transformation is a method for coordinate generation between an inner bounding surface $\vec{P}_1$ and outer bounding surface $\vec{P}_N$. To establish a particular distribution of mesh points on each bounding surface, a common parameterization $\vec{t}$ is chosen for each surface. This is equivalent to a coordinate description of the surfaces which yields the desired surface mesh when the parametric components of $\vec{t}$ are given a uniform discretization. With the parametric description, the inner and outer bounding surfaces are denoted by $\vec{P}_1(\vec{t})$ and $\vec{P}_N(\vec{t})$ respectively. At this stage, coordinates could be

generated along the straight line segments connecting points of common parametric value on each bounding surface as in Eq. 208. In continuation, parameterized intermediate surfaces $\vec{P}_2(\vec{t}),\ldots,\vec{P}_{N-1}(\vec{t})$ are introduced so that they can be used as controls over the internal form of the coordinates. The intermediate surfaces are not coordinated surfaces; but instead, are surfaces which are used to establish a vector field that is composed of tangent vectors to the coordinate curves spanning the coordinate system to connect bounding surfaces. It is also assumed that the collection of surfaces $\vec{P}_1(\vec{t})$, $\vec{P}_2(\vec{t}),\ldots,\vec{P}_N(\vec{t})$ is ordered from bounding surface to bounding surface. An illustration is given in Figure 12. For a fixed parameter value $\vec{t}$, there is a corresponding point on each surface. The piecewise linear curve obtained by connecting corresponding points is given by the dashed curve in Figure 12. From the figure, it can be observed that the tangent directions determined by the piecewise linear curve are piecewise constants. As $\vec{t}$ is varied, the field of tangent directions obtain their smoothness only in $\vec{t}$. To obtain smoothness in going from bounding surface to bounding surface, a sufficiently smooth interpolation must be performed. The result is a smooth vector field of undetermined magnitude which gives the desired tangential directions for coordinate curves connecting the bounding surfaces. A unique vector field of tangents is then obtained by correctly choosing magnitudes so that, on integration, the bounding surfaces are fit precisely.

In symbols, a vector field tangent to the piecewise-linear curves is given by

$$\vec{V}_k(\vec{t}) = A_k[\vec{P}_{k+1}(\vec{t}) - \vec{P}_k(\vec{t})] \quad , \tag{210}$$

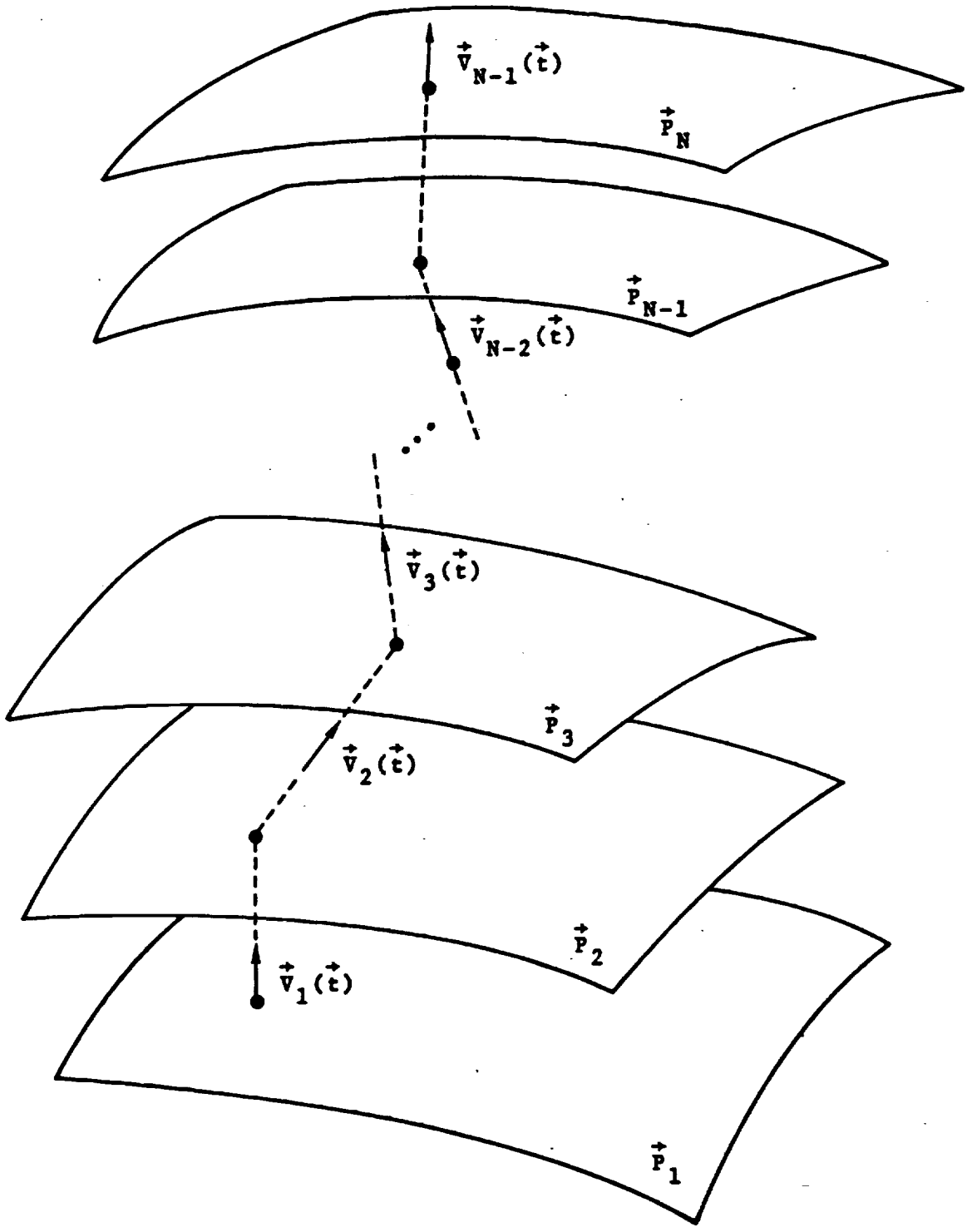

Figure 12. A Piecewise-Linear Curve and its Tangent Field

between the kth and $(k+1)^{\delta t}$ surfaces where k is taken to vary (if $N > 2$) from the first bounding surface to the final intermediate surface. These vectors are indicated in Figure 12. The coefficients A_k are scalars which determine the magnitude of the vectors but not the directions. An independent variable r is assumed for the spanning direction. A vector valued function which is discrete in r can now be defined as a map from r_k into $\vec{V}_k$ for a partition $r_1 < \ldots < r_{N-1}$ and for $k = 1,\ldots,N-1$. For notational simplicity, we will take $r_1 = 0$ and $r_{N-1} = 1$. A sufficiently smooth vector field $\vec{V}(r,t)$ is then obtained by a sufficiently smooth interpolation $\vec{V}(r_k,\vec{t}) = \vec{V}_k(\vec{t})$. With r as a continuous independent variable, the r-derivative of the coordinate transformation $\vec{P}(r,\vec{t})$ is equal to the interpolant. Specifically,

$$\frac{\partial \vec{P}}{\partial r} = \vec{V} = \sum_{k=1}^{n-1} \psi_k(r)\vec{V}_k(\vec{t}) \quad . \tag{211}$$

where $\psi_k(r_j)$ is unity at $k = j$ and vanishes otherwise. Since the coordinate transformation must be obtained from an integration in the r-variable, the interpolant ψ_k must be continuously differentiable up to an order which is one less than the level of smoothness desired for the coordinates. The construction of the local controls mentioned above will rely heavily upon the development of suitably smooth interpolation functions. If the integral of Eq. 211 has a constant of integration equal to $\vec{P}_1(\vec{t})$ and if the quantities $A_k\psi_k(r)$ integrate to unity over the domain $0 \leq r \leq 1$, then a coordinate transformation which matches the desired bounding surfaces is obtained. This also determines the original vector field since the coefficients must be given by

$$A_k = \left[\int_0^1 \psi_k(x)\,dx\right]^{-1} \quad , \tag{212}$$

for $k = 1,\ldots,n-1$. With this data, the multi-surface transformation is given by

$$\vec{P}(r,\vec{t}) = P_1(\vec{t}) + \sum_{k=1}^{N-1} \frac{\int_0^r \psi_k(x)\,dx}{\int_0^1 \psi_k(y)\,dy} [\vec{P}_{k+1}(\vec{t}) - P_k(\vec{t})] \; . \tag{213}$$

It is a simple matter to check that $P(0,\vec{t}) = P_1(\vec{t})$ and $P(1,\vec{t}) = P_N(\vec{t})$. In the latter case the result follows from a telescopic collapse of the summation. On examination of Eq. 212, it is also apparent that each interpolatory function ψ_k need only be determined up to any product with a nonzero real number. The geometric implication is that the vector field interpolation is an interpolation only on vector directions.

Polynomial Transformations

Some global implications of the multi-surface transformation can be illustrated by a sequence of polynomial examples where the ψ_k are of degree $N-2$ for $N = 2,3,4$. For $N = 2$ the polynomial of degree $N - 2 = 0$ is a constant function. On integration it is found that $A_1\psi_1$ is unity and that the polynomial two-surface transformation of Eq. 208 is obtained. The coordinate curves consist of a family of straight line segments connecting the bounding surfaces at common $\vec{t}$-values, and a second family of level (r = constant) curves which are the result of a uniform linear deformation along the line segments of the first family. Clearly, the only possible specifications are for positions on each surface, for angles on each surface, or for a position on one surface and an angle on the other. Consequently, there are only two degrees of freedom.

In the case with $N = 3$, another degree of freedom is added, the polymial degree is $N - 2 = 1$, and the partition is given by $0 = r_1 < r_2 = 1$. Each ψ_i must vanish at r_j if $i \neq j$ and must be nonzero at r_i. The simplest such functions are $\psi_1 = 1 - r$ and $\psi_2 = r$. Upon substitution into Eq. 213 and after some simplification, the polynomial three-surface transformation becomes

$$\vec{P}(r,\vec{t}) = (1-r)^2\vec{P}_1(\vec{t}) + 2r(1-r)\vec{P}_2(\vec{t}) + r^2\vec{P}_3(\vec{t}) \quad . \tag{214}$$

The coordinate curves connecting the bounding surfaces $\vec{P}_1$ and $\vec{P}_3$ are now biparabolic curves which leave $\vec{P}_1$ in the direction of $\vec{P}_2 - \vec{P}_1$ and end on $\vec{P}_3$ from the direction of $\vec{P}_3 - \vec{P}_2$. This should be clear on examination of .

$$\begin{aligned} \frac{\partial\vec{P}}{\partial r} &= 2(1-r)[\vec{P}_2(\vec{t}) - \vec{P}_1(\vec{t})] + 2r[\vec{P}_3(\vec{t}) - \vec{P}_2(\vec{t})] \\ &= 2[\vec{P}_2(\vec{t}) - \vec{P}_1(\vec{t})] + 2r[\vec{P}_3(\vec{t}) - 2\vec{P}_2(\vec{t}) + \vec{P}_1(\vec{t})] \quad , \end{aligned} \tag{215}$$

which is the derivative of Eq. 214 and a special case of Eq. 211. The remaining coordinate curves are the level curves of constant r which are deformations of the boundary curves along the biparabolic curves. An example of a transformation, generated from Eq. 214, is presented in Figure 13. In the example, the inner boundary $\vec{P}_1$ is an ellipse with a major axis of unity and a minor axis of .25. The outer boundary $\vec{P}_3$ and the intermediate curve $\vec{P}_2$, were generated respectively, 2.4 and 1.2, units away from the elliptical surface in the direction of the outward pointing unit normal vector. Then the outer boundary $\vec{P}_3$ was parameterized by its arc length. From the

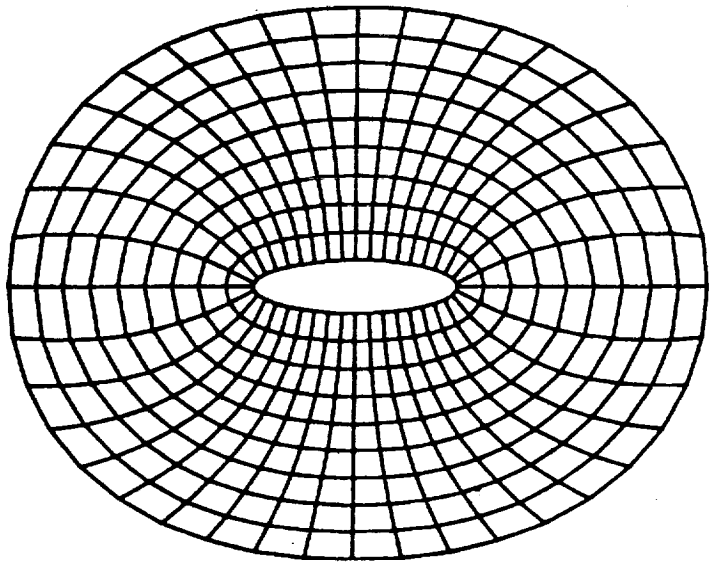

Figure 13. Coordinates generated from Eq. 214. Outwardly directed curves are biparabolic arcs; circumferential curves are uniformly distributed contours.

construction of $\vec{P}_2$, it is clear that the biparabolic curves must leave the elliptical surface orthogonally. With the concurrent specification of positions on each boundary, orthogonality on the outer boundary cannot be obtained. In summary, the boundary specifications of two positions and one angle is the most that can be applied. Alternatively, it would also be possible to specify two angles but only one position. The result is that there are only three degrees of freedom corresponding to $N = 3$.

The case $N = 4$ will lead to yet another degree of freedom. The geometric implication is that the curve which connects the bounding surfaces can inflect; and thereby, adjust to specifications of both angle and position on each bounding surface. This notion is consistent with the anticipated result of employing bicubic curves in the r-variable. Within the structure of the general multi-surface transformation an assumed partition $0 = r_1 < r_2 < r_3 = 1$ leads to the functions $\psi_1 = (r-1)(r-r_2)$,

$\psi_2 = r(r-1)$, and $\psi_3 = (r-r_2)r$ which are defined up to real multiples. The polynomial four-surface transformation is then given by

$$\vec{P}(r,\vec{t}) = (1-r)^2[1-a_1 r]\vec{P}_1(\vec{t}) + (a_1+2)(1-r)^2 r\vec{P}_2(\vec{t}) + r^2[1-a_2(1-r)]\vec{P}_4(\vec{t}) + (a_2+2)r^2(1-r)\vec{P}_3(\vec{t}) \quad , \tag{216a}$$

where

$$a_1 = \frac{2}{3r_2 - 1} \quad , \tag{216b}$$

and

$$a_2 = \frac{2}{3(1-r_2) - 1} \quad , \tag{216c}$$

As in the case with $N = 3$, it can be observed from Eq. 211 that the bounding curves are intersected at angles determined by the vectors $\vec{P}_2 - \vec{P}_1$ and $\vec{P}_4 - \vec{P}_3$, respectively. In this case, as in the previous case with $N = 3$, an example of a coordinate system around the same ellipse and with the same outer boundary is given in Figure 14 where it can be observed that the expected orthogonality at each bounding

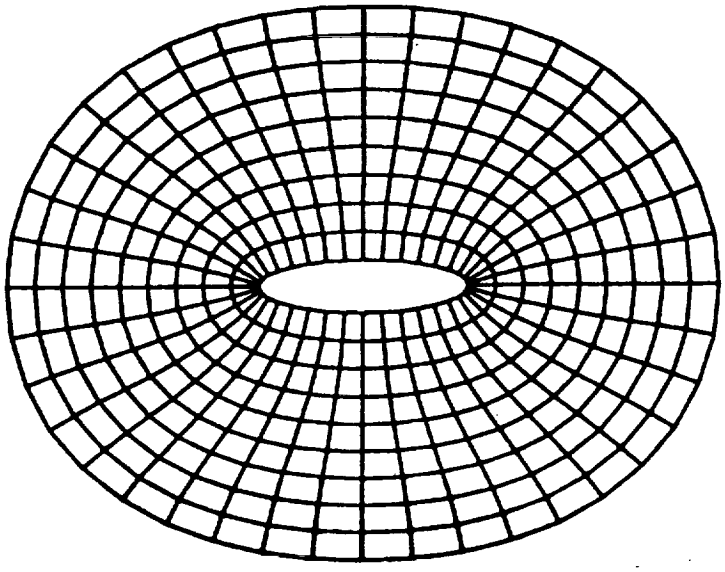

Figure 14. Coordinates generated from Eq. 216 with $B_1 = B_2 = 1/3$ in Eq. 223. Outwardly directed curves are bicubic arcs; circumferential curves are uniformly distributed contours.

surface is actually attained. This was produced by generating the intermediate curves $\vec{P}_2$ and $\vec{P}_3$ with parameterizations that orthogonally aligned them with the respective bouding curves $\vec{P}_1$ and $\vec{P}_4$. The displacement of each intermediate curve from its corresponding boundary was chosen to be equal to one sixth of the distance between the boundaries.

Uniform Distributions of Coordinate Surfaces

In both of the elliptical examples there is one common but subtle point which has some important consequences. It is simply that the coordinates are uniformly distributed between the bounding surfaces. This observation is apparent upon examination of the straight coordinate curves in Figures 13 and 14. Each is vertical or horizontal and is cut into equal increments by the crossing coordinate curves.

In the case with $N = 3$, the intermediate curve was generated to be halfway between the boundaries. The straight coordinate curves appeared when, for a given parameter value, the corresponding triple of points was colinear. Analytically, the r-dependence must vanish from Eq. 215; this means that the tangent vector to the straight coordinate curves are each constant vectors. The implication from Eq. 215 is that the intermediate curve $\vec{P}_2$ be halfway between the boundaries. Moreover, upon a substitution of this halfway condition, Eq. 215 becomes

$$\frac{\partial \vec{P}}{\partial r} = \vec{P}_3(\vec{t}) - \vec{P}_1(\vec{t}) \quad , \tag{217}$$

which is valid for each parametric value $\vec{t}$ where colinearity is satisfied. In addition, the transformation Eq. 214 reduces to the form of Eq. 208 except with a subscript 3 rather than 2. By continuity there is a uniform distribution of coordinate curves within some region containing the straight line segments. However, from Figure 13 it is clear that uniformity extends well beyond most regions of reasonable size. For a satisfactory explanation, further analysis is necessary. Since the uniformity here is measured in the outward direction from inner to outer bounding surfaces, it is reasonable to

consider projections onto the vector $\vec{P}_3 - \vec{P}_1$ which is aligned with the appropriate direction. To simplify the analysis, the scaled vector

$$\tilde{\tau} = \frac{\vec{P}_3 - \vec{P}_1}{\| \vec{P}_3 - \vec{P}_1 \|^2} \quad , \tag{218}$$

shall be used. Under dot product with the scaled vector, there is a relative projection in which the original vector $\vec{P}_3 - \vec{P}_1$ projects to unity. The projection of the vector $\vec{P}_2 - \vec{P}_1$, connecting the intermediate curve with the first bounding curve, is a number $C = (\vec{P}_2 - \vec{P}_1) \cdot \tilde{\tau}$ which is assumed to lie within the unit interval. The implication from this assumption is that the coordinate curves project to a monotone function of r. For each fixed $\tilde{\tau}$, the projection of the corresponding coordinate curve is given by

$$S_p(r,\vec{t}) = [\vec{P}(r,\vec{t}) - \vec{P}_1(\vec{t})] \cdot \tilde{\tau} \quad , \tag{219}$$

which is proportional to arc length along $\vec{P}_3 - \vec{P}_1$. The judicious choice of scale in Eq. 218 is now evident since $S_p(0,t) = 0$ and $S_p(1,t) = 1$. The r-derivative, which is obtained from Eq. 215 is given by

$$\frac{1}{2} \frac{\partial S_p}{\partial r} = C + r(1 - 2C) \quad . \tag{220}$$

On integration, with the constant determined by Eq. 219, the result is

$$S_p = r[2C + r(1 - 2C)] \quad , \tag{221}$$

where the desired uniformity will now be obtained if the quadratic term vanishes. When this occurs $C = 1/2$ and Eq. 221 reduces to the uniform distribution $S_p = r$. In summary, this choice of C is the natural generalization of the earlier halfway condition for straight lines.

In the case $N = 4$, we shall proceed directly to an examination of the relative projected arc length rather than start with the straight lines. There are now two intermediate surfaces, and two relative projections along $\vec{P}_4 - \vec{P}_1$. These are given by

$$C_1 = (\vec{P}_2 - \vec{P}_1) \cdot \tilde{\tau} \quad , \tag{222a}$$

and

$$C_2 = (\vec{P}_4 - \vec{P}_3) \cdot \tilde{\tau} \quad , \tag{222b}$$

where, in the same manner as before,

$$\tilde{\tau} = \frac{\vec{P}_4 - \vec{P}_1}{\| \vec{P}_4 - \vec{P}_1 \|^2} \quad . \tag{222c}$$

The projections are assumed to be positive so that S_p is monotone in r. From here, a short calculation, similar to the previous one, leads to the expression

$$S_p = r[3B_1 + 3(1 - 2B_1 - B_2)r + (3B_1 + 3B_2 - 2)r^2] \quad , \tag{223a}$$

where

$$B_1 = \frac{2r_2}{3r_2 - 1} C_1 \quad , \tag{223b}$$

and

$$B_2 = \frac{2(1-r_2)}{3(1-r_2)-1} C_2 \quad . \tag{223c}$$

A further calculation leads to the relationship

$$S_p(r,\vec{t}) + S_p(1-r,\vec{t}) = 1 + 3(B_1 - B_2)r(1-r) \quad , \tag{224}$$

which is a measure of symmetry in the relative projected arc length of Eq. 223. Absolute symmetry occurs when $B_1 = B_2$ for then the relative distance $S_p(r,\vec{t})$ from the inner boundary $\vec{P}_1$ is equal to the relative distance $1 - S_p(1-r,\vec{t})$ from the outer boundary $\vec{P}_4$. A sequence of symmetric examples are given with the elliptic coordinate systems in Figures 14 - 17. The most notable feature in these figures is that as $B_1 = B_2$ increases from 1/3 to unity, the distribution of coordinate curves, although symmetric, become concentrated in the center. Consequently, it is clear that symmetry is certainly a weaker condition than uniformity. For uniformity, the requirement is that the quadratic and cubic terms in S_p vanish. The implication is equivalent to $B_1 = B_2 = 1/3$. However, there is still some leeway since there is some freedom of choice in the selection of r_2. Since C_1 and C_2 are assumed to be positive, it follows from Eqs. 223b-c that the permissible selections are those for which $1/3 < r_2 < 2/3$. The relative projected distances from intermediate surfaces are then given by

$$C_1 = \frac{1}{2} - \frac{1}{6r_2} \quad ,$$

and (225)

$$C_2 = \frac{1}{2} - \frac{1}{6(1-r_2)} \quad ,$$

over the range of r_2. An example with $r_2 = 1/2$ was given in Figure 14 which was both symmetric and uniform. A further example is given in Figure 18 where a distribution function of the form in Eq. 209 was used in composition with a uniform transformation to pack points near an airfoil and its wake. A view of the airfoil region is given in Figure 19.

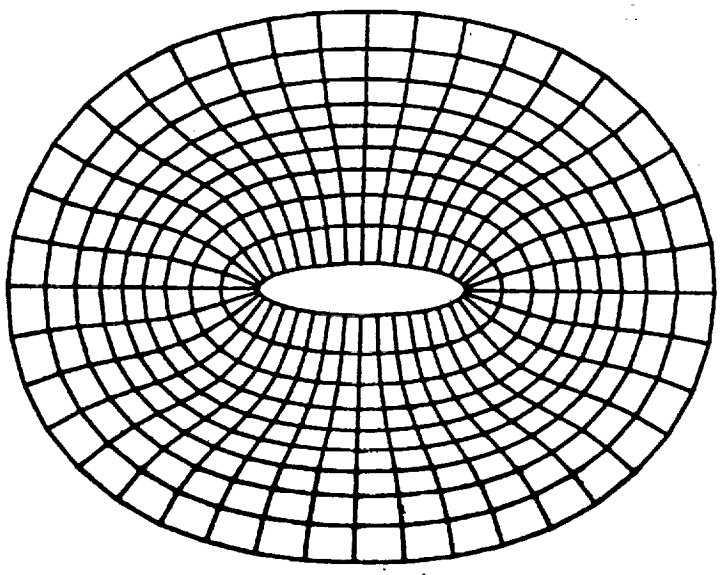

Figure 15. Coordinates from Eq. 216 with $B_1 = B_2 = 1/2$ in Eq. 223. The coordinates are symmetric with a mild concentration of curves in the center.

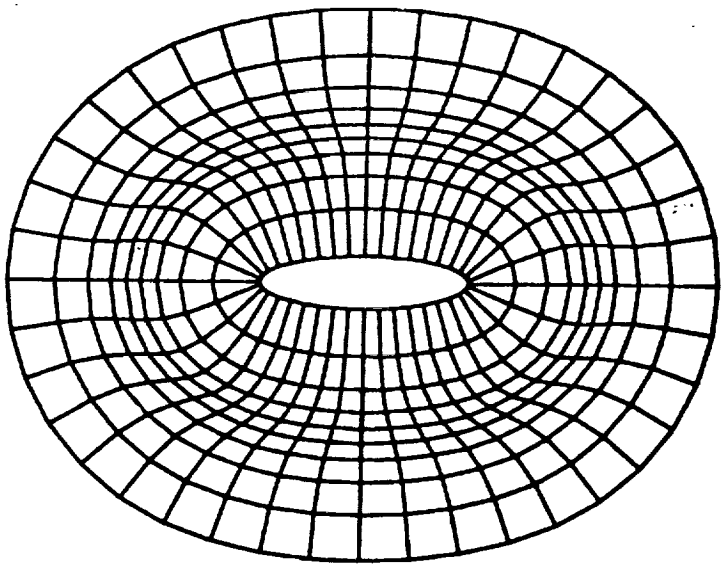

Figure 16. Coordinates from Eq. 216 with $B_1 = B_2 = 2/3$ in Eq. 223. The coordinates are symmetric with a concentration of curves in the center.

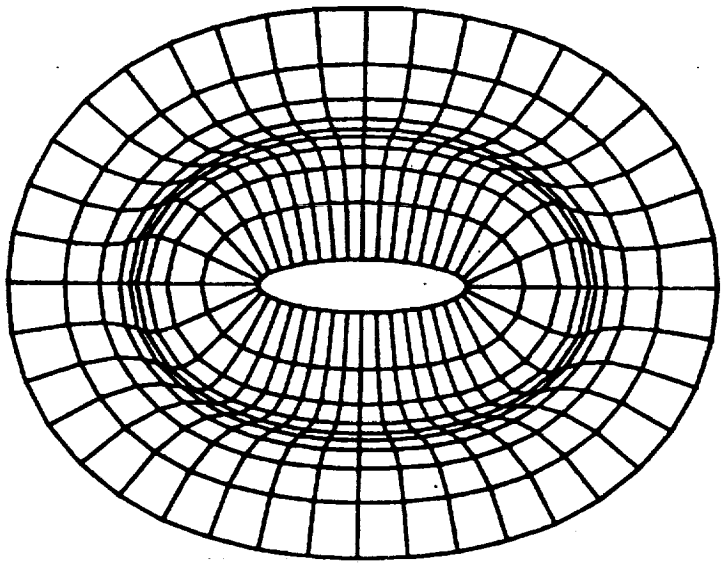

Figure 17. Coordinates from Eq. 216 with $B_1 = B_2 = 5/6$ in Eq. 223. The coordinates are symmetric with a severe concentration of curves in the center.

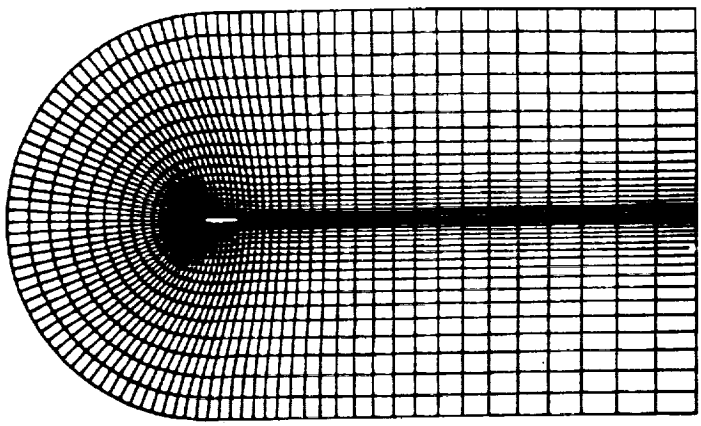

Figure 18. Coordinate system for a Joukowski airfoil with a branch cut.

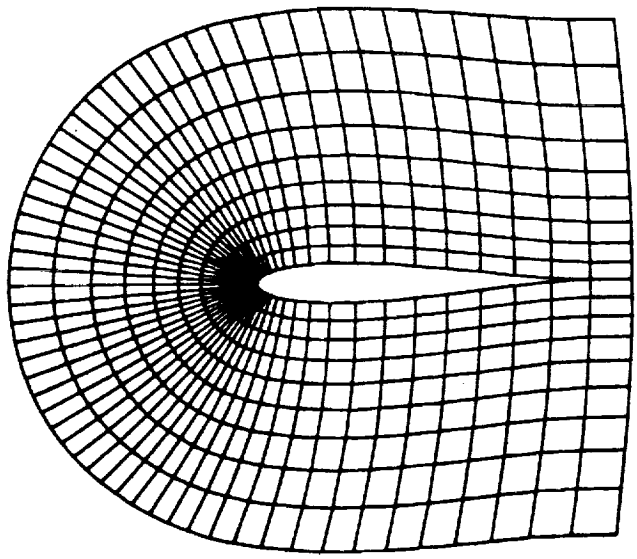

Figure 19. A detailed view of the coordinates near the airfoil surface.

Mesh point distributions on the airfoil (Figures 18 - 19) and on the elliptical bodies (Figures 13 - 17) were each obtained from geometric constructions. To concentrate mesh points in regions of higher curvature, the rate of turning of the unit normal vectors must be controlled. The method of control used in the examples is to create an auxiliary curve at a fixed distance in the normal convex direction, to tabulate its arc length, and to project the arc length tabulation back onto the original curve along its normal directions. The arc length tabulation is done cumulatively for each distinct component of the auxiliary curve as each purely convex or concave portion of a body is traversed in succession. As the distance is increased to an arbitrarily large value, each component of the auxiliary curve approaches a circular shape; hence, the rate of change of the nearly circular arc length (with respect to body arc length) is approximately proportional to curvature (the spherical indicatrix [1]). Consequently, when the distance is varied from zero towards infinity, the projected parameter varies from a body arc length parameter to a parameter whose rate of change is proportional to curvature. An illustration is given in Figure 20 where a convex portion of the body $\vec{P}_1$ is shown with an auxiliary curve at a distance of D units away. A uniform discretization of the auxiliary curve arc length is represented by equally spaced points on the auxiliary curve in Figure 20 and is projected onto the convex portion where a concentration of points at the higher curvature location can be observed explicitly.

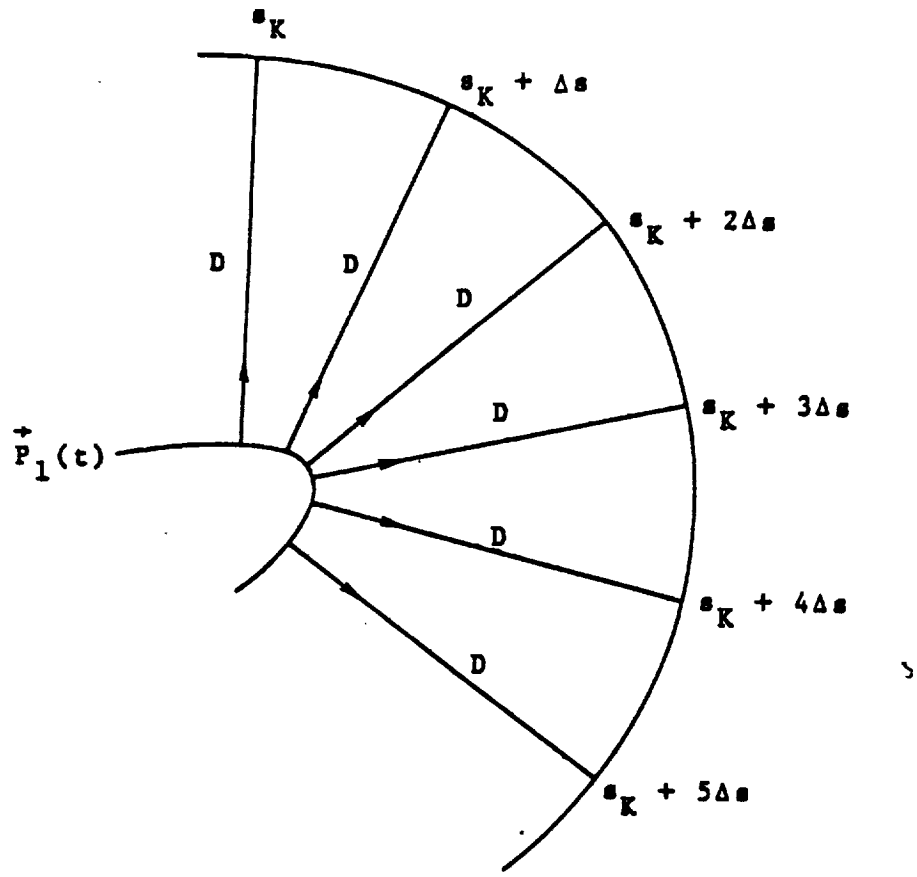

Figure 20. A Geometric Construction of a Curvature Sensitive Parameterization.

Transformations with Precise Local Controls

To establish local controls within the multi-surface transformations (Eq. 213), the interpolants ψ_k must vanish off of suitably small intervals. To add precision, uniformity controls must also be obtained in a parallel manner to the polynomial cases. Relative to uniform conditions, which can now be local conditions, any arbitrary distribution function can be applied in an undistorted fashion by a direct substitution of the function in place of r. The simplest local interpolants are the piecewise-linear functions which are nonvanishing over at most two intervals defined by the partition $0 = r_1 < r_2 < \ldots < r_{N-1} = 1$. An illustration is given in Figure 21 where distinct local interpolants are depicted for each partition point r_k.

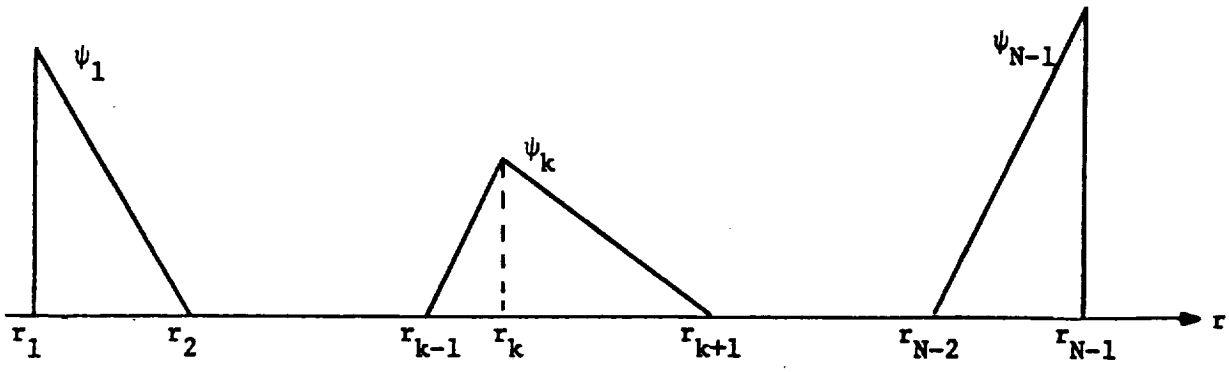

Figure 21. Piecewise Linear Local Interpolants for the Multi-Surface Transformation.

To simplify the form of the multi-surface transformation (Eq. 213), the height of each interpolant shall be adjusted so that each interpolant integrates to unity; hence, the integral normalization is incorporated into the interpolants and is removed from the explicit statement of the transformation. With the notation $h_i = r_{i+1} - r_i$ for $1 \leq i < N-1$, the integrals are obtained from triangular areas, and by direct observation, are given by $\psi_1(r_1)h_1/2$, $\psi_k(r_k)(h_{k-1}+h_k)/2$, and $\psi_{N-1}(r_{N-1})h_{N-2}/2$ in correspondence with the successive illustrations of Figure 21. When the integrals are set to unity, the heights become $\psi_1(r_1) = 2/h_1$, $\psi_k(r_k) = 2/(h_{k-1}+h_k)$, and $\psi_{N-1}(r_{N-1}) = 2/h_{N-2}$ in the same order as above. In correspondence, the explicit form of the normalized interpolants is given by

$$\psi_1(r) = \begin{cases} \frac{2}{h_1^2}(r_2 - r) & \text{for } r_1 \le r < r_2 \\ 0 & \text{for } r_2 \le r \le r_{N-1} \end{cases}$$

$$\psi_k(r) = \begin{cases} 0 & \text{for } r_1 \le r < r_{k-1} \\ \frac{2}{(h_{k-1}+h_k)h_{k-1}}(r - r_k) + \frac{2}{h_{k-1}+h_k} & \text{for } r_{k-1} \le r < r_k \\ \frac{2}{(h_{k-1}+h_k)h_k}(r_k - r) + \frac{2}{h_{k-1}+h_k} & \text{for } r_k \le r < r_{k+1} \\ 0 & \text{for } r_{k+1} \le r \le r_{N-1} \end{cases} \tag{226}$$

$$\psi_{N-1}(r) = \begin{cases} 0 & \text{for } r_1 \le r < r_{N-2} \\ \frac{2}{h_{N-2}^2}(r - r_{N-2}) & \text{for } r_{N-2} \le r \le r_{N-1} \end{cases}$$

In continuation, the corresponding integrals

$$G_i(r) = \int_0^r \psi_i(x)\,dx \tag{227}$$

are given by

$$G_1(r) = \begin{cases} 1 - \dfrac{1}{h_1^2}(r_2 - r)^2 & \text{for } r_1 \le r < r_2 \\ 1 & \text{for } r_2 \le r \le r_{N-1} \end{cases}$$

$$G_k(r) = \begin{cases} 0 & \text{for } r_1 \le r < r_{k-1} \\ \dfrac{(r - r_k)^2}{(h_{k-1} + h_k)h_{k-1}} + \dfrac{2(r - r_k)}{h_{k-1} + h_k} + \dfrac{h_{k-1}}{h_{k-1} + h_k} & \text{for } r_{k-1} \le r < r_k \\ -\dfrac{(r_k - r)^2}{(h_{k-1} + h_k)h_k} - \dfrac{2(r_k - r)}{h_{k-1} + h_k} + \dfrac{h_{k-1}}{h_{k-1} + h_k} & \text{for } r_k \le r < r_{k+1} \\ 1 & \text{for } r_{k+1} \le r \le r_{N-1} \end{cases} \tag{228}$$

$$G_{N-1}(r) = \begin{cases} 0 & \text{for } r_1 \le r < r_{N-2} \\ \dfrac{1}{h_{N-2}^2}(r - r_{N-2})^2 & \text{for } r_{N-2} \le r \le r_{N-1} \end{cases},$$

which, on substitution into the general multi-surface transformation (Eq. 213), leads to the local form

$$\vec{P}(r,t) = \vec{P}_k(t) + G_k(r)[\vec{P}_{k+1}(t) - \vec{P}_k(t)] + G_{k+1}(r)[\vec{P}_{k+2}(t) - \vec{P}_{k+1}(t)] , \tag{229}$$

which is valid on the interval $r_k \leq r \leq r_{k+1}$. Since $G_i(r_k)$ is unity for $1 \leq i \leq k-1$, there was a telescopic collapse of the first k terms in Eq. 213 to yield $\vec{P}_k(t)$; and since $G_i(r_{k+1})$ vanishes for $k+2 \leq i \leq N-1$, the last $N-k-3$ terms simply did not appear. The resultant local form of Eq. 229 can then be used to manipulate the coordinates for the r-values between r_k and r_{k+1} with only the three surfaces $\vec{P}_k$, $\vec{P}_{k+1}$ and $\vec{P}_{k+2}$ and without any outside influence. To delineate the curve segments in question, consider the interval endpoint evaluations

$$\vec{P}(r_k,t) = [1-G_k(r_k)]\vec{P}_k(t) + G_k(r_k)\vec{P}_{k+1}(t) \ ,$$

and (230)

$$\vec{P}(r_{k+1},t) = [1-G_{k+1}(r_{k+1})]\vec{P}_{k+1}(t) + G_{k+1}(r_{k+1})\vec{P}_{k+2}(t) \ ,$$

for each fixed t. Since $G_k(r_k)$ and $G_{k+1}(r_{k+1})$ are contained in the unit interval, the evaluations $\vec{P}(r_k,t)$ and $\vec{P}(r_{k+1},t)$ are observed from Eq. 230 to respectively lie on the line segments that connect $\vec{P}_{k+1}(t)$ with $\vec{P}_k(t)$ on one side and with $\vec{P}_{k+2}(t)$ on the other. An illustration for a fixed t value is given in Figure 22 where the curve is observed to maintain convexity, a property which can be shown analytically.

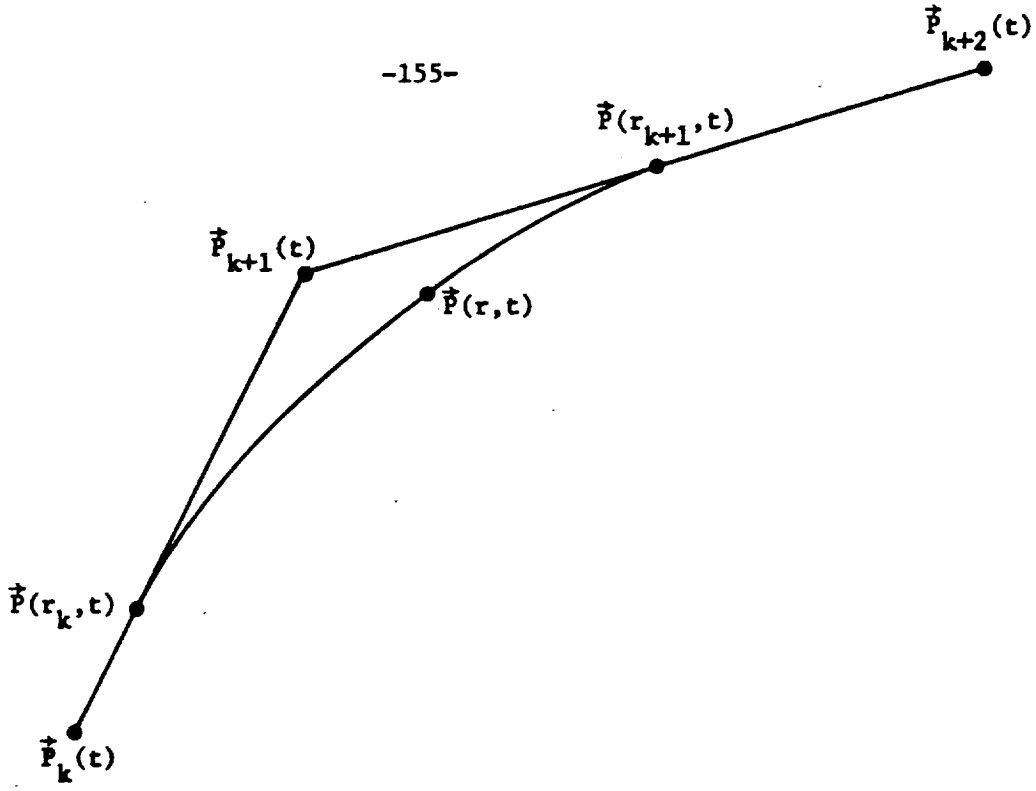

Figure 22. A Local Coordinate Curve Section from Eq. 229 on $r_k \leq r \leq r_{k+1}$.

To obtain a precise control over the rate of travel along the coordinate curve, the uniformity controls established in the polynomial case must be applied to the current local forms from either a local or global perspective. Indeed, the yardsticks for such rate measurements that were respectively given in Eqs. 218 and 222c can be replaced by virtually any other well-aligned vector field. A choice which can be used both locally and globally is to set

$$\vec{\tau}_{ij} = \frac{\vec{P}_i - \vec{P}_j}{\| \vec{P}_i - \vec{P}_j \|^2} \quad , \tag{231}$$

for $i > j$. When $i = N-1$ and $j = 1$, the yardstick vector for uniformity measurements reduces to the previous polynomial cases. Moreover, when $i = k+2$ and $j = k$, the rate along the smallest local units can be controlled with the placement of the local surfaces in the multi-surface construction for the given range of r. In the same manner as in the polynomial cases, let

$$C_{ij\ell} = (\vec{P}_{\ell+1} - \vec{P}_{\ell}) \cdot \tilde{\tau}_{ij} \quad , \tag{232}$$

be the relative projections of the line segments as $\ell = j, j+1, \ldots, i-1$ where the t dependence is assumed implicitly for notational convenience. The relative projected arc length measured from $\vec{P}_j$ is then defined to be

$$S_p(r,t) = [\vec{P}(r,t) - \vec{P}_j(t)] \cdot \tilde{\tau}_{ij}(t) \quad , \tag{233}$$

which for $r_k \leq r \leq r_{k+1}$ reduces to

$$S_p = C_{ijj} + C_{ij,j+1} + \ldots + C_{ij,k-1} + G_k(r)C_{ijk} + G_{k+1}(r)C_{ij,k+1}, \tag{234}$$

by direct application of Eq. 229. For uniformity, S_p must be linear in r, or equivalently, $\partial S_p/\partial r$ must be a constant. By substitution from Eq. 226, the r-derivative of S_p in Eq. 234 becomes

$$\begin{aligned} \frac{\partial S_p}{\partial r} &= \psi_k(r)C_{ijk} + \psi_{k+1}(r)C_{ij,k+1} \\ &= \frac{2}{h_k}\left\{ - \frac{C_{ijk}}{h_{k-1} + h_k} + \frac{C_{ij,k+1}}{h_k + h_{k+1}} \right\} r + \text{constants} \quad , \end{aligned} \tag{235}$$

which is a constant when

$$\frac{C_{ijk}}{h_{k-1} + h_k} = \frac{C_{ij,k-1}}{h_k + h_{k+1}} \quad . \tag{236}$$

From Eq. 232, the uniformity condition of Eq. 236 reduces to

$$\frac{(\vec{P}_{k+1} - \vec{P}_k) \cdot \tilde{\tau}_{ij}}{r_{k+1} - r_{k-1}} = \frac{(\vec{P}_{k+2} - \vec{P}_{k-1}) \cdot \tilde{\tau}_{ij}}{r_{k+2} - r_k} \quad , \tag{237}$$

where the definitions of h_ℓ were used. Clearly, uniformity depends upon the location of surfaces $\vec{P}_m$ and the choices of partition points. In the case when the partition is uniform, the condition reduces to

$$(\vec{P}_{k+2} - 2\vec{P}_{k+1} + \vec{P}_k) \cdot \tilde{\tau}_{ij} = 0 \quad , \tag{238}$$

which means that the discrete normal from $\vec{P}_{k+1}$ is orthogonal to the direction of uniformity measurement.

The development of local methods with uniformity conditions extends to higher levels of derivative continuity than the first order case considered here. The general theoretical development was performed by the present author under AFOSR Contract No. F49620-79-C-0132; and computer applications of the theory are currently being examined by the present author under NASA Lewis Research Center Contract NAS3-22117. Reports on both the theory and the computational applications will appear in [150] and with more detail in [151].

Solution Adaptive Meshes in the r-Direction

Relative to uniform conditions, distribution functions can be applied either locally or globally and either by a priori specification (as with Eq. 209 for attached boundary layers) or by an adaptive mesh technique. When an ADI method is used with coordinatewise implicit directions, the governing system of partial differential equations is solved as a sequence of two-point boundary value problems where the mesh can be adapted to the

solution along coordinate curves in the r-variable. By adapting only in the r-variable, nonsingularity of the entire transformation comes directly from the monotonicity of the r-distribution for each $\vec{t}$, given that the fixed underlying multi-surface transformation with uniform conditions is nonsingular. An example of adaptation in the r-direction (with the two-surface coordinates of Eq. 208) is given in the study of Yanenko et al. [82]. For two-point boundary value problems, adaptive techniques which preserve monotonicity have been based upon the minimization of truncation error ([75], [77], [79]) and upon geometric or analytic properties of the solution ([76], [78]). To maintain, consistency in directions other than r, only methods which do not add or substract mesh points can be considered. In addition, the adaptive techniques for two-point boundary value problems are generally implicit. The result is that an auxiliary equation or equations must be added to an existing system in order to obtain the benefits of a better mesh distribution. The balance then is between a mesh distribution which causes more rapid convergence and the amount of work necessary to obtain it relative to the same level of convergence with an a priori specification or a more dense mesh. With time-dependent problems, an explicit mesh adaption is an attractive alternative since techniques which closely follow solution properties can be developed without the creation of a possibly more complicated problem than was originally posed. Such an explicit construction can be entirely separated from the solution process by spatially lagging the mesh adaptation just enough to not influence the solution process on the current coordinate curve. For second order central difference procedures, the amount of lagging is just two coordinate curves behind the

current one. As a consequence, an extra line of solution data would have to be stored for the explicit adaptive process. To formulate an adaptive technique that is virtually independent of the numerical method used, a geometric technique will be outlined. Consider the velocity profile in Figure 23 which is taken through a separation bubble which could occur, for example, when a shock wave impinges upon an attached boundary layer.

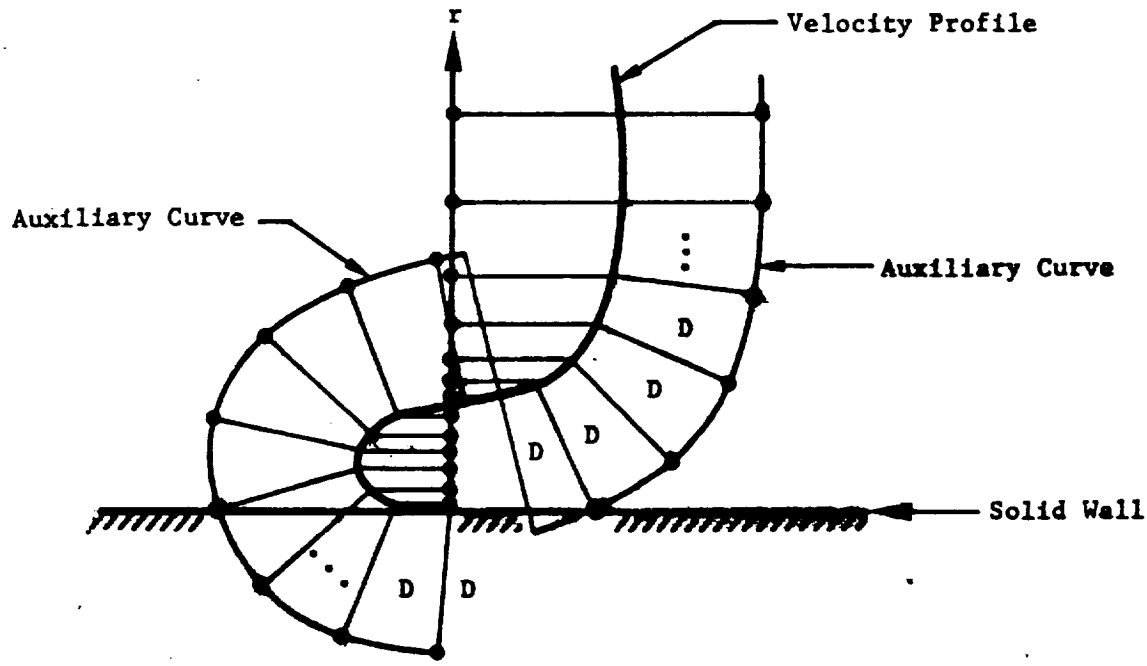

Figure 23. Adaptive mesh from the arc length of an auxiliary curve generated D units from a velocity profile.

If an equal arc length partition of the velocity profile were to be projected onto the r-direction axis (e.g., $\vec{P}_N - \vec{P}_1$), then the resultant mesh in r would be adequate for the resolution of the velocity gradients, but not for

velocity profile curvature which is a measure of the spatial rate of change in profile shape. To also include the cruvature effects, an auxiliary curve is constructed in the same fashion that was done for pointwise distributions on one-dimensional surfaces and illustrated in Figure 20. When the auxiliary curve is taken D units away in the convex normal direction, the projection of its arc length parameters along the normals gives us a velocity profile parameterization which varies from profile arc length to profile curvature concentrations as D varies from 0 to arbitrarily large values. Since the velocity profile in Figure 23 has an inflection point where convexity properties change, the auxiliary curve appears with two components. In the auxiliary curve arc length tabulation, the jump between components at the inflection point is <u>not</u> added to the arc length, but rather the arc length sum is computed up the inflection on the first component and is then continued by adding arc length staring from the inflection on the second component. In the figure, an equal arc length partition on the auxiliary curve is depicted by a sequence of dots where inflection point treatment can be readily observed. As in the case with surface parameterizations, the equally spaced dots on the auxiliary curve are projected onto the profile to yield a curvature sensitive distribution. When the profile distribution is projected orthogonally onto the r-direction axis, we obtain a distribution $R(r,\vec{t})$ which distributes mesh points to resolve regions where the velocity gradients (slopes) are large and where the gradients are rapidly changing (curvature). In the figure, the final images of the auxiliary curve partition points are displayed as a sequence of dots along the r-axis. Due to the geometric construction based upon arc length and projections, the distribution function

$R(r,\vec{t})$ is always strictly monotone; hence, when r is replaced by $R(r,\vec{t})$ in a fixed multi-surface transformation, nonsingularity will not be lost. Moreover, when uniformity in the r-variable is imposed for the fixed transformation, the distribution is inserted without distortion which is absolutely necessary in such a process. In applications of such a geometric technique, some consideration has to be given to the treatment of local oscillations (wiggles) in a numerical solution. Some filtering or smoothing must clearly be applied when needed. To compare the difference between implicit and explicit solution adaptation, Ablow and Schecter [76] have examined two point boundary value problems with both an arc length and a curvature control to obtain a rather complex implicit relationship. With more generality in the implicit approach, White [78] has developed a method based on arbitrary monitor functions.

REFERENCES

[1] D. Laugwitz, Differential and Riemannian Geometry, Academic Press, Press, New York (1965).

[2] R. L. Bishop and S. I. Goldberg, Tensor Analysis on Manifolds, McMillan, New York (1968).

[3] J. Serrin, Mathematical principles of classical fluid mechanics, Handbuch der Physik, Bd. VIII, ed. S. Flugge and C. Truesdell, Springer-Verlag, Berlin (1959).

[4] J. O. Hinze, Turbulence, McGraw-Hill, New York (1959).

[5] B. E. Launder and D. B. Spalding, Mathematical Models of Turbulence, Academic Press, New York (1972).

[6] W. P. Jones and B. E. Launder, The prediction of laminarization with a two-equation model of turbulence, International Journal of Heat and Mass Transfer, Vol. 15 (1972).

[7] T. Cebeci and A. M. O. Smith, Analysis of Turbulent Boundary Layers, Academic Press, New York (1974).

[8] A. A. Townsend, The Structure of Turbulent Shear Flows, Second Ed., Cambridge University Press (1976).

[9] P. Moin, N. N. Mansour, W. C. Reynolds, and J. H. Ferziger, Large eddy simulation of turbulent shear flow, Sixth Intl. Conf. Numer. Methods in Fluid Dynamics, Springer-Verlag Lecture Notes in Physics, Vol. 90 (1978).

[10] J. H. Ferziger and D. C. Leslie, Large eddy simulation: A predictive approach to turbulent flow computation, Proc. Fourth AIAA Computational Fluid Dynamics Conference (1979), pp. 234-246.

[11] A. Einstein, The Meaning of Relativity, Fifth Ed., Princeton University Press (1956).

[12] R. Alder, M. Bazin, and M. Schiffer, Introduction to General Relativity, McGraw-Hill, New York (1965).

[13] G. C. McVittie, General Relativity and Cosmology, University of Illinois Press (1965)

[14] G. C. McVittie, A systematic treatment of moving axes in hydrodynamics, Proc. Royal Society, A, 196 (1949), pp. 285-300.

[15] F. Walkden, The equations of motion of a viscous compressible gas referred to an arbitrarily moving co-ordinate system, Royal Aircraft Establishment, Technical Report No. 66140, England (1966).

[16] H. J. Gibeling, S. J. Shamroth, and P. R. Eiseman, Analysis of strong interaction dynamic stall for laminar flow on airfoils, NASA CR 2969 (1978).

[17] G. Birchoff and S. MacLane, A Survey of Modern Algebra, Revised Ed., Macmillan, New York (1962).

[18] J. N. Franklin, Matrix Theory, Prentice-Hall, Englewood Cliffs, NJ (1968).

[19] H. Flanders, Differential Forms with Applications to the Physical Sciences, Academic Press, New York (1963).

[20] I. M. Singer and J. A. Thorpe, Lecture Notes on Elementary Topology and Geometry, Scott, Foresman, and Co., (1967).

[21] R. W. MacCormack, The effect of viscosity in hypervelocity impact cratering, AIAA Paper 69-354 (1969).

[22] R. M. Beam and R. F. Warming, An implicit finite-difference algorithm for hyperbolic systems in conservation-law form, J. Computational Physics, Vol. 22 (1976), pp. 87-110.

[23] M. Vinokur, Conservation equations of gasdynamics in curvilinear coordinate systems, J. Computational Physics, Vol. 14 (1974), pp. 105-125.

[24] H. Viviand, Formes conservatives des equations de la dynamique des gaz, La Recherche Aérosp., No. 1974-1 (1974), pp. 65-66.

[25] P. R. Eiseman and A. P. Stone, A generalized Hodge theory, J. Differential Geometry, 9 (1974), pp. 169-176.

[26] P. R. Eiseman and A. P. Stone, A note on a differential concomitant, Proc. Amer. Math. Soc., 53 (1975), pp. 179-185.

[27] P. R. Eiseman and A. P. Stone, Conservation laws of fluid dynamics - a survey, SIAM Review, 22 (1980), pp. 12-27.

[28] A. Rizzi and H. Bailey, Finite-volume solution of the Euler equations for steady three-dimensional transonic flow, Proc. of the Fifth International Conference on Numerical Methods in Fluid Dynamics, Springer-Verlag Lecture Notes in Physics, Vol. 59 (1976).

[29] J. L. Steger, Implicit finite-difference simulation of flow about arbitrary two-dimensional geometries, AIAA Journal, Vol. 16 (1978), pp. 679-686.

[30] P. R. Eiseman, A unification of unidirectional flow approximations, Proc. of the Sixth International Conference on Numerical Methods in Fluid Dynamics, Springer-Verlag Lecture Notes in Physics, Vol. 90 (1978), pp. 185-192.

[31] A. Jameson, Iterative solution of transonic flows over airfoils and wings including flows at Mach 1, Communications in Pure and Applied Mathematics, Vol. 27 (1974), pp. 283-309.

[32] E. M. Murman and J. D. Cole, Calculation of plane steady transonic flows, AIAA Journal, Vol. 9 (1971), pp. 114-121.

[33] B. Lakshminarayana and J. H. Horlock, Generalized expressions for secondary vorticity using intrinsic coordinates, J. Fluid Mechanics, Vol. 59 (1973), pp. 97-115.

[34] J. H. Horlock and B. Lakshminarayana, Secondary flows; theory, experiment, and application in turbomachinery aerodynamics, Annual Rev. Fluid Mechanics, Vol. 5 (1973), p. 247.

[35] S. V. Patankar and D. B. Spalding, A calculation procedure for heat, mass, and momentum transfer in three-dimensional parabolic flows, International Journal of Heat and Mass Transfer, Vol. 15 (1972), p. 1787.

[36] L. S. Caretto, R. M. Curr, and D. B. Spalding, Two numerical methods for three-dimensional boundary layers, Comp. Methods Appl. Mech. and Eng., 1 (1972), p. 39.

[37] S. G. Rubin and T. C. Lin, A numerical method for three-dimensional viscous flow: applications to the hypersonic leading edge, J. Computational Physics, Vol. 9 (1972), pp. 339.

[38] T. C. Lin and S. G. Rubin, Viscous flow over a cone at moderate incidence. Part 2 - Supersonic boundary layer, J. Fluid Mechanics, Vol. 59, Part 3 (1973), p. 593.

[39] W. R. Briley, Numerical method for predicting three-dimensional steady viscous flow in ducts, J. Computational Physics, Vol. 14 (1974), pp. 8-28.

[40] P. R. Eiseman, H. McDonald, and W. R. Briley, A method for computing three-dimensional viscous diffuser flows, United Technologies Research Center Report R76-911737-1 (1975).

[41] P. R. Eiseman, R. Levy, H. McDonald, and W. R. Briley, Development of a three-dimensional turbulent duct flow analysis, NASA CR-3029 (1978).

[42] P. R. Dodge, Numerical method for 2D and 3D viscous flows, AIAA J., Vol. 15, No. 7 (1977), pp. 961-965.

[43] D. L. Dwoyer, Application of a velocity-split Navier-Stokes solution technique to external flow problems. Proc. Fourth AIAA Computational Fluid Dynamics Conference (1979), pp. 36-44.

[44] W. S. Helliwell and S. C. Lubard, An implicit method for three dimensional viscous flow with applications to cones at angles of attack, Computers and Fluids, Vol. 3 (1975), p. 83.

[45] J. V. Rakich and S. C. Lubard, Numerical computation of viscous flows on the lee side of blunt shapes flying at supersonic speeds, Aerodynamic Analyses Requiring Advanced Computers, Part I. NASA SP-347 (1975).

[46] R. I. Issa and F. C. Lockwood, On the prediction of two-dimensional supersonic viscous interactions near walls, AIAA Journal, Vol. 15, No. 2 (1977), pp. 182-188.

[47] R. I. Issa and F. C. Lockwood, A hybrid marching integration procedure for the prediction of two-dimensional supersonic boundary layers, ASME Journal of Fluid Engr. (1977), pp. 205-212.

[48] G. Fix and G. Strang, An Analysis of the Finite Element Method, Prentice-Hall, Englewood Cliffs, NJ (1973).

[49] R. W. MacCormack and A. J. Paullay, The influence of the computational mesh on accuracy for initial value problems with discontinuous or nonunique solutions, Computers and Fluids, Vol. 2 (1974), pp. 339-361.

[50] A. W. Rizzi and M. Inouye, Time-split finite volume method for three-dimensional blunt body flow, AIAA Journal, Vol. 11, No. 11 (1973), pp. 1478-1485.

[51] A. Jameson and D. A. Caughey, A finite volume method for transonic potential flow calculations, Proc. Third AIAA Computational Fluid Dynamics Conference (1977), pp. 35-54.

[52] M. J. Fritts and J. P. Boris, The Lagrangian solution of transient problems in hydrodynamics using a triangular mesh, J. Computational Physics, Vol. 31 (1979), pp. 173-215.

[53] A. Lerat and J. Sidès, Numerical simulation of unsteady transonic flows using the Euler equations in integral form, 21st Annual Conference on Aviation and Astronautics, Tel-Aviv and Haifa, Israel (1979)

[54] S. G. Rubin and P. K. Khosla, Polynomial interpolation methods for viscous flow calculations, J. Computational Physics, Vol. 24 (1977), pp. 217-244.

[55] S. B. Margolis, Time dependent solution of a pre-mixed laminar flame, J. Computational Physics, Vol. 27 (1978), pp. 410-427.

[56] C. deBoor and B. Swartz, Collocation at Gaussian points, SIAM J. Numerical Analysis, Vol. 10 (1973), pp. 582-606.

[57] D. Gottlieb and S. A. Orszag, Numerical Analysis of Spectral Methods: Theory and Applications, CBMS-NSF Regional Conference Series in Applied Mathematics, No. 26, SIAM (1977).

[58] H. B. Keller, A new difference scheme for parabolic problems, Numerical Solution of Partial Differential Equations - II, Bert Hubbard, ed., Academic Press (1971), pp. 327-350.

[59] S. F. Wornom, A critical study of higher-order numerical methods for solving the boundary-layer equations, Proc. Third AIAA Computational Fluid Dynamics Conference (1977), pp. 61-71.

[60] M. Ciment and S. H. Leventhal, A note on the operator compact implicit method for the wave equation, Mathematics of Computation, Vol. 32 (1978), pp. 143-147.

[61] J. P. Boris and D. L. Book, Flux corrected transport. I. SHASTA, a fluid transport algorithm that works, J. Computational Physics, Vol. 11 (1973), pp. 38-69.

[62] D. L. Book, J. P. Boris, and K. Hain, Flux corrected transport II. Generalizations of the method, J. Computational Physics, Vol. 18 (1975), pp. 248-283.

[63] J. P. Boris and D. L. Book, Flux corrected transport III. Minimal error FCT algorithms, J. Computational Physics, Vol. 20 (1976), pp. 397-431.

[64] B. van Leer, Towards the ultimate conservation difference scheme, V. A second order sequel to Gudunov's method, J. Computational Physics, Vol. 32 (1979), pp. 101-136.

[65] M. G. Crandall and A. Majda, Monotone difference approximations for scalar conservation laws, Mathematics of Computation, Vol. 34 (1980), pp. 1-22.

[66] A. J. Chorin, Random choice solution of hyperbolic systems, J. Computational Physics, Vol. 22 (1976), pp. 517-533.

[67] A. J. Chorin, Vortex sheet approximation of boundary layers, J. Computational Physics, Vol 27 (1978), p. 428.

[68] M. M. Hafez, J. C. South, and E. M. Murman, Artificial compressibility methods for numerical solutions of the transonic full potential equation, AIAA J. (1979), pp. 838-844.

[69] A. Harten, The Artificial compression method for computation of shocks and contact discontinuities: I. Single conservation laws, Comm. Pure Applied Mathematics, Vol. 39 (1977), pp. 611-638.

[70] H. B. Keller, Numerical solutions of bifurcation and nonlinear eigenvalue problems, Applications of Bifurcation Theory, P. Rabinowitz, ed., Academic Press, New York (1977), pp. 359-384.

[71] R. Meyer-Spasche and H. B. Keller, Numerical study of Taylor-vortex flows between rotating cyclinders, California Institute of Technology Report (June, 1978).

[72] J. Canosa and R. Gomes de Oliveira, A new method for the solution of the Schrodinger equation, J. Computational Physics, Vol. 5 (1970), pp. 188-207.

[73] S. Pruess, Solving linear boundary value problems by approximating the coefficients, Mathematics of Computation, Vol. 27 (1973), pp. 551-562.

[74] I. Babuška and W. C. Rheinboldt, Error estimates for adaptive finite element computations, SIAM J. Numer. Anal., Vol. 15 (1978), pp. 736-754.

[75] M. Lentini and V. Pereyra, An adaptive finite difference solver for nonlinear two-point boundary value problems with mild boundary layers, SIAM J. Numerical Analysis, Vol. 14 (1977), pp. 91-111.

[76] C. M. Ablow and S. Schechter, Campylotropic coordinates, J. Computational Physics, Vol. 27 (1978), pp. 351-362.

[77] C. M. Ablow, S. Schechter, and W. H. Zwisler, Note selection for two-point boundary-value problems, submitted to J. Computational Physics.

[78] A. B. White, Jr., On selection of equidistributing meshes for two-point boundary-value problems, SIAM J. Numerical Analysis, Vol. 16 (1979), pp. 472-502.

[79] B. L. Pierson and P. Kutler, Optimal nodal point distribution for improved accuracy in computational fluid dynamics, AIAA Paper 79-0272 (1979).

[80] H. A. Dwyer, R. J. Kee, and B. R. Sanders, An adaptive grid method for problems in fluid mechanics and heat transfer, Proc. Fourth AIAA Computational Fluid Dynamics Conference (1979), pp. 195-203.

[81] N. N. Yanenko, E. A. Kroshko, V. V. Liseikin, V. M. Fomin, V. P. Shapeev, and Yu. A. Shitov, Methods for the construction of moving grids for problems of fluid dynamics with big deformations, Proc. Fifth International Conference on Numerical Methods in Fluid Dynamics, Springer-Verlag Lecture Notes in Physics, Vol. 59 (1976), pp. 454-459.

[82] N. N. Yanenko, V. M. Kovenya, V. D. Lisejkin, V. M. Fomin, and E. V. Vorozhtsov, On some methods for the numerical simulation of flows with complex structure, Proc. Sixth International Conference on Numerical Methods in Fluid Dynamics, Springer-Verlag Lectures Notes in Physics, Vol. 90 (1978), pp. 565-578.

[83] R. P. Federenko, The speed of convergence of one iterative process, USSR Comp. Math. and Math. Phys., Vol. 4 (1964), pp. 227-235.

[84] N. S. Bakhvalov, On the convergence of a relaxation method with natural constraints on the elliptic operator, USSR Comp. Math. and Math. Phys., Vol. 6 (1966), pp. 101-135.

[85] A. Brandt, Multi-level adaptive solution to boundary value problems, Mathematics of Computation, Vol. 31 (1977), pp. 333-391.

[86] A. Brandt, Multi-level adaptive techniques (MLAT) for singular-perturbation problems, ICASE Report No. 78-18 (1978).

[87] R. A. Nicolaides, On the ℓ^2 convergence of an algorithm for solving finite element equations, Mathematics of Computation, Vol. 31 (1977), pp. 892-906.

[88] J. C. South and A. Brandt, Application of a multi-level grid method to transonic flow calculations, Transonic Flow Problems in Turbomachinery, ed. by T. C. Adamson and M. F. Platzer, Hemisphere, Washington (1977).

[89] A. Jameson, Acceleration of transonic potential flow calculations on arbitrary meshes by the multiple grid method, Proc. Fourth AIAA Computational Fluid Dynamics Conference (1979), pp. 122-146.

[90] K. Stewartson, On the asymptotic theory of separated and unseparated fluid motion, Proc. International Symposium Modern Developments in Fluid Dynamics, ed. by J. Rom, SIAM (1977), pp. 305-322.

[91] O. R. Burggraf, Some recent developments in computation of viscous flows, Proc. Fifth International Conference on Numerical Methods in Fluid Dynamics, Springer-Verlag Lecture Notes in Physics, Vol. 59 (1976), pp. 52-64.

[92] M. D. van Dyke, Perturbation Methods in Fluid Dynamics, Academic Press (1964), also Parabolic Press.

[93] T. A. Zang and M. Y. Hussaini, Mixed spectral/finite difference approximations for slightly viscous flows, to be presented at the Seventh International Conference on Numerical Methods in Fluid Dynamics.

[94] S. H. Bokhari, M. Y. Hussaini, and S. A. Orszag, Numerical simulation of high Reynolds number three-dimensional compressible flow, to be presented at the Seventh International Conference on Numerical Methods in Fluid Dynamics.

[95] H. H. Rachford, Jr. and M. F. Wheeler, An H^{-1} Galerkin procedure for the two-point boundary value problem, Mathematical Aspects of Finite Elements in Partial Differential Equations, Academic Press, New York (1974), pp. 353-382.

[96] I. Lindemuth and J. Killeen, Alternating direction implicit techniques for two-dimensional magnetohydrodynamic calculations, J. Computational Physics, Vol. 13 (1973), pp. 181-208.

[97] W. R. Briley and H. McDonald, Solution of the three-dimensional compressible Navier-Stokes equations by an implicit technique, Proc.

Fourth International Conference on Numerical Methods in Fluid Dynamics, Lecture Notes in Physics, Vol. 35, Springer-Verlag, Berlin (1975).

[98] R. M. Beam and R. F. Warming, An implicit factored scheme for the compressible Navier-Stokes equations, AIAA J., Vol. 16 (1978), pp. 393-402.

[99] R. M. Beam and R. F. Warming, An implicit factored scheme for the compressible Navier-Stokes equations II: The numerical ODE connection, Proc. Fourth AIAA Computational Fluid Dynamics Conference (1979), pp. 1-13.

[100] R. W. MacCormack, An efficient explicit-implicit-characteristic method for solving the compressible Navier-Stokes equations, Computational Fluid Dynamics, ed. by H. B. Keller, SIAM-AMS Proceedings, Vol. 11 (1978), pp. 130-155.

[101] W. F. Ballhaus, A. Jameson, and J. Albert, Implicit approximate factorization schemes for the efficient solution of steady transonic flow problems, AIAA J., Vol. 16 (1978), pp. 573-579.

[102] T. L. Holst, A fast conservative algorithm for solving the transonic full potential equation, Proc. Fourth AIAA Computational Fluid Dynamics Conference (1979), pp. 109-121.

[103] R. Varga, Matrix Iterative Analysis, Prentice-Hall, Englewood Cliffs, NJ (1962).

[104] R. D. Richtmyer and K. W. Morton, Difference Methods for Initial Value Problems, 2nd. Ed., Wiley Interscience, 4 (1967).

[105] R. F. Warming and R. M. Beam, On the construction and application of implicit factored schemes for conservation laws, Computational Fluid Dynamics, ed. by H. B. Keller, SIAM-AMS Proceedings, Vol. 11 (1978), pp. 85-129.

[106] J. Douglas and J. E. Gunn, A general formulation of alternating direction methods, Numerische Mathematik, Vol. 6 (1964), pp. 428-453.

[107] A. Jameson and E. Turkel, Implicit schemes and LU decompositions, ICASE Report No. 79-24 (1979)

[108] J. L. Steger and R. W. Warming, Flux vector splitting of the inviscid gasdynamic equations with application to finite difference methods, NASA Tech. Memo. 78605 (1979).

[109] J. Douglas and T. Dupont, Alternating-Direction Galerkin methods on rectangles, Numerical Solution of Partial Differential Equations - II, Academic Press, New York (1971), pp. 133-214.

[110] A. R. Mitchell, Computational Methods in Partial Differential Equations, Wiley, New York (1969).

[111] P. R. Eiseman, H. McDonald, and R. Levy, A method for computing flows over an ogival body, United Technologies Research Center Report R77-912536-8 (1978).

[112] E. Engquist and A. Majda, Absorbing boundary conditions for the numerical simulation of waves, Mathematics of Computation, Vol. 31 (1977), pp. 629-651.

[113] G. W. Hedstrom, Non-reflecting boundary conditions for nonlinear hyperbolic systems, to appear in J. Computational Physics.

[114] D. H. Rudy and J. C. Strikwerda, A non-reflecting outflow boundary condition for subsonic Navier-Stokes calculations, ICASE Report No. 79-2, to appear in J. Computational Physics.

[115] D. H. Rudy and J. C. Strikwerda, Boundary conditions for subsonic compressible Navier-Stokes calculations, ICASE Report No. 79-18, submitted to Computers and Fluids.

[116] B. Gustafsson and H. O. Kreiss, Boundary conditions for time-dependent problems with an artificial boundary, J. Computational Physics, Vol. 30, (1979), pp. 333-351.

[117] B. Gustafsson and A. Sundström, Incompletely parabolic systems in fluid dynamics, SIAM J. of Applied Mathematics, Vol. 35 (1978), pp. 343-357.

[118] D. Gottlieb, M. Gunzburger, and E. Turkel, On numerical boundary treatment for hyperbolic systems, ICASE Report No. 78-13 (1978).

[119] J. Oliger and A. Sundström, Theoretical and practical aspects of some initial boundary value problems in fluid dynamics, SIAM J. Applied Mathematics, Vol. 35 (1978), pp. 419-446.

[120] D. Gottlieb and E. Turkel, Boundary conditions for multi-step finite difference methods for time-dependent equations, J. Computational Physics, Vol. 26 (1978), pp. 181-196.

[121] T. J. Wearle, Errors arising from irregular boundaries in ADI solutions of the shallow water equations, International J. Numer. Meth. Engr., Vol. 14 (1979), pp. 921-931.

[122] J. M. Gary, On boundary conditions for hyperbolic difference schemes, J. Computational Physics, Vol. 26 (1978), pp. 339-351.

[123] C. K. Chu and A. Serney, Boundary conditions in finite difference fluid dynamic codes, J. Computational Physics, Vol. 15 (1974), pp. 476-491.

[124] P. J. Roache, Computational Fluid Dynamics, Hermosa Publishers, Albuquerque, NM, Revised Edition (1976).

[125] D. J. Rose and R. A. Willoughby, editors, Sparse Matrices and Their Applications, Plenum Press, New York (1972).

[126] J. R. Bunch and D. J. Rose, editors, Sparse Matrix Computations, Academic Press, New York (1976).

[127] T. Theodorsen and I. E. Garrick, General potential thoery of arbitrary wing sections, NACA TR No. 452 (1933).

[128] D. C. Ives, A modern look at conformal mapping including multiply connected regions, AIAA J., Vol. 14 (1976), pp. 1006-1011.

[129] D. C. Ives and J. F. Liutermoza, Analysis of transonic cascade flow using conformal mapping and relaxation techniques, AIAA J., Vol. 15 (1977), pp. 647-652.

[130] B. Grossman and R. E. Melnik, The numerical computation of the transonic flow over two-element airfoil systems, Proc. Fifth International Conference on Numerical Methods in Fluid Dynamics, Lecture Notes in Physics, Vol. 59, Springer-Verlag, Berlin (1976), pp. 220-227.

[131] O. L. Anderson, Calculation of internal viscous flows in axisymmetric ducts at moderate to high Reynolds numbers, to appear in Computers and Fluids.

[132] P. Henrici, Applied and Computational Complex Analysis, Vol. 1, Wiley, New York (1974).

[133] R. T. Davis, Numerical methods for coordinate generation based on Schwartz-Christoffel transformations, Proc. Fourth AIAA Computational Fluid Dynamics Conference (1979), pp. 180-194.

[134] L. C. Woods, The Theory of Subsonic Plane Flow, Cambridge University Press (1961).

[135] D. A. Caughey, A systematic procedure for generating useful conformal mappings, International Journal on Numerical Methods in Engineering, Vol. 12 (1978), pp. 1651-1657.

[136] P. R. Eiseman, A multi-surface method of coordinate generation, J. Computational Physics, Vol. 33 (1979), pp. 118-150.

[137] W. D. McNally, FORTRAN program for generating a two-dimensional orthogonal mesh between two arbitrary boundaries, NASA TN D-6766.

[138] R. A. Graves, Jr., Application of a numerical orthogonal coordinate generator to axisymmetric blunt bodies, NASA TM 80131 (1979).

[139] J. L. Steger and D. S. Chaussee, Generation of body fitted coordinates using hyperbolic partial differential equations, FSI Report 80-1 (1980).

[140] G. Starius, Constructing orthogonal curvilinear meshes by solving initial value problems, Numerische Mathematik, Vol. 28, Fasc. 1 (1977), pp. 24-48.

[141] P. R. Eiseman, Orthogonal coordinates from specified metrics, ICASE Internal Report No. 11 (1979).

[142] J. F. Thompson, F. C. Thames, and C. W. Mastin, Automatic numerical generation of body-fitted curvilinear coordinate system for field containing any number of arbitrary two-dimensional bodies, J. Computational Physics, Vol. 15 (1974), pp. 299-319.

[143] P. R. Eiseman, A coordinate system for a viscous transonic cascade analysis, J. Computational Physics, Vol. 26 (1978), pp. 307-338.

[144] G. O. Roberts, Computational meshes for boundary layer problems, Proc. Second International Conference on Numerical Methods in Fluid Dynamics, Ed. M. Holt, Springer-Verlag (1970), p. 171.

[145] U. Ghia, K. N. Ghia, and C. J. Studerus, Use of surface-oriented coordinates in the numerical simulation of flow in a turbine cascade, Proc. Fifth International Conference on Numerical Methods in Fluid Dynamics, Lecture Notes in Physics, Vol. 59, Springer-Verlag (1976), pp. 197-204.

[146] J. F. Thompson, F. C. Thames, and C. W. Mastin, TOMCAT - A code for numerical generation of boundary-fitted curvilinear coordinate systems on fields containing any number of arbitrary two-dimensional bodies, J. Computational Physics, Vol. 24 (1977), pp. 274-302.

[147] M. H. Protter and H. F. Weinberger, Maximum Principles in Differential Equations, Prentice-Hall, Englewood Cliffs, NJ (1967).

[148] J. L. Steger and R. L. Sorenson, Automatic mesh-point clustering near a boundary in grid generation with elliptic parital differential equations, J. Computational Physics, Vol. 33 (1979), pp. 405-416.

[149] P. R. Eiseman, Three-dimensional coordinates about wings, Proc. Fourth AIAA Computational Fluid Dynamics Conference (1979), pp. 166-174.

[150] P. R. Eiseman, Coordinate generation with precise controls, to be presented at the Seventh International Conference on Numerical Methods in Fluid Dynamics.

[151] P. R. Eiseman, Coordinate generation with precise controls over mesh properties, manuscript in preparation.

Errata

Page	Line	Appears As	Should Be
36	21	stree-energy	stress-energy
44	17	W	$\vec{W}$
46	Fig. 5	$F_2 \otimes (-dx^1)$	$-F_2 \otimes (-dx^1)$
79	Eq. 150a	$\frac{\partial H_i}{\partial t}$	$\frac{\partial H_i}{\partial \tau}$
80	2	t comes	τ comes
81	Eq. 151	$\frac{\partial H_i}{\partial t}$	$\frac{\partial H_i}{\partial \tau}$
88	2 of Eq. 168	$\frac{\partial H}{\partial p_r^k}$	$\frac{\partial H_i}{\partial p_r^k}$
93	2	(P_r^k)	(u^ℓ) and (p_r^k) respectively
94	Eq. 178b	$-E_0^j$	$-3E_0^j$
99	21	Schwartz	Swartz
103	Fig. 10	Z'	X'
103	Fig. 10	X'	Z'
105	3	field of	field of orthogonal
119	Eq. 200	J =	J = det
122	18	sysem	system
123	Eq. 204	x^4	x^3
128	24	the same shape	a good location
131	21	mathcing	matching
132	14	[147]	[29]
133	6	coordinator	coordinates
141	3	bouding	boumding
157	Eq. 237	$\vec{P}_{k+2} - \vec{P}_{k-1}$	$\vec{P}_{k+2} - \vec{P}_{k+1}$
160	2	cruvature	curvature
160	15	staring	starting